

**ADDITIVE MANUFACTURING METHODS FOR ELECTROACTIVE
POLYMER PRODUCTS**

by

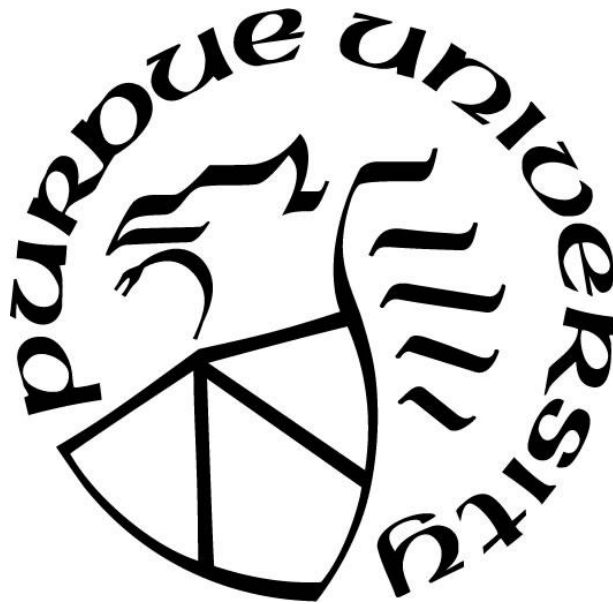
Trevor J. Mamer

A Thesis

Submitted to the Faculty of Purdue University

In Partial Fulfillment of the Requirements for the degree of

Master of Science



Department of Engineering Technology

West Lafayette, Indiana

May 2019

**THE PURDUE UNIVERSITY GRADUATE SCHOOL
STATEMENT OF COMMITTEE APPROVAL**

Dr. Brittany Newell, Chair

Department of Engineering Technology

Dr. José García-Bravo, Co-Chair

Department of Engineering Technology

Dr. Suranjan Panigrahi

Department of Engineering Technology

Assistant Professor Davin Huston

Department of Engineering Technology

Approved by:

Dr. Duane D. Dunlap

Head of the Graduate Program

To my family, it isn't quite a Ph.D. in Life but I'm working on it.

*To TheMidnightPostOffice, your mic wasn't broken. I heard you the whole
time. :slammed: :waitingforterv:*

ACKNOWLEDGMENTS

This work was sponsored in part by the National Science Foundation under grant CNS-1726865, the Purdue Polytechnic Institute, and Kinex Medical company. The work accomplished here would also not have been possible without the insight and assistance provided by my committee members, Brittany Newell, José García, Suranjan Panigrahi, and Davin Huston. Additionally, assistance by my peers was essential in getting done all that was accomplished here. I would like to extend a humble thank you to: David Gonzales for all his help and contributions that served as the foundations for my research. To Laura Vallejo for all her incredibly helpful critiques that fixed problems before they ever started. To Jorge Leon for all his blessings and the laughter he brought to the lab. To Ridhi Deo for all the coffee. To Taylor Zigon for answering all my questions pertaining to his research. To Mohammad Javad Mirshojaeian Hosseini, who's incredibly generous contributions led to the setup of critical software and hardware. To Mohamad Rusydi Mohamad Yasin for his instrumental help in setting up and acquiring the data for the stretch tests. To Cole Maynard for helping me survive all the work outside of research. Lastly to all my family and friends outside of the lab who support me. To each and every one of them; you are missed, and your support is felt every day. Thank you.

TABLE OF CONTENTS

LIST OF TABLES	7
LIST OF FIGURES	8
GLOSSARY	11
ABSTRACT.....	12
CHAPTER 1. INTRODUCTION	13
1.1 Purpose.....	14
1.2 Research Questions.....	14
1.3 Deliverables	15
1.4 Significance.....	15
1.5 Assumptions.....	15
1.6 Delimitations.....	16
1.7 Limitations	16
CHAPTER 2. REVIEW of LITERATURE.....	17
2.1 Introduction.....	17
2.2 Methodology of the Review.....	17
2.3 Electroactive Polymers	19
2.3.1 EAP Manufacturing.....	21
2.4 Additive Manufacturing.....	22
2.4.1 Printer Types & Materials	22
2.5 Preliminary Samples	22
2.6 Preliminary Testing.....	23
2.7 Preliminary Results.....	24
CHAPTER 3. RESEARCH METHODOLOGY.....	27
3.1 Introduction.....	27
3.2 Material and Printer Choice	28
3.3 Design Choice.....	29
3.4 Manufacturing.....	33
3.5 Testing.....	40
3.5.1 Pre & Post Stretch Measurements	40

3.5.2 Application Testing	42
CHAPTER 4. RESULTS	46
4.1 Manufacturing.....	46
4.2 Resting Values – Pre-Stretch	54
4.3 Application Testing – Sensors	65
4.4 Resting Values – Post-Stretch.....	80
4.5 Application Testing -Actuators.....	92
CHAPTER 5. SUMMARY, CONCLUSIONS, and RECOMMENDATIONS.....	96
5.1 Manufacturing.....	96
5.2 Pre & Post Stretch Resting Values.....	97
5.3 Application Testing - Sensors.....	99
5.4 Application Testing - Actuators.....	100
5.5 Concluding Statements	101
5.6 Future Work	101
LIST of REFERENCES.....	104

LIST OF TABLES

Table 2.1 - Consistency Test with PE873	25
Table 3.1 - Annealing settings	38
Table 4.1 - PE873 Pre-Stretch Resting Capacitance Values.....	54
Table 4.2 PE873 Pre-Stretch Resting Capacitance Values Continued	55
Table 4.3 – Fluorine Rubber Ink Pre-Stretch Resting Capacitance Values	55
Table 4.4 – Fluorine Rubber Ink Pre-Stretch Resting Capacitance Values Continued	56
Table 4.5 - Parker Pre-Stretch Resting Capacitance Values.....	56
Table 4.6 - Parker Pre-Stretch Resting Capacitance Values Continued	56
Table 4.7 - ETPU Pre-Stretch Resting Capacitance Values	57
Table 4.8 - ETPU Long Pre-Stretch Resting Capacitance Values Continued	57
Table 4.9 - PE873 Sensors & Actuators Pre-Stretch Initial Resting Resistance Values	59
Table 4.10 – Fluorine Rubber Sensor & Actuator Initial Resting Resistance Values	60
Table 4.11 - Number of dropped values during stretch test.....	80
Table 4.12 - PE873 Post-Stretch Resting Capacitance Values	81
Table 4.13 - PE873 Post-Stretch Resting Capacitance Values Continued	81
Table 4.14 – Fluorine Rubber Ink Post-Stretch Resting Capacitance Values	82
Table 4.15 - Fluorine Rubber Ink Post-Stretch Resting Capacitance Values Continued	82
Table 4.16 – Parker & Grease Post-Stretch Resting Capacitance Values	83
Table 4.17 – Parker & Grease Post-Stretch Resting Capacitance Values Continued.....	83
Table 4.18 - PE873 Sensors & Actuators Post-Stretch Initial Resting Resistance Values.....	87
Table 4.19 - Fluorine Rubber Ink Sensors & Actuators Post-Stretch Initial Resting Resistance Values	88
Table 4.20 – Actuator high voltage testing physical diameter changes.....	93
Table 4.21 - Average and Standard Deviation for Actuator high voltage testing physical diameter changes.....	94
Table 4.22 - Actuator high voltage testing electrical values.....	95
Table 4.23 - Average and Standard Deviation for Actuator high voltage testing electrical changes	95

LIST OF FIGURES

Figure 2.1 - Concept Map Venn Diagram for Search.....	18
Figure 2.2 - Concept Map for Concept Hierarchy	18
Figure 2.3 - Visual of the electronic EAP working principle (Gonzalez et al., 2019).....	21
Figure 2.4 - Actuator Prototype with PE873 Ink	23
Figure 2.5 - PE873 Repeatability Test.....	23
Figure 2.6 – Capacitance Change per Step Count	25
Figure 2.7 – Change in Capacitance per Step.....	26
Figure 3.1 - Methodology Flow Chart	27
Figure 3.2 - Manufacturing Steps	30
Figure 3.3 - Actuator Samples Visual.....	30
Figure 3.4 - Sensor Samples Visual.....	31
Figure 3.5 - Example of layering in CAD designs.....	31
Figure 3.6 – Reference Parker-Hannifin Sensor Sample	32
Figure 3.7 - Additively Manufactured Sensor Sample	32
Figure 3.8 - Reference Grease Sample	33
Figure 3.9 - Conductive ink sample.....	33
Figure 3.10 - Dielectric blank being strained on iris stretcher prior to actuation testing	35
Figure 3.11 - Student developed circuit writer front panel and settings used.....	36
Figure 3.12 - Makerbot settings for dielectric and EPTU printing.....	37
Figure 3.13 - Makerbot settings for dielectric and ETPU printing.....	37
Figure 3.14 - Lulzbot Bed Temperature Climb and Drop Rates for annealing	38
Figure 3.15 - Lulzbot used for dielectric printing and annealing	39
Figure 3.16 - Makerbot used for sensor dielectric printing & ETPU	39
Figure 3.17 – Custom made circuit writer used for electrode application.....	40
Figure 3.18 - Front panel and settings for frequency sweep software	41
Figure 3.19 - Locations for resistance measurements for sensor samples	41
Figure 3.20 - Locations for resistance measurements for actuator samples	42
Figure 3.21 - Stretch Test Setup	43
Figure 3.22 - Front panel and settings for capacitance over time sensor application testing	43

Figure 3.23 - Example of Tracker setup and front panel	44
Figure 3.24 - Acrylic ring for holding strain on actuator samples	45
Figure 3.25 - Example of a strained actuator sample.....	45
Figure 4.1 - Sensor sample dielectric blanks	46
Figure 4.2 - Actuator sample dielectric blank.....	47
Figure 4.3 - Sensor initial ink pad in progress	48
Figure 4.4- Sensor initial ink pad in progress, side view	48
Figure 4.5 - Sensor initial ink pad immediately post-ink printing.....	48
Figure 4.6 - Sensor sample warping at start of annealing process.....	49
Figure 4.7 - Actuator initial ink pad in progress.....	49
Figure 4.8 - Actuator ink pad warping at start of annealing process	50
Figure 4.9 - All sensors samples complete, post final annealing.....	50
Figure 4.10 - PE873 Actuators post final annealing	51
Figure 4.11 - All Fluorine Rubber Ink samples, post final annealing.....	51
Figure 4.12- Pre & post additional anneal capacitance results Fluorine Rubber Ink sensor samples.....	52
Figure 4.13 - Pre & post additional anneal capacitance results Fluorine Rubber Ink actuator samples.....	52
Figure 4.14 - Missing fingers for blue clips on PE873 Samples 2 & 5	53
Figure 4.15 – Fluorine Rubber Ink actuator post additional annealing	54
Figure 4.16 - Parker all Sensors Combined Frequency Sweep Plot pre-stretch	61
Figure 4.17 - PE873 All Sensors Combined Frequency Sweep Plot pre-stretch.....	62
Figure 4.18 - Fluorine Rubber Ink All Sensors Combined Frequency Sweep Plot pre-stretch....	62
Figure 4.19 - Fluorine Rubber Ink Actuator Combined Frequency Sweeps Plot pre-stretch.....	63
Figure 4.20 - PE873 Actuator Combined Frequency Sweeps Plot pre-stretch.....	63
Figure 4.21 - ETPU Frequency combined frequency sweeps plot pre-stretch	64
Figure 4.22 - Parker Sensor Samples Post-Stretch Test	65
Figure 4.23 - Fluorine Rubber Ink Post-Stretch Test Front Side.....	66
Figure 4.24 - Fluorine Rubber Ink Post-Stretch Test Rear side.....	66
Figure 4.25 – PE873 Post-Stretch Test Front Side	67
Figure 4.26 – PE873 Post-Stretch Test Rear Side	67

Figure 4.27 - ETPU initial samples front side post stretch test	68
Figure 4.28 - ETPU initial samples back side post stretch test.....	68
Figure 4.29 - Separation at the reading trace ETPU initial sample	69
Figure 4.30 - Read trace on Fluorine Rubber Ink Sample	69
Figure 4.31 - Read trace on PE873 Sample	70
Figure 4.32 - Parker capacitance over strain.....	71
Figure 4.33 - Fluorine Rubber Ink capacitance over strain unbroken samples	72
Figure 4.34 – Fluorine Rubber Ink capacitance over strain broken samples.....	73
Figure 4.35 - ETPU Samples capacitance over strain.....	74
Figure 4.36 - PE873 capacitance over strain	75
Figure 4.37 - All samples, including Fluorine Rubber Ink broken samples	76
Figure 4.38 - Additive Samples only, including Fluorine Rubber Ink broken samples	77
Figure 4.39 - All samples, broken Fluorine Rubber Ink samples removed	78
Figure 4.40 - Additive Samples, broken Fluorine Rubber Ink samples removed.....	79
Figure 4.41 - PE873 Sensors Change in Resting Capacitance Plot	84
Figure 4.42 - Fluorine Rubber Sensors change in resting capacitance plot.....	84
Figure 4.43 - Parker Sensors change in resting capacitance plot.....	85
Figure 4.44 - PE873 Actuator sensors change in resting capacitance	85
Figure 4.45 - Fluorine Rubber ink actuator changes in resting capacitance.....	86
Figure 4.46 - Parker Sensor frequency sweep post stretch test.....	89
Figure 4.47 - PE873 Sensor frequency sweep post stretch test	90
Figure 4.48 - Fluorine Rubber Ink Sensor frequency sweep post stretch test	90
Figure 4.49 – Grease actuator frequency sweep post stretch test	91
Figure 4.50 - PE873 actuator frequency sweep post stretch test	91
Figure 4.51 - Fluorine Rubber Ink actuator frequency sweep post stretch test	92
Figure 5.1 - Fluorine Rubber Ink Sample 2 during stretch testing	99
Figure 5.2 - DuPont resistance over strain plot(Dupont, 2014).....	100
Figure 5.3 - Example of Cellink printer.....	102
Figure 5.4 - Example of Cellink printer accuracy.....	102
Figure 5.5 - Example of Cellink printer accuracy.....	103

GLOSSARY

DEFINITIONS

1. *Electroactive Polymer (EAP)*: polymers that exhibit alterations in physical size or shape while experiencing the stimulation of an electric field(Newell & García-Bravo, n.d.).
2. *Additive manufacturing*: A form of manufacturing where material is added, most commonly in layers to create a product. The opposite of subtractive manufacturing. Commonly associated with 3D printing.
3. *Young Modulus*: A measure of the ability of a material to withstand changes in length when under lengthwise tension or compression(Gonzalez, 2018).
4. *Thermoplastic Polyurethane (TPU)*: any class of polyurethane plastics that possesses properties such as elastic behavior under traction and contractile forces(Gonzalez, García Bravo, & Newell, 2019)(Gonzalez, 2018).
5. *Electronic Thermoplastic Polyurethane (ETPU)*: Thermoplastic Polyurethane combined with carbon black conductive particles to create a conductive TPU product.

ABSTRACT

Author: Mamer, Trevor, J. MS

Institution: Purdue University

Degree Received: May 2019

Title: Additive Manufacturing Methods for Electroactive Polymer Products

Committee Chair: Brittany Newell

Electroactive polymers are a class of materials capable of reallocating their shape in response to an electric field while also having the ability to harvest electrical energy when the materials are mechanically deformed. Electroactive polymers can therefore be used as sensors, actuators, and energy harvesters. The parameters for manufacturing flexible electroactive polymers are complex and rate limiting due to number of steps, their necessity, and time intensity of each step. Successful additive manufacturing processes for electroactive polymers will allow for scalability and flexibility beyond current limitations, advancing the field, opening additional manufacturing possibilities, and increasing output. The goal for this research was to use additive manufacturing techniques to print conductive and dielectric substrates for building flexible circuits and sensors. Printing flexible conductive layers and substrates together allows for added creativity in design and application.

CHAPTER 1. INTRODUCTION

Electroactive polymer (EAP) technologies have seen significant development since the 1990s, yet despite advances in the electroactive polymer field, manufacturing of EAPs products remains complex and underdeveloped. Additive manufacturing has likewise seen significant advances in development in recent years, making the additive manufacturing machines themselves not only more cost effective but also more capable. Improved capability of additive manufacturing stems from not only the ability to print more complex shapes but also the ability to print with more types of materials. Combining higher cost effectiveness with increased printer capability can reduce the complexity in the manufacturing process of electroactive polymers products.

Manufacturing of EAP products is complex, with all steps being necessary for a successful product. Automated manufacturing of EAP products is even more so. Evidence of corporate manufacturing processes that are open for public viewing demonstrate long assembly lines with the need for hand fitting, roll to roll processes, and complex electrode material applicators. EAPs are most commonly constructed of two material types in three layers. The dielectric layer is commonly a 3M style VHB(3M, n.d.), silicone, or similar material. The electrode layer is subsequently applied to the dielectric layer. The similarity between hand application and methods such as sputtering are that they either require human intervention or complex and expensive machinery. The use of hand work or complex machinery limits not only what design can be created but also the flexibility and scalability of production. Hand fabrication techniques always creates some sort of variability, not to mention that hand work is often slow. Complex and expensive machinery such as press cutters, dies, and sputtering machines are effective in manufacturing EAP products but are lacking in the ability to adapt to new designs and materials.

Research into the field often states that further work or infrastructure improvements are required for complete implementation. While there exists documentation on EAP manufacturing at a corporate level(Hannifin Parker, n.d.), the documentation is limited in its quantity and in its exact detailing of the process and materials. Often, research papers note that in order for EAP materials to evolve out of the developmental state, further work and development needs to occur at many levels of the EAP infrastructure, especially including development of manufacturing processes(Dynamics & Forum, 2001). The problems addressed by this study are the limited

automated and semi-automated manufacturing methods for the creation of electroactive polymers sensors and actuators. Within the scope, electroactive polymer materials that can be produced with automated methods must be developed and tested.

1.1 Purpose

From literature review, numerous research articles and patents are available, but the quantity of manufacturing methods for EAPs are significantly limited. (Benslimane, Kiil, & Tryson, 2010; Hannifin Parker, n.d.). Likewise, manufacturing methods for EAP products also lags behind what the industrial market needs for consumer production. A website facilitated by Dr. Yoseph Bar-Cohen, a prominent figure in the field of EAP research, documents companies providing EAP materials and products (Bar-Cohen, n.d.). The webpage titled “EAP material and product manufacturers” lists only fifteen companies of which only three sell fully realized products and not just materials or samples(Bar-Cohen, n.d.). A research grant written by Dr. Brittany Newell describes the potential for additive manufacturing as a viable process for the creation of EAP products(Newell & Garcia Bravo, n.d.). The decision to use additive manufacturing exclusively stems from the opportunity created by the advancements in additive manufacturing hardware, software, and materials intersecting with the need for additional manufacturing methods in the EAP field. The purpose is to address the short comings of current manufacturing limitations of EAP by utilizing additive manufacturing to create an EAP sensor and actuator. The fundamental layers of an EAP, the inner dielectric layer and outer electrode layers, will be manufactured using exclusively additive techniques, culminating in the creation of an entirely additive manufactured sensor and actuator.

1.2 Research Questions

The questions/hypotheses to be answered were as follows: Can an operational sensor and actuator, of comparable performance to traditionally created reference examples, be manufactured using exclusively additive manufacturing? What material types are suitable for additive production of EAPs? What is the specialized process behind the additive manufacturing of EAPs? The answers to these questions are critical to validating the additive manufacturing process as viable for EAPs.

1.3 Deliverables

The deliverables of were project will be documenting and profiling of the additive process for both types of material, as well as profiling of the characteristics and feedback from the dielectric sensors and actuators. For the two inks, five samples of both the actuator design and the sensor design will be created for comparison against an equal number of reference designs from traditional manufacturing processes.

1.4 Significance

The field of manufacturing EAPs is significant for many reasons, though a specific reason is that future technologies operational in the here-and-now are limited in reach because of the manufacturing limitations. Technologies such as artificial muscles, gearless actuators, flexible sensors, and wearables technologies all directly involve or benefit from EAP technology. Yet, due to manufacturing complexities and cost the aforementioned technologies cannot permeate the consumer market in mass and even EAPs that manifest in reality are limited in functionality. The field of manufacturing electroactive polymers is additionally significant because the technology is capable of filtering into applications such as robotics, prosthetics, muscle-like actuators, flexible sensors and the like (Rossiter, Walters, & Stoimenov, 2009). Finding and documenting the materials that are capable of being used in additive manufacturing processes would allow for an entirely additively manufactured electroactive polymer actuator, sensor, or other device. Additive manufacturing brings to the table creative solutions, simplified processes, and flexibility of materials and design that is lacking in the current field. Opening the possibilities for types of manufacturing for EAPs will accelerate not only the development of EAP technology but also its implementation in mainstream products.

1.5 Assumptions

1. The first and foremost assumption is that as an additive manufacturing process, all results from the process will be constructed using an automated process.
2. Laboratory equipment can produce and test electroactive polymers.
3. Dielectric material will extrude uniformly.
4. Conductive material will extrude uniformly.

1.6 Delimitations

Sensor and actuator designs will be limited to a single variation each. While electroactive polymers can be made into a variety of shapes and designs, only a single variation of sensor and actuator will be created for consistency in testing. Both the sensor and actuator fall into the dielectric EAP category under the electronic EAP umbrella. The single dielectric material and two conductive inks will be the only materials used in the additive manufacturing process, other material and ink types will not be explored. Additionally, low voltage circuitry design and testing will not be explored.

1.7 Limitations

The additive manufacturing machinery being used consist of an extruder type filament printer for the dielectric material, an automated circuit writer for the conductive material, and an air pressure assisted syringe printer for the conductive material. A constantly growing field of different types of printers and additive manufacturing machinery exist; however, the available machinery is of the aforementioned type. The type of printer being used inherently limits the types of material that can be used because of the compatibility necessary between the material and the printer. Utilizing additive manufacturing inherently limits the possibility of material types that can be used for both the dielectric layer as well as the electrode layer. The printers possess limits as well to resolution both in the control of material deposition and control of the extruder head. The minimum layer thickness with a 0.4mm nozzle is between 0.050mm to 0.5mm(“LulzBot TAZ 6,” n.d.) using the Lulzbot Taz 6. The circuit printer has been tested to a trace width accuracy of 0.2032mm with low viscosity inks and 0.3048mm-0.508mm with high viscosity inks(Zigon, 2017).

CHAPTER 2. REVIEW of LITERATURE

2.1 Introduction

The introduction into the review of literature began with the grant proposal drafted by Dr. Newell and Dr. García-Bravo for research into additive manufacturing of EAP sensors and actuators. Preliminary testing of materials and additive manufacturing machinery further assisted in narrowing down the scope of the literature review to the specific material types and machinery that would be used. Additive manufacturing machines come in many styles and types, such as Stereolithography (SLA), Fused Filament Modeling (FFM), Digital Light Processing (DLP), and an ever-increasing array different processes to deposit and cure materials of all types. Each type of printer comes with its own material limitations and design constraints. As such, focusing on a specific type of printer assists in determining what material types can be used. With EAP products, electrode layers are commonly created with a conductive grease, meaning extrusion or ink jet style printing would be the most applicable (Pabst et al., 2011). Following the preliminary search and tests, a focused literature review was undertaken.

2.2 Methodology of the Review

Figure 1 and Figure 2 work together to depict how the concepts of this research interact and overlap. Figure 1 depicts the purpose of this research in its center, that being the additive manufacture of an EAP sensor & actuator. The important aspect of Figure 2 was the depiction of how the hierarchy of the concepts works and how deciding what aspect to focus on at one level influences the options for focus on the next. Specifically, the choice of an additive manufacturing process defines the types of potential materials to be used in the creation of the sensors and actuators.

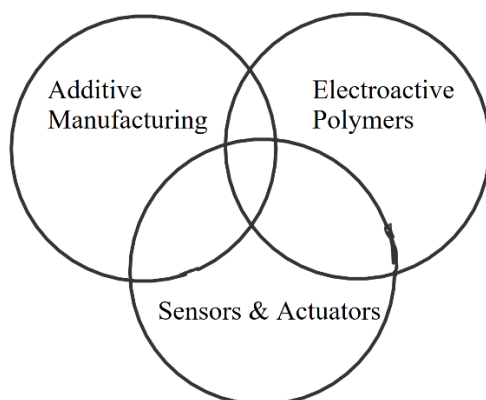


Figure 2.1 - Concept Map Venn Diagram for Search

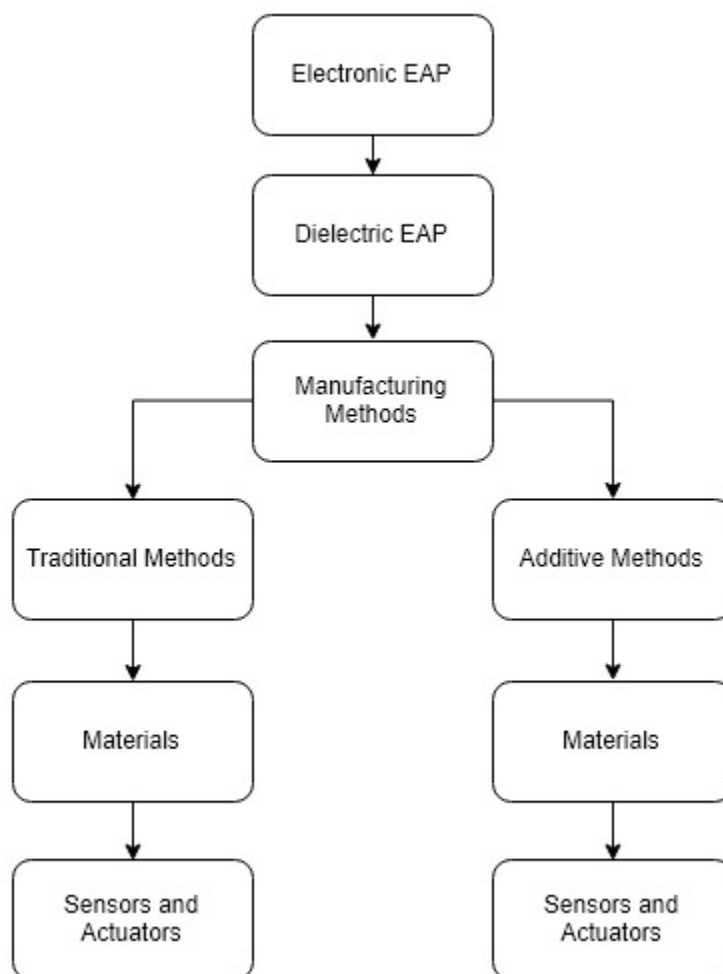


Figure 2.2 - Concept Map for Concept Hierarchy

2.3 Electroactive Polymers

Electroactive polymers are a class of material with the capability to alter size and shape in response to an electrical field while also being capable of functioning as an electrical energy harvester when mechanically deformed. EAPs are commonly separated into two categories, electronic EAP and Ionic EAP(Bar-Cohen, 2018). Electronic EAPs consist of polymers that alter shape or size due to electron movement during a response from an electric field. Ionic EAPs exhibit the same physical change characteristics as the Electronic EAP however due to the movement of ions in response to an electrical field. A further distinction is that Electronic EAPs are usually dry and Ionic EAPs are usually wet and contain electrolytes. Electronic EAPs are the focus of the research done here. The origins of EAPs can be traced back to the 1880s with Wilhelm Rontgen's experiments with dielectric elastomer actuators(Keplinger, Kaltenbrunner, Arnold, & Bauer, 2010). However, the late 1990's is often credited as the modern start of development into EAPs. The late 1990's and early 2000's was an especially prolific time in the development of EAPs due to the focus on new material types for EAP use and the a focus on pre-strain for enhanced actuation(Burchfiel et al., 2000). Since the late 90's and early 2000's research and production of EAPs has centered around the use cases of sensors and actuators. EAP actuators have been highly prevalent due to potential outcomes as artificial muscles. Electronic EAPs are especially suited to the role of artificial muscles; research samples showing the capability to arm wrestle humans and lift 10 gallons of water(Bar-Cohen, 2005).

The pertinent electrical concepts of the electronic EAPs are the capacitance equation (Equation 1)(Wang et al., 2015) and the effective pressure being applied to provoke actuation(Equation 6)(R. E. Pelrine, Kornbluh, & Joseph, 1998). For Equation 1, C is equal to capacitance, ϵ is the permittivity of free space, ϵ_{TPU} is the permittivity of the dielectric material (in the research here that is the TPU material), A is the surface area of the electrode pad, and z is the distance between the electrode layers.

$$C = \epsilon * \epsilon_{TPU} * \frac{A}{z} \quad (\text{Equation 1})$$

In order to relate the applied electrical field to a mechanical deformation, the following relationships can be used. The electrostatic energy U of an elastomer dielectric layer with opposing charges Q and -Q on the front and back of the layer is seen in Equation 2.

$$U = \frac{0.5*Q^2}{C} = \frac{0.5*Q^2*z}{\epsilon*\epsilon_{TPU}*A} \quad (\text{Equation 2})$$

Changing the stored electrostatic energy dU for a change dz in thickness and dA in area can be seen in Equation 3.

$$dU = \left(\frac{0.5*Q^2}{\epsilon*\epsilon_{TPU}*A} \right) * dz - \left(\frac{0.5*Q^2*z}{\epsilon*\epsilon_{TPU}*A} \right) * \frac{dA}{A} \quad (\text{Equation 3})$$

Equation 3 can be rewritten into Equation 4 through application of the constraint that $A*z$ equals a constant ($dA/A = -dz/z$).

$$dU = \left(\frac{Q^2}{\epsilon*\epsilon_{TPU}*A} \right) * dz \quad (\text{Equation 4})$$

The equation for effective mechanical pressure which is applied to the top surface of the electrodes can now be adapted from Equation 4 and is depicted in Equation 5.

$$p = \left(\frac{1}{A} \right) * \frac{dU}{dz} = \left(\frac{Q^2}{\epsilon*\epsilon_{TPU}*A^2} \right) \quad (\text{Equation 5})$$

Lastly, keeping in mind that the electric field E is equivalent to $E = \frac{Q}{\epsilon*\epsilon_{TPU}*A}$, effective pressure can be expressed as Equation 6.

$$p = \epsilon * \epsilon_{TPU} * E^2 \quad (\text{Equation 6})$$

The incompressible nature of materials such as the elastomers used in EAP actuators means that, because volume has to be conserved, the elastomer will expand in the planar direction to account for the decrease in thickness (Gonzalez, 2018) (R. E. Pelrine et al., 1998). In order for the expansion to occur in the first place, effective pressure needs to overcome the Young's Modulus of the material. The TPU being used in this research has been shown to have a dielectric constant of 6.32 ± 0.30 and a Young's modulus range of 3.04 MPa to 6.21 MPa (Gonzalez et al., 2019). A visual of the principle in action can be seen in Figure 2.3.

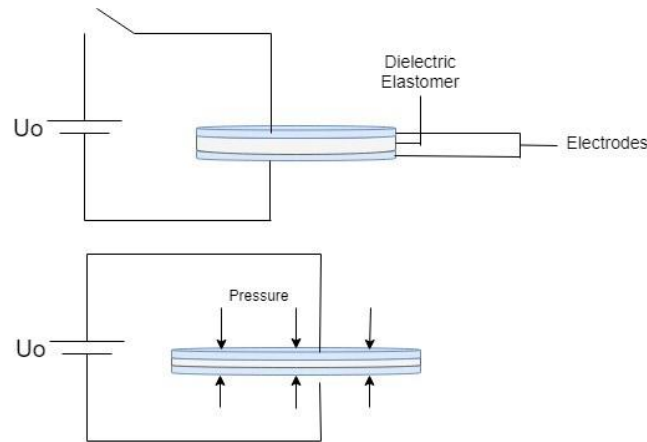


Figure 2.3 - Visual of the electronic EAP working principle (Gonzalez et al., 2019)

2.3.1 EAP Manufacturing

The manufacturing of EAPs is a challenge that has limited the proliferation of the technology into the mass consumer market and hampered the rate of further development in the field. Current practice of EAP manufacturing is to either manufacture by hand (a common method used in academic research), use highly complex and expensive production line (a common method for companies producing EAP products such as Parker-Hannifin(Hannifin Parker, n.d.)) or a combination of the two. EAPs are inherently difficult to produce at scale because of the difficulty in handling and manufacturing the two fundamental layers of an EAP: an elastic dielectric material and an elastic conductive material. Further complicating the production process is the necessity of straining the dielectric layer to enhance actuation(R. Pelrine et al., 2003). The difficulty in handling and production leads to the usage of roll to roll processes, presses for die cutting, and sputtering for electrode application. The aforementioned processes, while effective at producing operational EAP sensors and actuators, limits the rate of overall production; not to mention the frequency of design and material changes. Further, processes such as sputtering for the electrode and roll to roll processes to maintain pre-strain are complex and costly, limiting the opportunities for the usage in academic research and development.

2.4 Additive Manufacturing

Commonly referred to as 3D printing, additive manufacturing shares a similar timeframe of the 1980's and early 2000s for early modern development(Kodama, 1981). Additive manufacturing is the process of adding material layer upon layer (rather than cutting away or removing material) until a finished design is completed. The additive manufacturing processes utilized by 3D printers are capable of complex designs not possible with traditional subtractive manufacturing methods, such as automotive wheels with interlocking and hollow spokes("HRE Performance Wheels," 2018).

2.4.1 Printer Types & Materials

When discussing additive manufacturing and specifically 3D printing, it is important to note the types of 3D printing and the accompanying material compatibility. If 3D printing is going to be utilized in a manufacturing process, an initial decision needs to be made of whether a specific type of printer or a specific type of material will be used. Material type will limit printer type and vice versa. Knowing which takes precedent is a crucial first step. For example, if a digital light modeling (DLP) printer is going to be utilized in a manufacturing process then materials normally reserved for fused filament modeling (FFM) or electron beam melting (EBM) will not be compatible. Likewise, if titanium is the choice of material then printer types such as DLP and FFM may be incompatible.

2.5 Preliminary Samples

Preliminary samples and testing were undertaken in order to become acquainted with the materials and machinery that will be used. Figure 2.4 and Figure 2.5 depict cured designs that were used in the testing of PE873 ink as both an actuator and sensor(Conductor, n.d.). After the testing of the samples depicted in Figure 2.4, the sample in Figure 2.5 was manufactured to test multiple samples and simultaneously a preliminary complete additive process. Figure 2.5 was created to preliminarily test the exclusive additive process for sensors as well as preliminarily test for consistency between identical print designs.

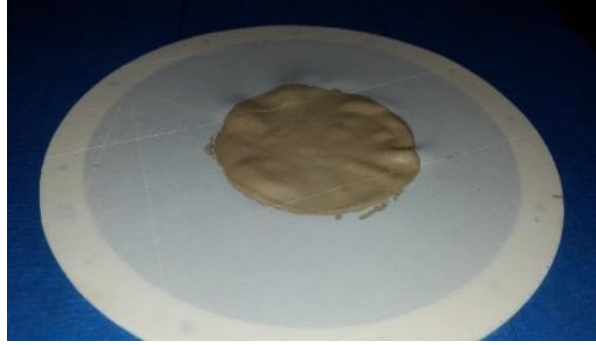


Figure 2.4 - Actuator Prototype with PE873 Ink

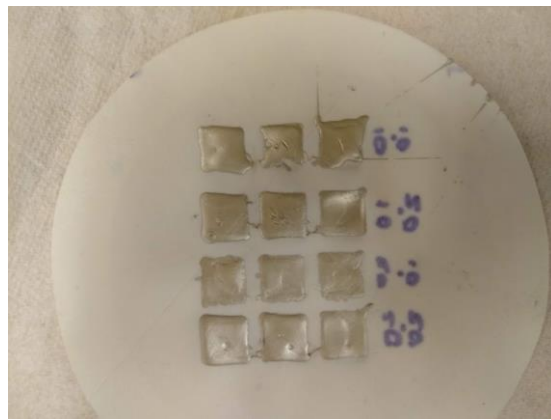


Figure 2.5 - PE873 Repeatability Test

2.6 Preliminary Testing

The large pads were tested for capacitance and substrate compatibility. The samples were strained using an iris stretcher, which uniformly stretches materials through attachment at twelve distinct points in the material (Romo-Estrada, Newell, & García-Bravo, 2018). The capacitance of the material was measured as the material was strained at ten distinct levels. The iris stretcher utilizes a micro-stepper driving system (Romo-Estrada et al., 2018). Each distinct iteration resulted in one thousand steps of the iris stretcher's stepper motor and about 5 mm of expansion in the dielectric substrate diameter. Capacitance and pad diameter were recorded at each iteration. Image analysis was performed to calculate the pad and dielectric substrate diameters. Iteration 1 was taken with the material on the stretcher and at a point where the stretcher moves from loading to its resting. Iteration 2 – 10 were an additional 1000 steps per iteration. The final iteration, iteration 11, was taken when the substrate relaxed back to resting, relaxing the

dielectric substrate and the electrode pad. The final iteration allowed for the recording of the change in capacitance at rest caused by the previous iterations. Capacitance was recorded with a Protek LCR Meter Z8200 at 1 kHz.

The testing for the multiple pad samples seen in Figure 2.5 involved measuring the resting capacitance of the capacitors using the same Protek LCR Meter Z8200 at 1 kHz as the previous testing. The results for the multiple sample testing can be seen in Table 2.1.

2.7 Preliminary Results

Preliminary results for the manufacturing process showed promising trends for the use of the designed additive manufacturing process. The sensors in particular indicated favorable returns that are consistent in response. Figure 2.6 and Figure 2.7 depicted the relative consistency and linear response of the sensors' capacitance level to the amount of strain being placed on them.

Table 2.1 - Consistency Test with PE873

Trial Version	Speed	Overlap	Capacitance (pF)
1	10	10	22.7
1	10	10	16.1
1	10	10	20.5
2	10	20	26.7
2	10	20	5.1
2	10	20	24.5
3	20	10	21.5
3	20	10	22.6
3	20	10	22.2
4	20	20	23.3
4	20	20	25.7
4	20	20	24.9
Grand Mean			21.3

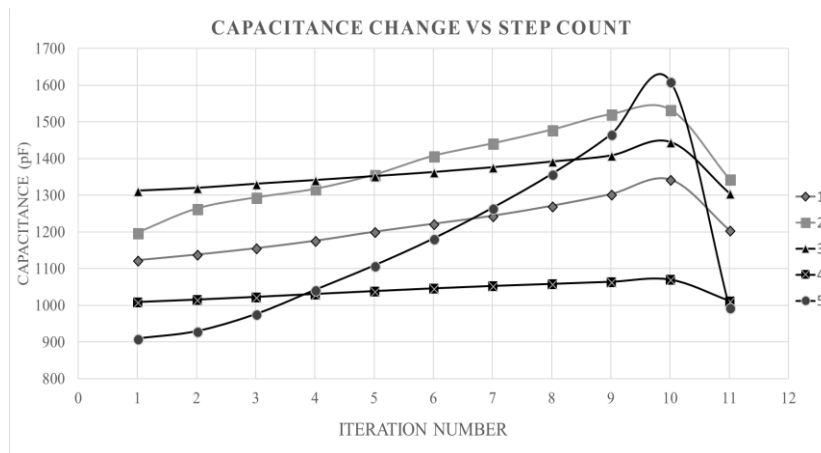


Figure 2.6 – Capacitance Change per Step Count

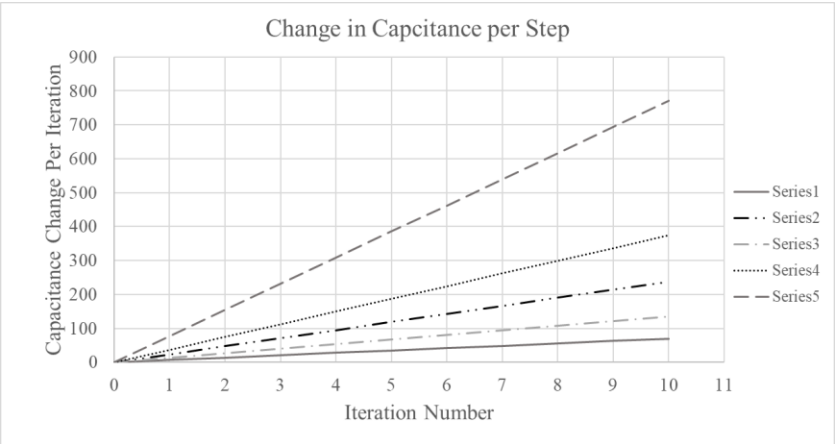


Figure 2.7 – Change in Capacitance per Step

The combination of preliminary testing between the single pad and multiple pad samples demonstrated the capability of the additive manufacturing process used initially in this research to create not only operating sensors, but to also create repeatable samples of consistent, if not quite identical, attributes.

CHAPTER 3. RESEARCH METHODOLOGY

3.1 Introduction

The final deliverable for this project was profiling of the manufacturing process, from material types and printer settings to the resulting products from the process. Profiling a manufacturing process makes this research developmental in style. The manufacturing process was iterated on and developed, with the sensor and actuator deliverables validating the effectiveness of the development and manufacturing processes. Population number and designs were carefully selected to provide a meaningful base for analysis as well as mirror real world designs in order to have meaningful comparisons. Figure 3.1 depicts the logic flow from start to finish for the experimental procedure.

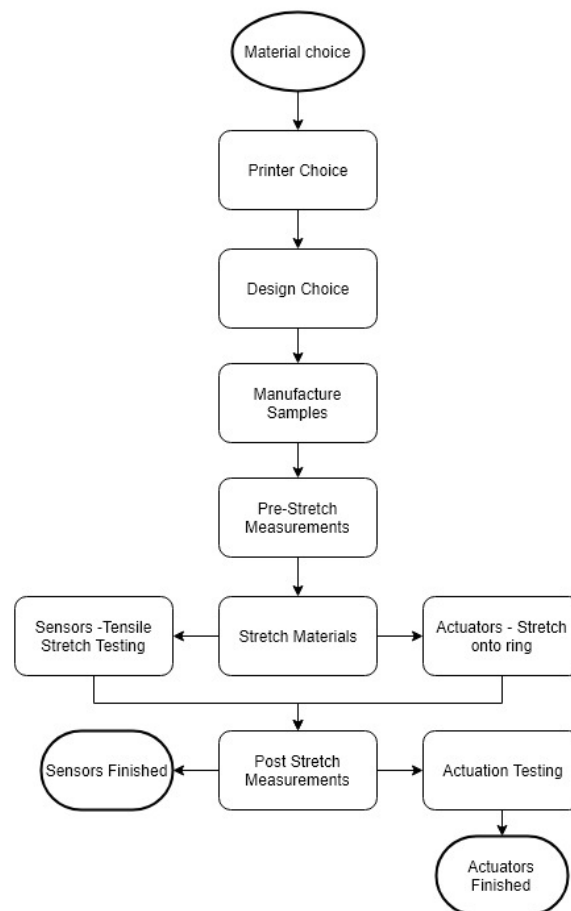


Figure 3.1 - Methodology Flow Chart

3.2 Material and Printer Choice

Material choice marks the beginning of the methodology flow chart because of the necessity to determine which material types met both requirements of being EAP capable and additive manufacturing compatible. Material types for both the dielectric material and the conductive material had been successfully used in additive manufacturing processes, though separately from each other. The accomplishments and characterization of FFM capable TPU and syringe deposition capable conductive inks informed the decision to pursue both the TPU and conductive inks as well as the FFM and syringe deposition printers.

The dielectric material used both in the preliminary and final manufacturing was the Diabase X60 Ultra Flexible filament. The Diabase TPU material possesses a Shore A hardness of 60 and has been proven to function as a dielectric in EAP applications in research applications (Gonzalez et al., 2019; Mamer, Newell, & García Bravo, 2018). While the TPU used has been proven capable both in a 3D printing context and an EAP context; the conductive inks used here have only been proven in an additive process. The conductive inks were narrowed down to two options: DuPont's PE873 and a fluorine rubber-based ink. The fluorine rubber ink was produced in academia by a collaborator and had a fluorine rubber base combined with surfactant and silver flakes making it conductive (Matsuhisa et al., 2015). The aforementioned collaborator was also the supplier for the fluorine rubber ink. The original usage case for both inks were intended to be in electronic textiles. The flexibility and elasticity of the PE873 and the Fluorine Rubber ink because of original use cases made for ideal candidates in an electronic EAP application. DuPont points to TPU by name as an appropriate substrate for application (Conductor, n.d.).

Materials tend to be either conductive but not stretchable or stretchable but not conductive. Further limiting the potential options for the electrode material used here was that the material not only had to combine stretch capability and conductivity but also be additive manufacturing compatible. Both the DuPont ink and the Fluorine Rubber ink are conductive while being stretchable and just so happen to be additive manufacturing capable when using the correct style printer. The Fluorine Rubber ink has been tested to maintain conductivity (182 S/cm^{-1}) at 215% strain (Matsuhisa et al., 2015), making for an ideal material in the EAP context. Additionally DuPont also documents testing and results of strain on the PE series of materials and details the benefits of strain relief design, while also noting a sheet resistivity of $<75 \text{ m}\Omega\text{sq}/25\mu\text{m}$ (Dupont,

2014). A final addition to the list of electrode layer materials is an Electric TPU (ETPU) filament capable of additive manufacturing through FFM printers. The ETPU filament is similar to the standard TPU filament used for the dielectric material however the ETPU gains the conductivity from carbon black. The TPU base of the ETPU provides for the ability to stretch while the carbon black provides the conductivity. While not as flexible as the conductive inks, the ETPU advertises a shore hardness A of 95. The ETPU was a candidate worth pursuing.

Manufacturing results will center exclusively on the additive only samples and not the reference samples. Final manufacturing was split amongst four printers: the student developed circuit writer, the Cellink+ BioPrinter, the Lulzbot Taz 6, and the MakerBot Replicator 2X. The Lulzbot and the Makerbot manufactured the dielectric only layer (referred to here as dielectric blanks). The Lulzbot printed the actuator dielectric blanks while the Makerbot manufactured the sensor dielectric blanks and ETPU samples. Additionally, the Lulzbot also functioned as the hot plate for the annealing of the conductive ink.

3.3 Design Choice

The design of both the actuator and sensor samples was meant to resemble the reference samples. The Parker-Hannifin EAP evaluation kit sensors were used as the reference comparison for the sensor samples. In order to mimic the reference sensor design, the additively produced sensor design incorporated a three-layer rectangular design. The additively produced sensor samples were meant to mimic the Parker-Hannifin samples, matching the electrode surface area in order to create a base for consistency in testing. The actuator reference sample consists of hand applied conductive grease applied to the same additively produced TPU used in the additive exclusive samples. The hand applied conductive grease in a circular shape on TPU mirrors the manufacturing approach commonly used in research. While using a hand application does introduce enhanced variability in physical size and material deposition, it is still the most common form of EAP manufacturing in academic research. The circular shape was chosen because of the prevalence of the design in research and because the strain application device used here is designed to provide a uniform circular stretch. The circular design is a research proven and robust design that is also capable of being translated to an additive design. Figure 3.5 depicts the CAD model used for construction of the ETPU samples. Additionally, Figure 3.5 also provides a visual representation of the layering of all samples, both sensor and actuator. Both

sensor and actuator designs use the same layering as depicted in Figure 3.5, albeit the actuators using a circular rather than rectangular design as can be seen in Figure 3.6 through Figure 3.9.

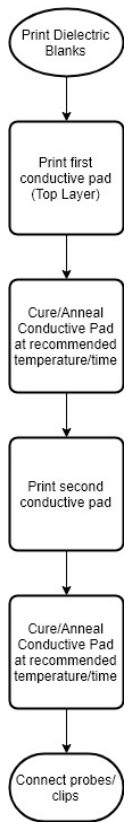


Figure 3.2 - Manufacturing Steps

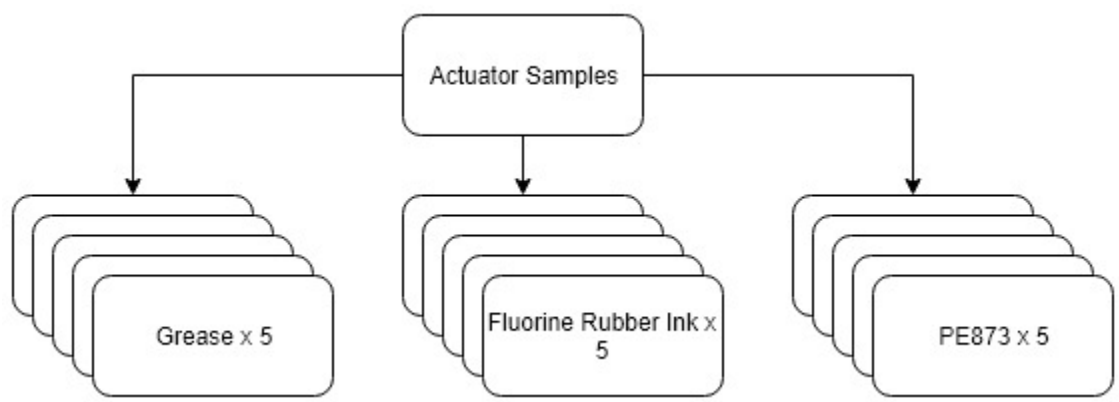


Figure 3.3 - Actuator Samples Visual

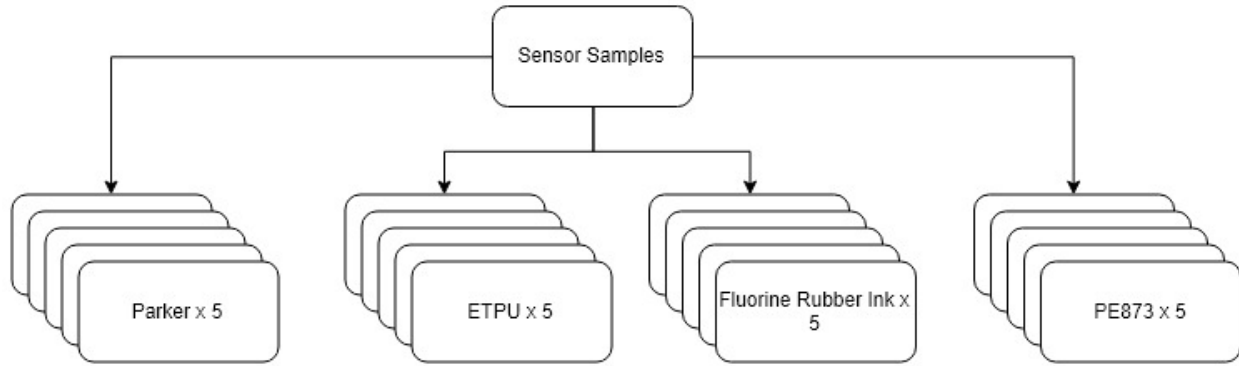


Figure 3.4 - Sensor Samples Visual

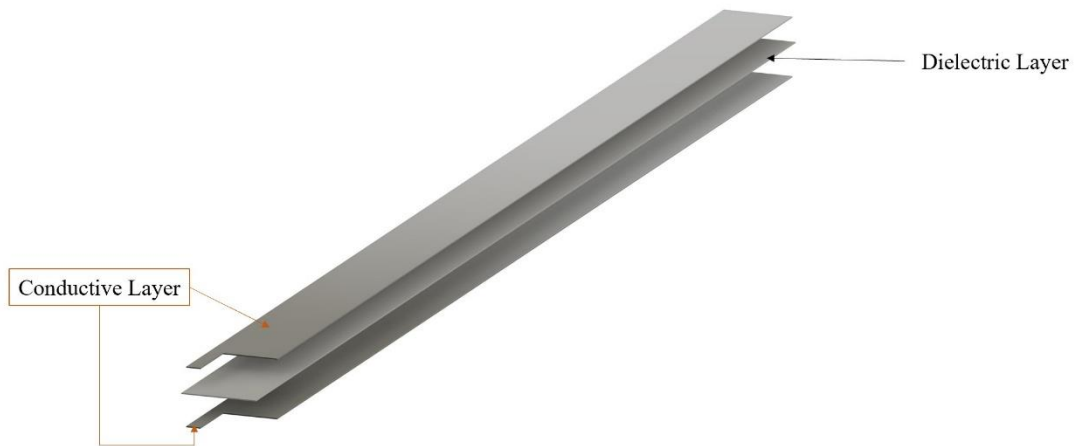


Figure 3.5 - Example of layering in CAD designs



Figure 3.6 – Reference Parker-Hannifin Sensor Sample



Figure 3.7 - Additively Manufactured Sensor Sample

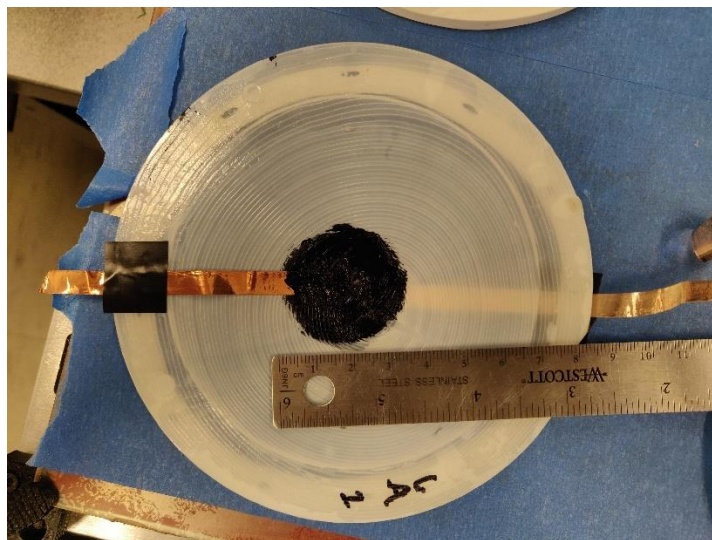


Figure 3.8 - Reference Grease Sample



Figure 3.9 - Conductive ink sample

3.4 Manufacturing

The dielectric material was manufactured using a combination of a Lulzbot Taz6 for the actuators and a Makerbot Replicator 2X for the sensors. The electrode material was applied

using a student developed circuit writer(Zigon, 2017) and a CellInk+ Bio Printer. The Makerbot Replicator 2X also printed the ETPU material. The dual heads of the Makerbot allowed it to print the ETPU and TPU samples in full in one print cycle. The aforementioned machines were selected because they have demonstrated the ability to create operating EAP products in preliminary testing and were compatible with the chosen materials. Further, the Lulzbot also functioned as the annealing hot bed for the conductive materials. The Lulzbot's heated bed was chosen for the annealing process as the bed was both capable of annealing the conductive materials at the correct temperature and fitting in with the original research prompt to create EAP products using solely additive manufacturing methods.

The CAD model for the dielectric layer of sensor samples specifies a 0.60mm thickness. Using a nozzle diameter of 1.75mm and the settings depicted in Figure 3.12 and Figure 3.13, the Makerbot Replicator 2X was capable of printing the ten dielectric sensor sample blanks to a $0.60\text{mm} \pm 0.10\text{mm}$ thickness. The CAD model for the ETPU samples included the same dielectric model used in the printing of the dielectric blanks with the addition of two 0.1mm thick layers of ETPU. The printer settings for both the TPU and ETPU extruders were identical. The Makerbot Replicator 2X was capable of printing the completed ETPU samples to an overall thickness of $0.8\text{mm} \pm 0.15\text{mm}$. The CAD model for the dielectric actuator blanks specifies a thickness of 0.20mm on the edge of which is a collar 0.8mm thick. The additional thickness on the collar is meant to combat premature tearing of the actuator sample while it is being strained prior to actuation as seen in Figure 3.10. The Lulzbot was capable of printing the fifteen required samples to a $0.20\text{mm} \pm 0.02\text{mm}$ thickness.



Figure 3.10 - Dielectric blank being strained on iris stretcher prior to actuation testing

The relationship between the needle size (gauge) and printer settings were crucial to successfully applying a cohesive layer of conductive ink. While the relationship between nozzle diameter and printer settings is critical to all additive manufacturing processes, the relationship is especially pertinent to the conductive ink and circuit writer printer used here. Due to the limitations of the student developed printer (namely the combination of the extrusion screw, syringe, and the lack of viscosity in the ink itself), the decision was made to use an 18 gauge needle, slow the printer down from its default travel speed of 20 mm/s to 10mm/s, set retraction to zero, and set extrusion to the allowable maximum of extrusion every 1mm. At 18 gauge the nozzle was larger in actual practice than in the software. A smaller nozzle, 25 gauge, was chosen in software in order to create an over extrusion. The same can be accomplished by increasing overlap percentage as well. However, in the preliminary samples the combination of under sizing the nozzle in software with the slower speed and no retraction created enhanced cohesion in the first layer because of over deposition of the conductive ink. Application of a cohesive first layer was critical in order to use the minimum amount of conductive material to achieve the desired results. The final electrode layers added $0.2\text{mm} \pm 0.02\text{mm}$ of thickness to the dielectric blanks.

Initial annealing parameters, time and temperature, were informed by the recommended specifications from the respective creators of the ink. The annealing process is crucial for both the PE873 and the Fluorine Rubber ink as it allows for solvent in the ink to evaporate. The removal of the solvent solidifies the material while improving the electrical properties (reduction

in resistance). Dupont suggests the use of 100 C° to 160 C° for two to ten minutes in an oven(Conductor, n.d.). The Fluorine Rubber ink annealing parameters were recommended to be done in two stages, 90C° for an hour and 120C° for an additional hour. Final annealing parameters were selected based on information from the inventor and from experimental testing. An important additional note for Table 3.1 is that the time for annealing includes the temperature ramp up. The temperature noted in Table 3.1 is the temperature to set the bed to, not the temperature to start at. At the end of the time allotted in Table 3.1, the heated bed was deactivated, and the sample being annealed was allowed to cool to room temperature (30 C° ± 3 C° in the test environment here).

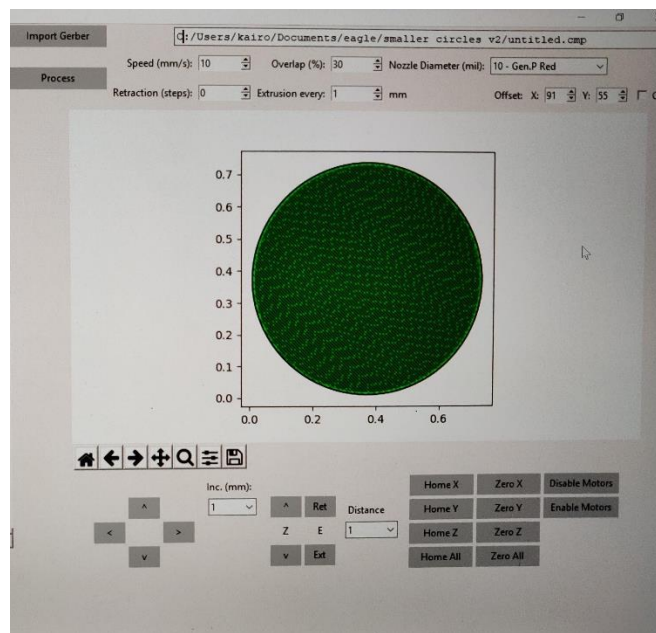


Figure 3.11 - Student developed circuit writer front panel and settings used

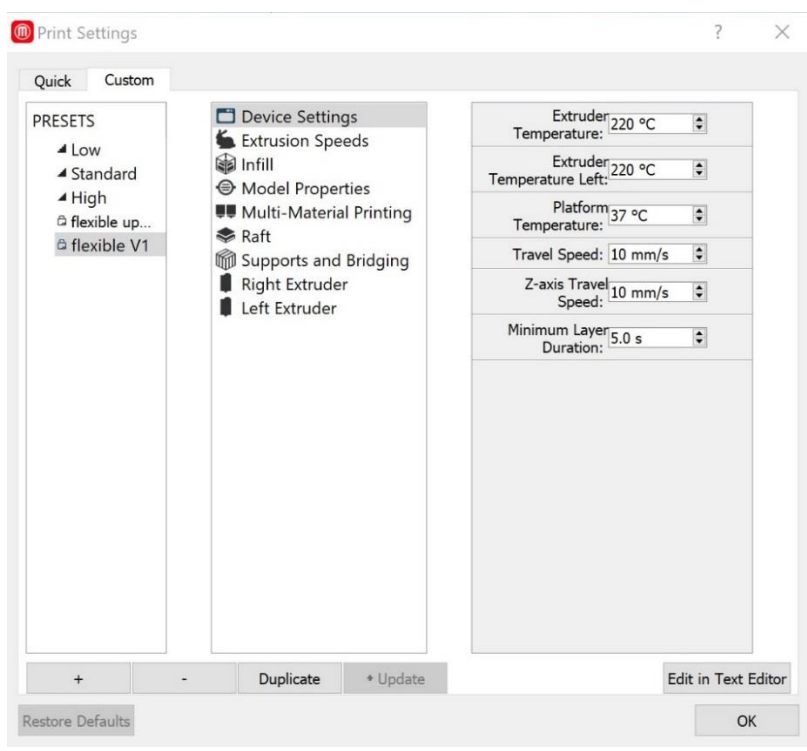


Figure 3.12 - Makerbot settings for dielectric and EPTU printing

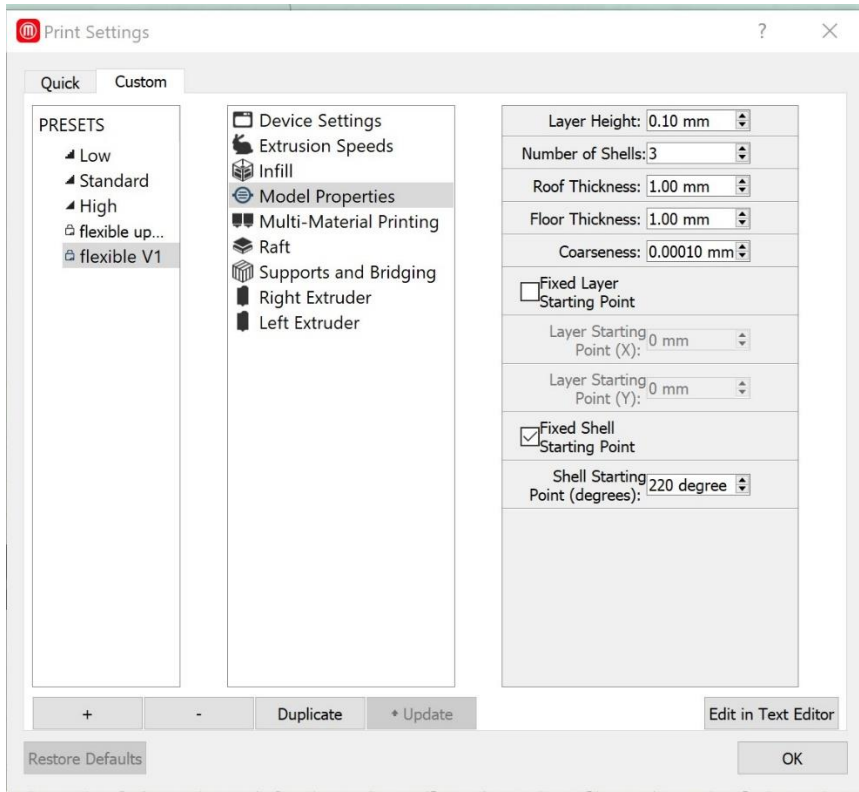


Figure 3.13 - Makerbot settings for dielectric and ETPU printing

Table 3.1 - Annealing settings

Initial and Final Annealing Settings							
		Initial			Final		
		Grease	Fluorine Rubber	PE873	Grease	Fluorine Rubber	PE873
Step 1 (top layer)	Bed Temp (Celsius)	None	90	110	None	110	110
	Time (Minutes)	None	60	15	None	40	15
Step 2 (bottom layer)	Bed Temp (Celsius)	None	120	110	None	110	110
	Time (Minutes)	None	60	15	None	40	15
Step 3 (top layer)	Bed Temp (Celsius)	None	120	None	None	110	None
	Time (Minutes)	None	60	None	None	40	None
Step 4 (bottom layer)	Bed Temp (Celsius)	None	120	None	None	110	None
	Time (Minutes)	None	60	None	None	40	None

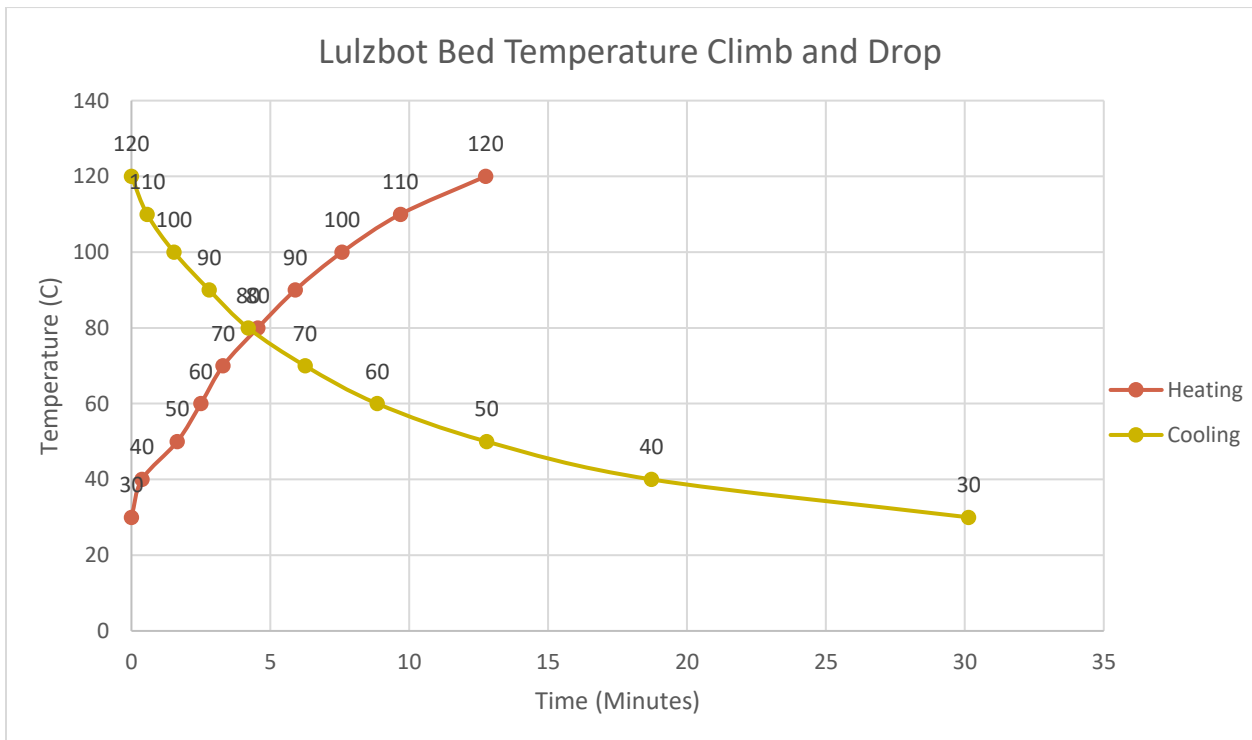


Figure 3.14 - Lulzbot Bed Temperature Climb and Drop Rates for annealing

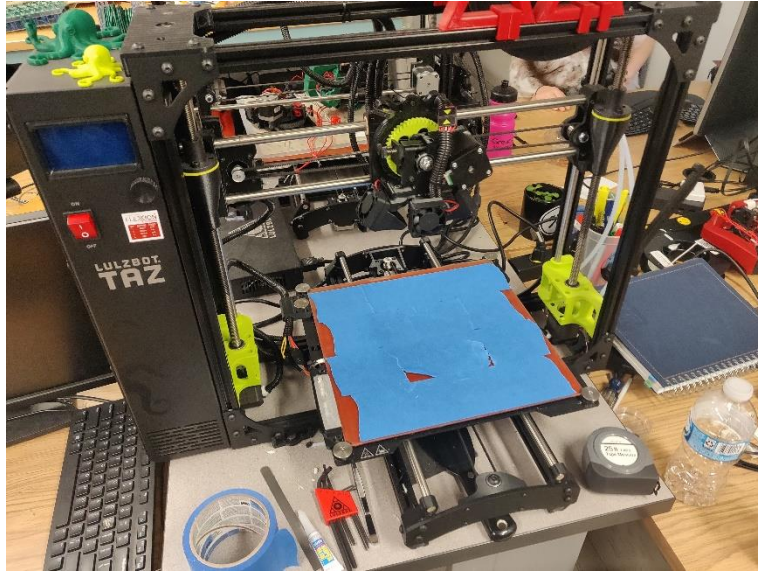


Figure 3.15 - Lulzbot used for dielectric printing and annealing

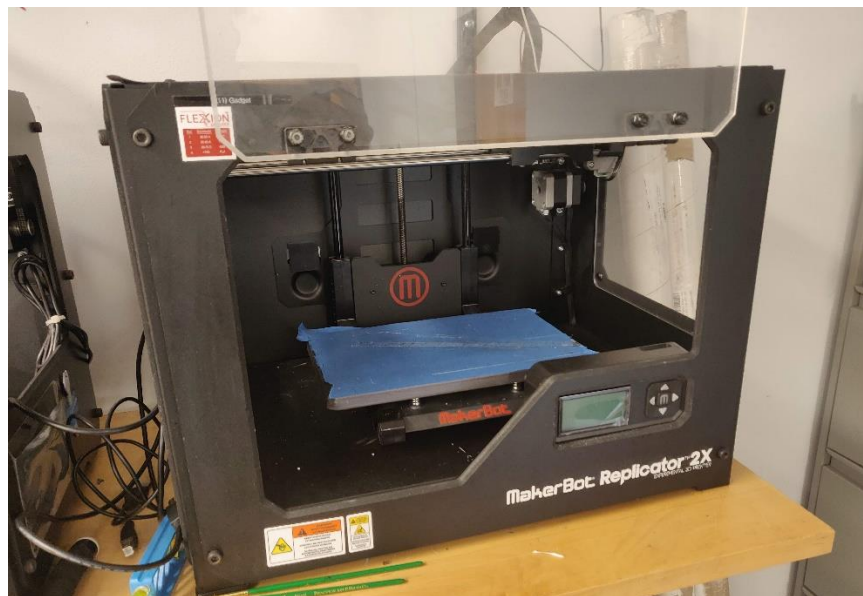


Figure 3.16 - Makerbot used for sensor dielectric printing & ETPU

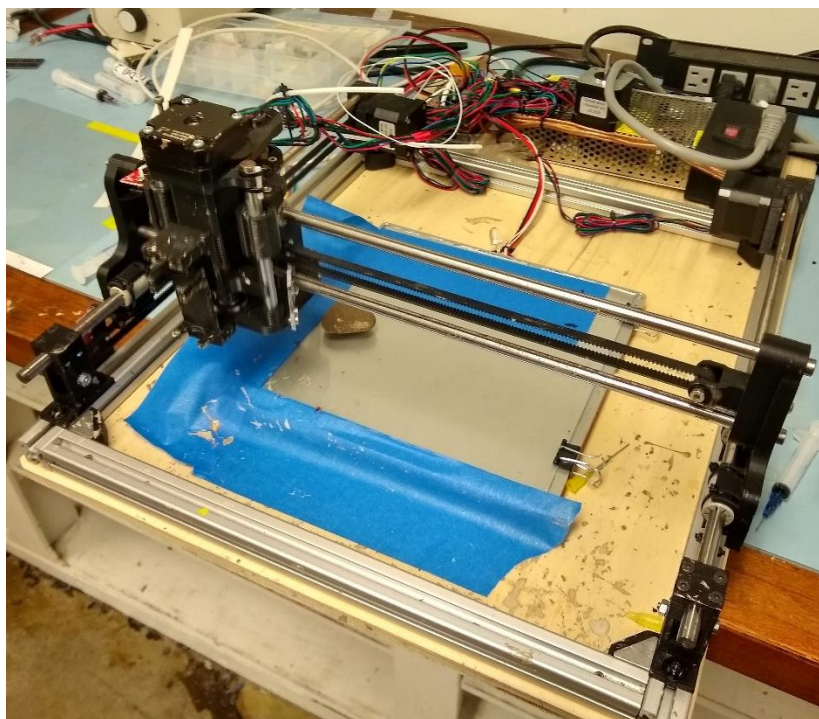


Figure 3.17 – Custom made circuit writer used for electrode application

3.5 Testing

Testing of the produced samples was twofold. Resting capacitance and resistance values were taken pre and post stretch of the samples. Application testing was the second phase and unique to the sensor and actuator samples. The sensor application testing consisted of testing capacitance values while stretching the samples. The actuator application testing consisted of applying high voltage to the samples in order to test actuation potential.

3.5.1 Pre & Post Stretch Measurements

Pre and post stretch measurements for capacitance and resistance were accomplished using a Protek LCR Meter Z8200 at 1 kHz. For both the actuators and sensors the capacitance values were taken from single points; using the casing pick up points on the sensors and copper tape applied to the center of the circle for the actuators. The same points were used for capacitance measurements using a frequency sweep from 100Hz to 10000Hz on a NF ZM2372 LCR Meter. The settings for the NF ZM2372 in the frequency sweep tests can be seen in Figure 3.18, which contains the front panel of the LabVIEW application being used to store the values from the NF ZM2372 remotely. Resistance measurements were taken across four points of the

front and back of each sample. The resistance measurement locations can be seen in Figure 3.19 for the sensors and Figure 3.20 for the actuators. The resting values were taken for analysis of consistency in the output (finished samples) of the manufacturing process.

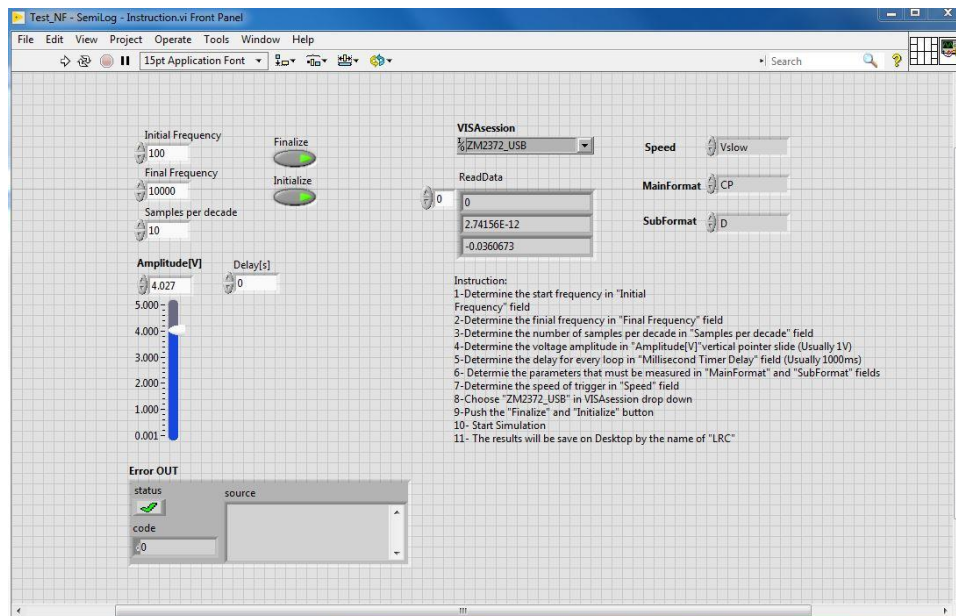


Figure 3.18 - Front panel and settings for frequency sweep software



Figure 3.19 - Locations for resistance measurements for sensor samples



Figure 3.20 - Locations for resistance measurements for actuator samples

3.5.2 Application Testing

Application testing was specific to both the sensors and actuators. The sensor application testing consisted of placing the sensors in an Applied Test Systems Inc tensile strength testing machine and stretching the samples to 50 percent strain as seen in Figure 3.21. Each sensor sample across the three subsets was adjusted to have an active stretching conductive length of 33.5mm, thus making 16.75mm a 50 percent strain. Displacement in the tensile strength tester was a constant 1.524mm per minute. Capacitance was recorded for the duration of the stretch in order to create capacitance over strain percentage plots. Data acquisition for sensor application testing consisted of the same hardware as the frequency sweep setup in conjunction with modified software. A LabVIEW application based on the LabVIEW application used for the frequency sweep was used, modified to track capacitance over time rather than capacitance over frequency as depicted in Figure 3.22. Settings for voltage, Delay, and speed were kept the same, the only difference being a stagnant frequency signal of 1kHz.



Figure 3.21 - Stretch Test Setup

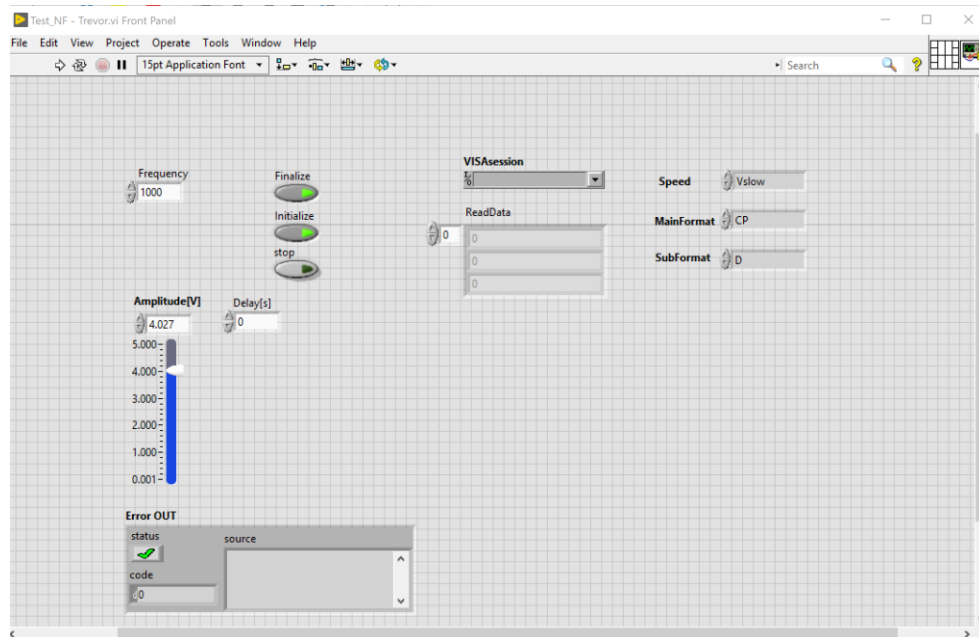


Figure 3.22 - Front panel and settings for capacitance over time sensor application testing

Actuation application testing consisted of placing the actuator samples under high voltages. Prior to the high voltage testing itself was the requirement to add strain to samples. Straining the sample is shown to enhance actuation (Burchfiel et al., 2000). Acrylic rings (Figure 3.24) were created to hold the actuators in a state of 60% strain for high voltage actuation testing. The actuator samples were held to the acrylic ring with Duro Super Glue. The applied voltage



Figure 3.24 - Acrylic ring for holding strain on actuator samples

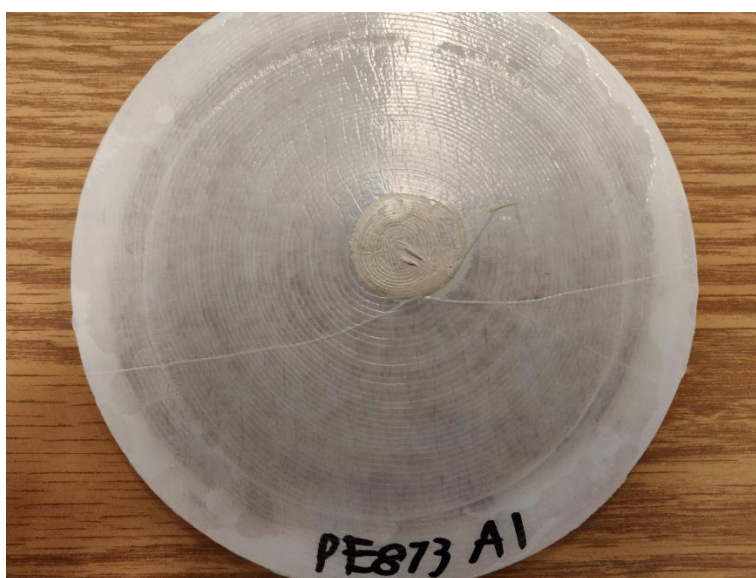


Figure 3.25 - Example of a strained actuator sample

CHAPTER 4. RESULTS

4.1 Manufacturing

Manufacturing followed the steps outlined in Figure 3.2. Minor changes and adjustments were made to the annealing process as required. The changes to the annealing process are detailed later in this section.

Per the manufacturing steps in Figure 3.2, the dielectric layer prints were finished first. The actuators and sensors were manufactured on the Lulzbot and Makerbot respectively, allowing the samples to be printed simultaneously. The sensor samples were printed multiples at a time, which is why the samples have two connected lines. The connected lines were not part of the CAD design, but instead were an unintended result of the printing process. The final output for the sensor dielectric blanks can be seen in Figure 4.1. The dielectric blanks were printed one at a time, an example of the final output of which can be seen in Figure 4.2.

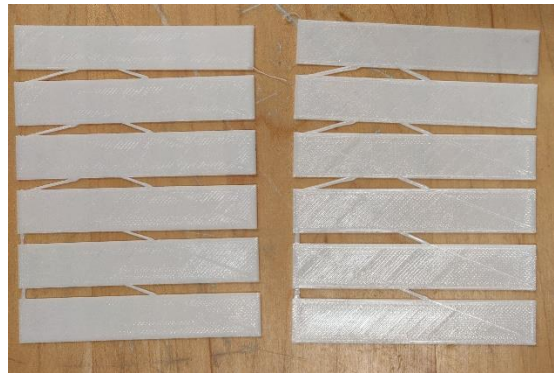


Figure 4.1 - Sensor sample dielectric blanks



Figure 4.2 - Actuator sample dielectric blank

Following the completion of the both the sensor and actuator dielectric blanks, the initial conductive pads (top side) were applied and annealed. Following the front side application and annealing, the reverse side was applied and annealed. Both sensor and actuator samples front and back side printing were completed start to finish, however with notable observations. All applications of conductive ink to the TPU resulted in warping of the sample. The warping of the samples is at the maximum post conductive ink application, at the start of and during the annealing process (warping can be seen in Figure 4.5, Figure 4.6, and Figure 4.8). The warping occurred in the same or similar fashion for both the PE873 ink as well as the Fluorine Rubber Ink.

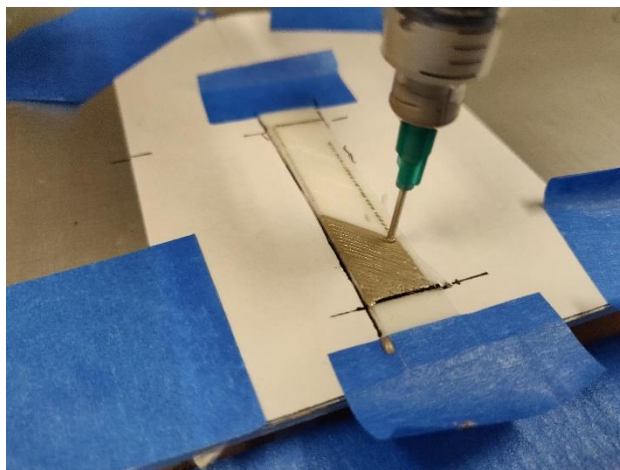


Figure 4.3 - Sensor initial ink pad in progress

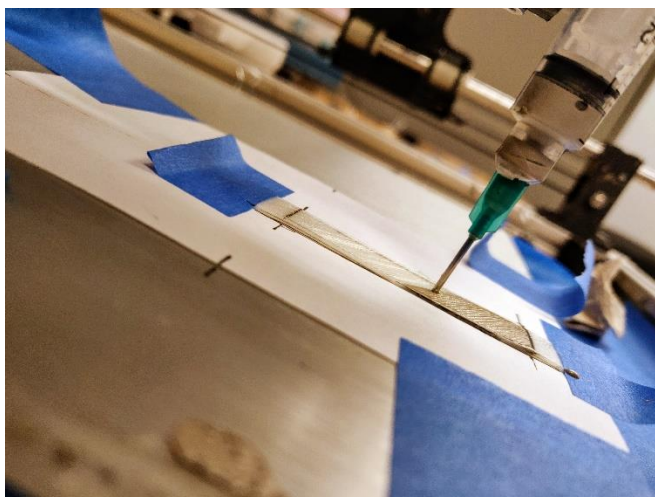


Figure 4.4- Sensor initial ink pad in progress, side view

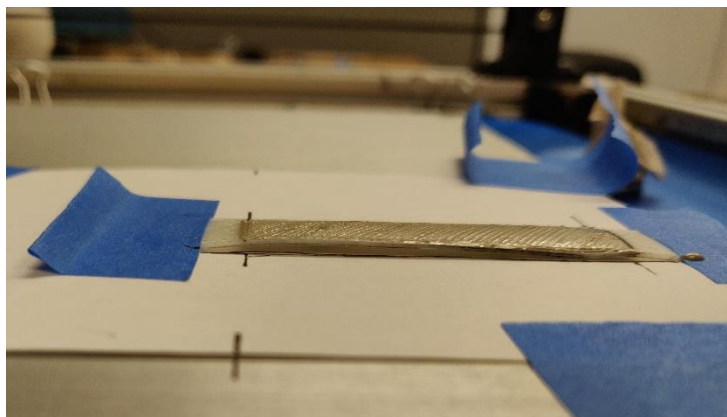


Figure 4.5 - Sensor initial ink pad immediately post-ink printing

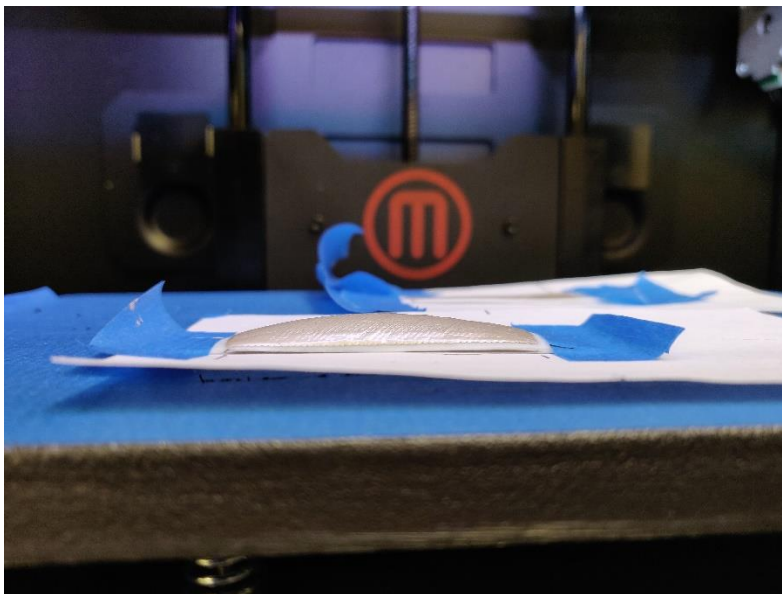


Figure 4.6 - Sensor sample warping at start of annealing process

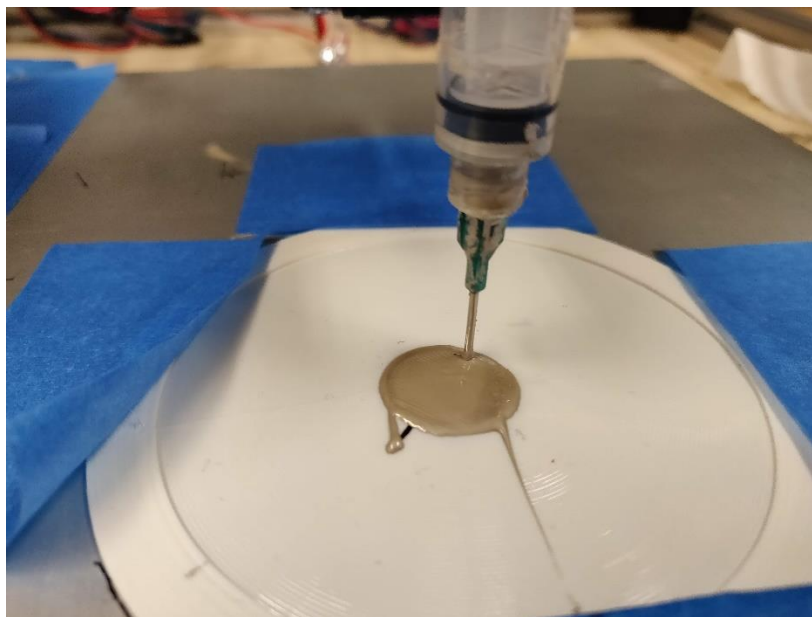


Figure 4.7 - Actuator initial ink pad in progress

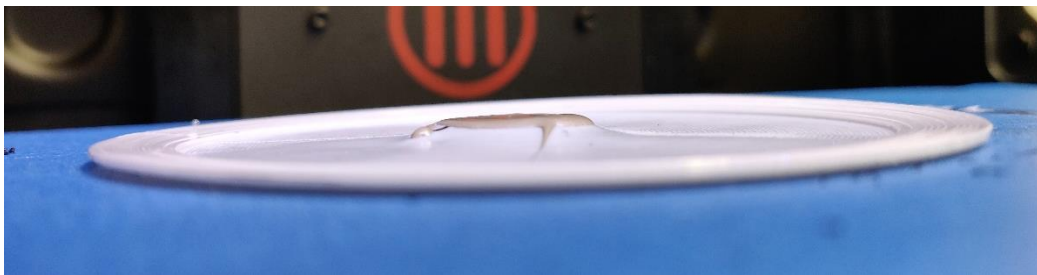


Figure 4.8 - Actuator ink pad warping at start of annealing process

Despite the warping, all samples returned to a flat and level resting state post annealing. The warping is assumed to be due to interaction of the solvents in the inks with the dielectric substrate. As the inks are annealed and the solvent evaporates, the dielectric materials returns to its original state. The finished samples for both sensor and actuator are depicted in Figure 4.9, Figure 4.10, and Figure 4.11.



Figure 4.9 - All sensors samples complete, post final annealing

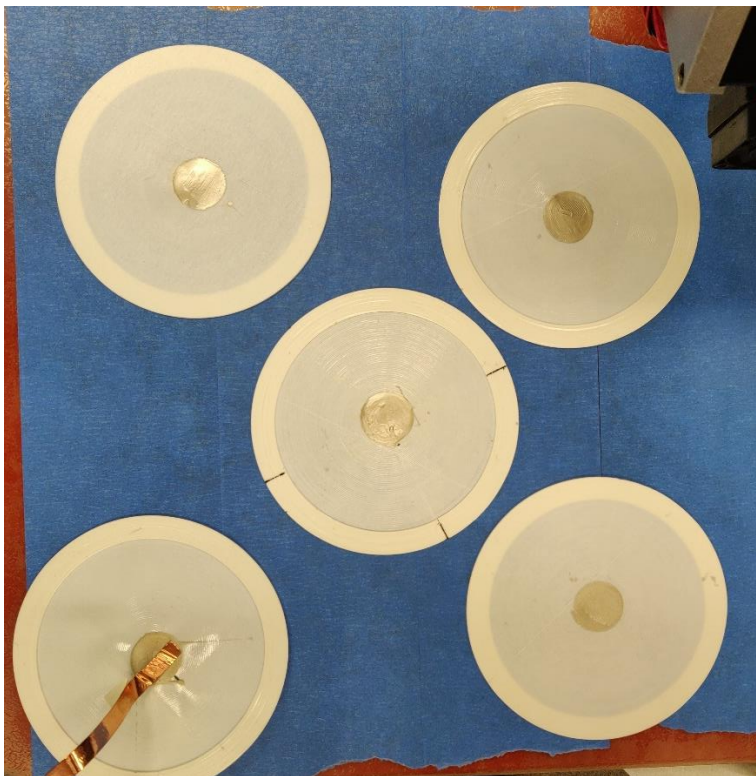


Figure 4.10 - PE873 Actuators post final annealing



Figure 4.11 - All Fluorine Rubber Ink samples, post final annealing

A notable finding post annealing is that in the Fluorine Rubber ink samples (both actuators and sensors), the initial two steps in the annealing process were not sufficient in producing desired electrical properties. Upon recommendation from the creators of the Fluorine Rubber Ink, steps three and four from Table 3.1 were added to the annealing process. The post third and fourth step results increased the capacitance level of both the sensors and actuator samples, the results of which can be seen in Figure 4.12 and Figure 4.13. In Figures 4.12 and 4.13 pre-anneal represents steps one and two while post-anneal represents steps three and four. While the third and fourth annealing steps were successful in increasing capacitance levels of all

samples, the additional annealing steps had negative effects on the mechanical properties as seen in Figure 4.15.

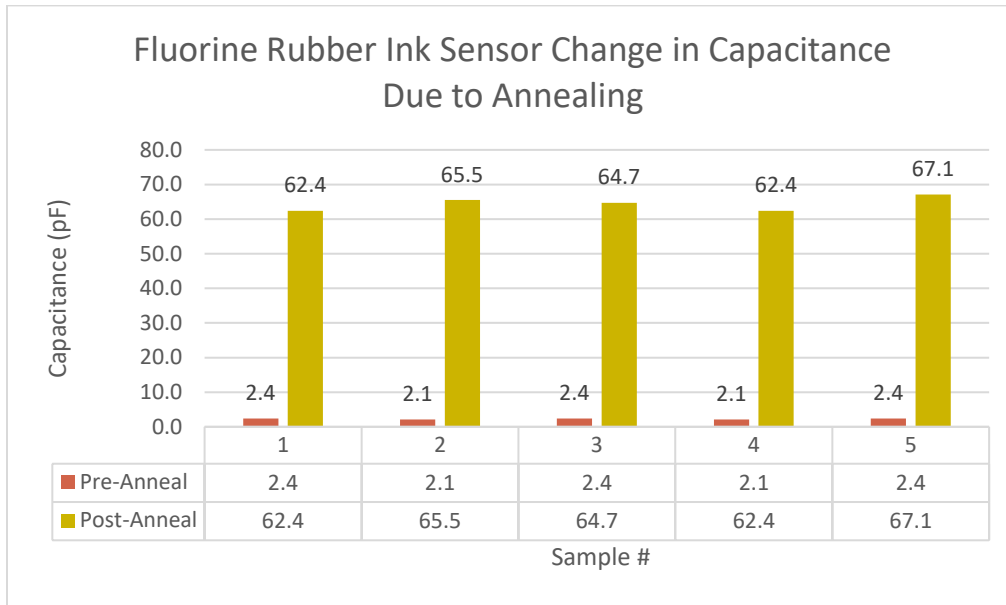


Figure 4.12- Pre & post additional anneal capacitance results Fluorine Rubber Ink sensor samples

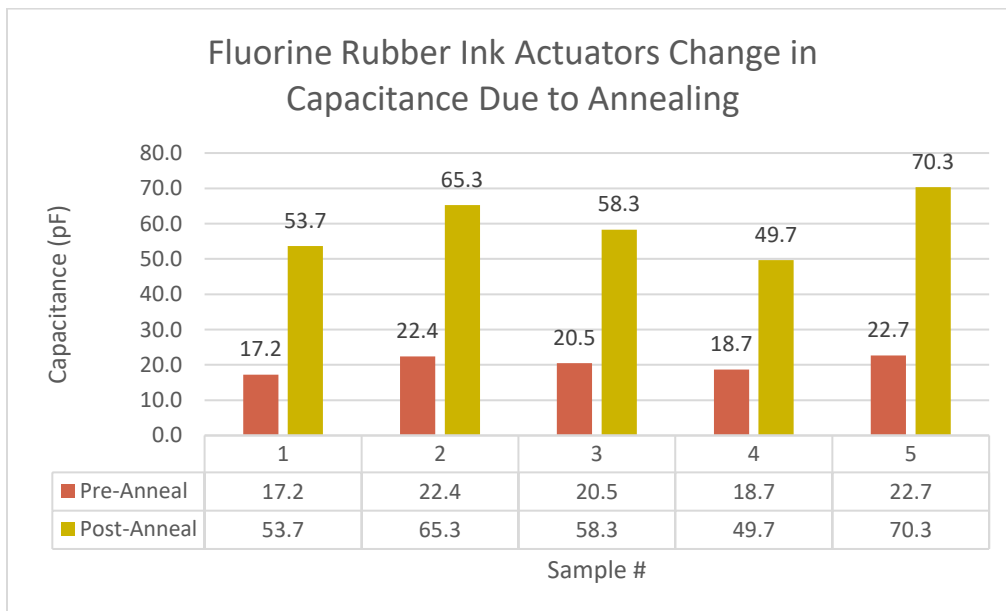


Figure 4.13 - Pre & post additional anneal capacitance results Fluorine Rubber Ink actuator samples

While the manufacturing completed start to finish on the initial run of the final set of samples, initial runs were not without faults. Notably, two issues arose that required reprinting or correcting before testing could resume. One of the two issues was missing fingers for the blue clip contact points on the front side of two of the PE873 sensor samples Figure 4.14. The second issue was with the annealing process when using the Fluorine Rubber ink. The initial strategy to use steps one and two in the annealing chart (Table 3.1) was not producing meaningful changes in the electrical properties of the Fluorine Rubber ink conductive pads. Across all sensor and actuator samples using the Fluorine Rubber ink, post recommended annealing temperatures and times, resistance values were wildly fluctuating in the megaohms range and capacitance values were considerably lower than the PE873 samples. An additional round of annealing was applied to both the sensor and actuator samples of the Fluorine Rubber ink; one hour at 120C° for the top and then repeated one hour at 120C° on the bottom (the third and fourth steps in Table 3.1). The additional annealing, while successful at reducing resistance levels and increasing capacitance levels, made a portion of conductive layer fall apart as can be seen in Figure 4.15. While the sensors samples were still capable of undergoing testing, four of the five actuator samples broke either before or during straining prior to actuation testing. Thus, the decision was made to reprint the broken Fluorine Rubber ink actuator samples and reprint them using the Cellink+ Bioprinter and annealing at the updated annealing settings. The reprinted Fluorine Rubber ink actuator samples underwent the same manufacturing process for the dielectric layer. The reprinted Fluorine Rubber Ink actuators were successful in the manufacturing stage and went on to be used in the rest of the testing sections.



Figure 4.14 - Missing fingers for blue clips on PE873 Samples 2 & 5



Figure 4.15 – Fluorine Rubber Ink actuator post additional annealing

4.2 Resting Values – Pre-Stretch

Following the manufacturing stage, resting resistance and capacitance measurements were taken from all samples including reference prior to stretching. In addition to the single value resting capacitance acquisitions, capacitance frequency sweeps were done as well for all samples.

Table 4.1 - PE873 Pre-Stretch Resting Capacitance Values

PE 873 Sensor Samples	
	Resting Capacitance (pF)
S1	62.2
S2	60.2
S3	53.3
S4	61.1
S5	55.1
PE 873 Actuator Samples	
	Resting Capacitance (pF)
S1	67.8
S2	61.8
S3	71.2
S4	59.7
S5	31.0

Table 4.2 PE873 Pre-Stretch Resting Capacitance Values Continued

PE873 Sensors				
Average (pF)	Stddev (pF)	Min (pF)	Max (pF)	Broken
58.4	3.5	53.3	62.2	0
PE873 Actuators				
Average (pF)	Stddev (pF)	Min (pF)	Max (pF)	Broken
58.3	14.2	31	71.2	0

Table 4.3 – Fluorine Rubber Ink Pre-Stretch Resting Capacitance Values

Fluorine Rubber Ink Sensor Samples	
	Resting Capacitance (pF)
S1	62.4
S2	65.5
S3	64.7
S4	62.4
S5	67.1
Fluorine Rubber Ink Actuator Samples	
	Resting Capacitance (pF)
S1	53.7
S2	65.3
S3	58.3
S4	49.7
S5	70.3
Fluorine Rubber Ink Actuator Samples reprint	
	Resting Capacitance (pF)
S1	58.8
S2	111.3
S3	58.3
S4	80.7
S5	84.2

Table 4.4 – Fluorine Rubber Ink Pre-Stretch Resting Capacitance Values Continued

Fluorine Rubber Ink Sensors				
Average (pF)	Stddev (pF)	Min (pF)	Max (pF)	Broken
64.4	1.8	62.4	67.1	0
Fluorine Rubber Ink actuator original				
Average (pF)	Stddev (pF)	Min (pF)	Max (pF)	Broken
59.5	7.5	49.7	70.3	0
Fluorine Rubber Ink actuator reprints				
Average (pF)	Stddev (pF)	Min (pF)	Max (pF)	Broken
78.7	19.5	58.3	111.3	0

Table 4.5 - Parker Pre-Stretch Resting Capacitance Values

Parker Sensor Samples	
	Resting Capacitance
S1	355.1
S2	324.3
S3	321.7
S4	339.7
S5	358.3

Table 4.6 - Parker Pre-Stretch Resting Capacitance Values Continued

Parker Sensors				
Average (pF)	Stddev (pF)	Min (pF)	Max (pF)	Broken
339.8	15.1	321.7	358.3	0

Table 4.7 depicts the resting capacitance results from the ETPU samples. The early results for the samples of equivalent size and shape to the conductive ink samples returned low capacitance values, within the noise floor of the LCR meter. Longer samples (241mm in length versus 71mm in length for the standard samples) were created in order to test if a scaled-up version could create enough of a capacitance value to escape the noise floor or if the values in of the original were representative of all samples using the ETPU. The long samples, which became known as ETPU Long sensor samples did produce larger capacitance values than the initial samples. The manufacturing process, layer thickness, and materials were consistent for both the standard and long ETPU samples. The only parameter that changed was the length of the sample in order to increase surface area of the electrode and thus in theory increase capacitance overall.

Due to the instability of the initial ETPU sensor capacitance readings, the range rather than the values were included in Table 4.7.

Table 4.7 - ETPU Pre-Stretch Resting Capacitance Values

Full ETPU Sensor Samples	
	Resting Capacitance (pF)
S1	0.2 - 0.7
S2	0.2 - 0.6
S3	0.3 - 0.7
S4	0.3 - 0.8
S5	0.2 - 0.7
Full ETPU Long Sensor Samples	
	Resting Capacitance (pF)
S1	11.2
S2	6.8
S3	7.4
S4	6.3
S5	6.4

Table 4.8 - ETPU Long Pre-Stretch Resting Capacitance Values Continued

ETPU Long Sensors				
Average (pF)	Stddev (pF)	Min (pF)	Max (pF)	Broken
7.6	1.8	6.3	11.2	0

The resistance values recorded were at the surface level of the electrode, at the four points located in Figure 3.19 and Figure 3.20. The resistance values were captured using a four pole two probe setup on an LCR meter, the Protek LCR Meter Z8200. The resistance values recorded here speak more to the consistency with which the conductive particles in each ink proliferated through the single layer applied than it does as just raw resistance readings. Resistance values for the ETPU samples (both the initial size and the long samples) were not added to the tables in this section because they did not return any resistance values. The resistance values for the ETPU samples fluctuated wildly in the megaohms region, not remaining stable enough with any of the ETPU samples to take meaningful measurements. The

aforementioned behavior with the ETPU also occurred on several locations of the conductive inks. Any location where wildly fluctuating values occurred, an N/A was recorded.

Table 4.9 - PE873 Sensors & Actuators Pre-Stretch Initial Resting Resistance Values

PE 873 Sensor Samples - Front Side – Ohms						
	Resting Resistance Location 1	Resting Resistance Location 2	Resting Resistance Location 3	Resting Resistance Location 4	Average	
S1	2.909	1.545	1.443	1.188	1.771	
S2	2.332	1.575	0.671	0.739	1.329	
S3	4.201	2.416	1.810	2.263	2.673	
S4	3.644	2.143	1.916	2.568	2.568	
S5	3.750	1.531	1.630	3.715	2.657	
PE 873 Sensor Samples - Back Side - Ohms						
	Resting Resistance Location 1	Resting Resistance Location 2	Resting Resistance Location 3	Resting Resistance Location 4	Average	
S1	1.905	1.265	0.960	0.548	1.170	
S2	2.638	1.590	1.266	0.777	1.568	
S3	84.330	9.105	73.560	45.910	53.226	
S4	1.367	0.738	0.664	1.056	0.956	
S5	4.180	0.581	0.967	3.580	2.327	
PE 873 Actuator Samples - Front Side - Ohms						
	Resting Resistance Location 1	Resting Resistance Location 2	Resting Resistance Location 3	Resting Resistance Location 4	Average	
S1	1.482	1.554	0.808	0.791	1.159	
S2	0.530	0.672	0.423	0.487	0.528	
S3	11.871	8.450	22.164	4.532	11.754	
S4	N/A	N/A	N/A	N/A	0.000	
S5	N/A	N/A	N/A	N/A	0.000	
PE 873 Actuator Samples - Back Side - Ohms						
	Resting Resistance Location 1	Resting Resistance Location 2	Resting Resistance Location 3	Resting Resistance Location 4	Average	
S1	0.420	2.530	0.471	1.602	1.256	
S2	0.541	0.632	0.592	0.556	0.580	
S3	55.320		367.000	275.550	174.468	
S4	104.720	157.120	201.980	152.700	154.130	
S5	N/A	N/A	N/A	N/A	0.000	

Table 4.10 – Fluorine Rubber Sensor & Actuator Initial Resting Resistance Values

Fluorine Rubber Sensor Samples - Front Side - Ohms						
	Resting Resistance Location 1	Resting Resistance Location 2	Resting Resistance Location 3	Resting Resistance Location 4	Average	
S1	0.638	0.329	0.137	0.262	0.342	
S2	0.213	0.170	0.023	0.026	0.108	
S3	0.190	0.158	0.033	0.034	0.104	
S4	1.534	1.498	0.156	0.164	0.838	
S5	0.690	0.505	0.283	0.312	0.448	
Fluorine Rubber Sensor Samples - Back Side - Ohms						
	Resting Resistance Location 1	Resting Resistance Location 2	Resting Resistance Location 3	Resting Resistance Location 4	Average	
S1	1.607	0.480	0.331	1.072	0.873	
S2	0.907	0.514	0.154	0.536	0.528	
S3	2.380	2.040	0.663	0.621	1.426	
S4	4.933	7.700	0.198	0.180	3.253	
S5	1.535	0.913	0.488	0.480	0.854	
Fluorine Rubber Actuator Samples - Reprint - Front Side - Ohms						
	Resting Resistance Location 1	Resting Resistance Location 2	Resting Resistance Location 3	Resting Resistance Location 4	Average	
S1	0.320	0.324	0.174	0.136	0.239	
S2	0.660	0.735	0.331	0.369	0.524	
S3	0.175	0.215	0.132	0.109	0.158	
S4	0.711	2.210	0.230	0.444	0.899	
S5	0.251	0.430	0.173	0.156	0.253	
Fluorine Rubber Actuator Samples - reprint - Back Side - Ohms						
	Resting Resistance Location 1	Resting Resistance Location 2	Resting Resistance Location 3	Resting Resistance Location 4	Average	
S1	0.139	0.117	0.084	0.087	0.107	
S2	0.644	0.559	0.260	0.276	0.435	
S3	0.297	0.325	0.232	0.207	0.265	
S4	0.853	2.090	0.362	0.421	0.932	
S5	0.516	0.354	0.182	0.225	0.319	

Frequency sweeps were also part of the battery of resting recordings in order to add more substance to the capacitance values. Capacitance frequency sweep curves give a view with improved clarity into the performance of capacitors. For the research done here, it also adds to the comparison between the reference samples and the additively produced samples by providing measurements throughout a range of frequencies.

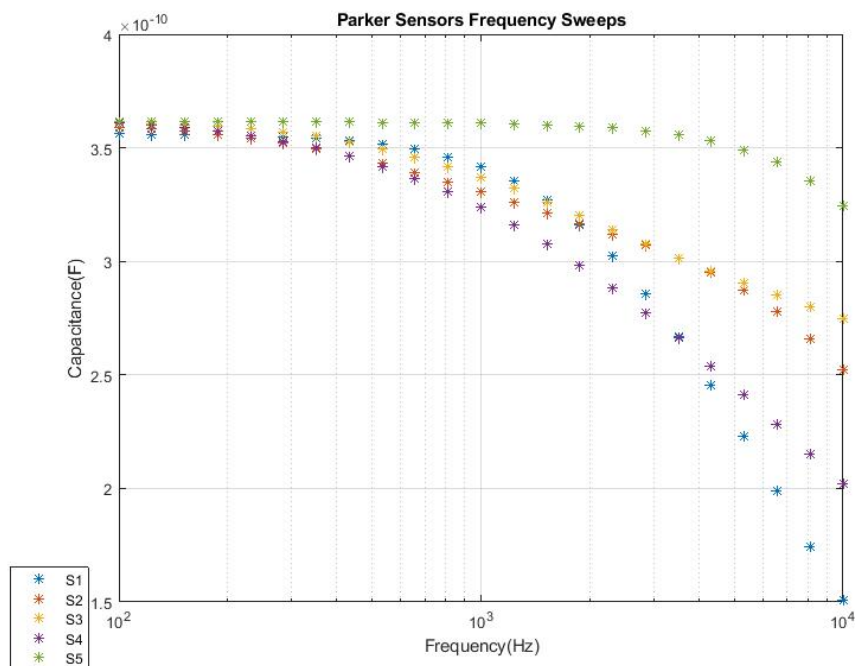


Figure 4.16 - Parker all Sensors Combined Frequency Sweep Plot pre-stretch

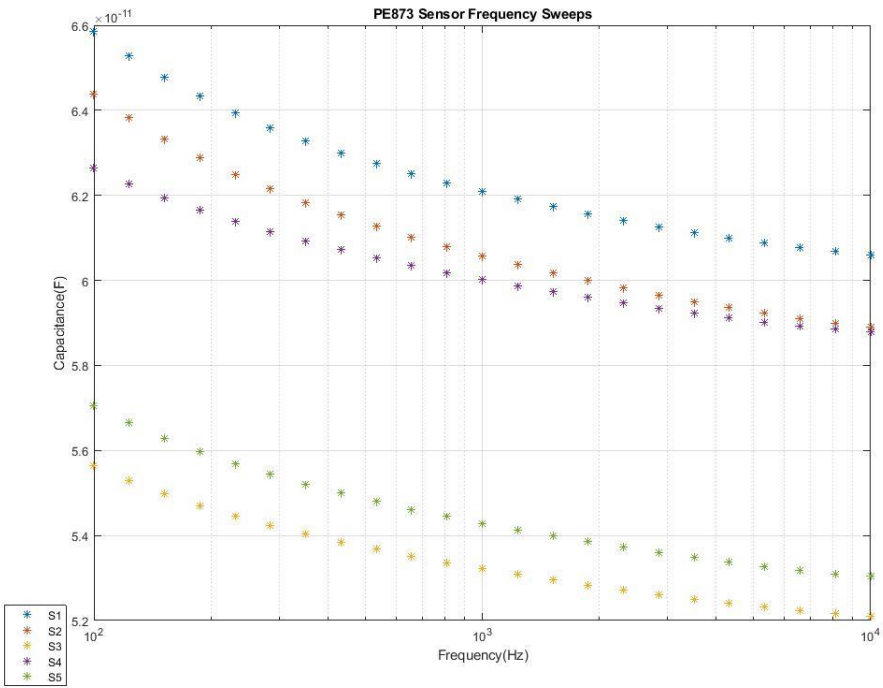


Figure 4.17 - PE873 All Sensors Combined Frequency Sweep Plot pre-stretch

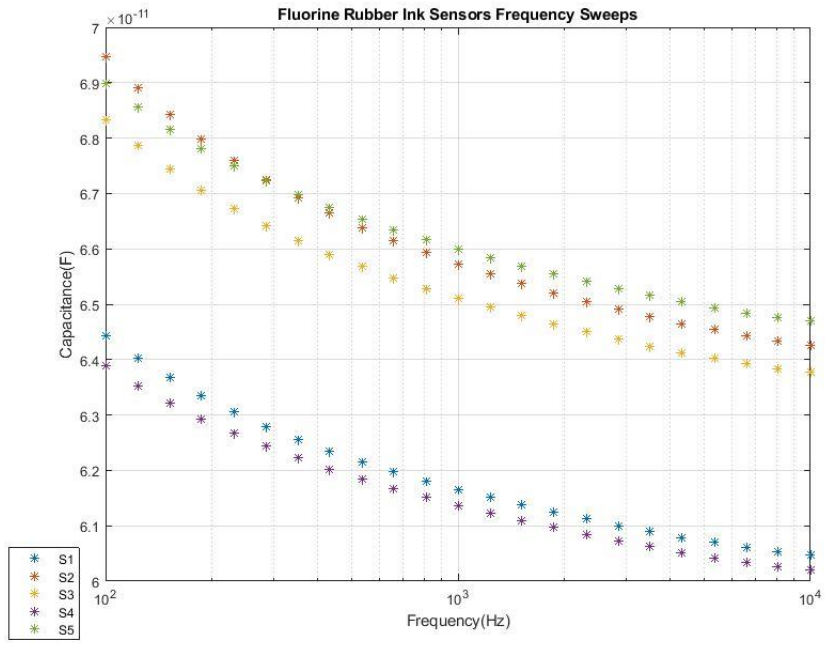


Figure 4.18 - Fluorine Rubber Ink All Sensors Combined Frequency Sweep Plot pre-stretch

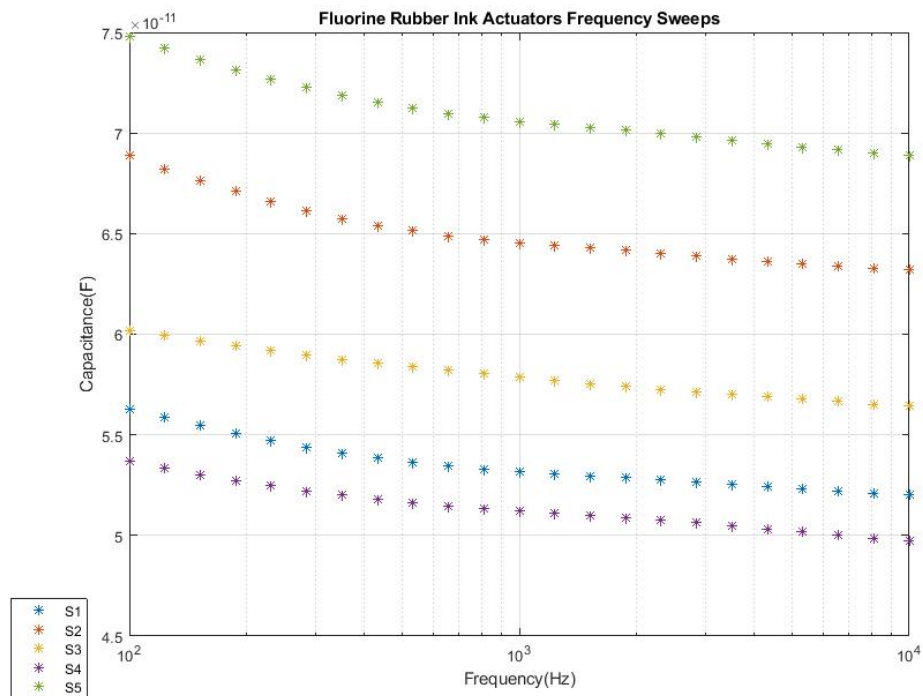


Figure 4.19 - Fluorine Rubber Ink Actuator Combined Frequency Sweeps Plot pre-stretch

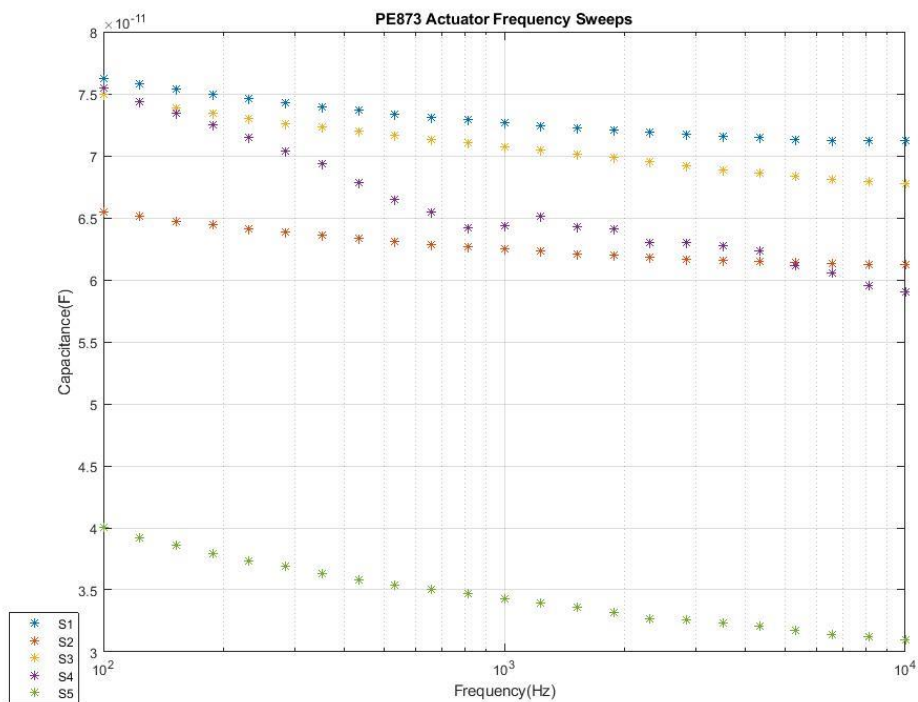


Figure 4.20 - PE873 Actuator Combined Frequency Sweeps Plot pre-stretch

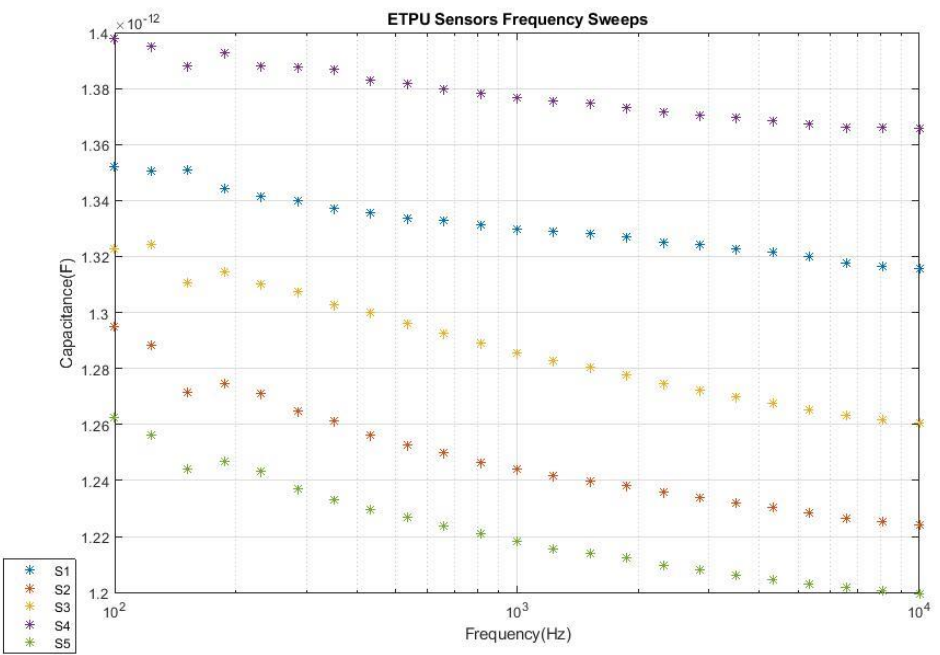


Figure 4.21 - ETPU Frequency combined frequency sweeps plot pre-stretch

4.3 Application Testing – Sensors

Capacitance values were recorded throughout the duration of the stretching process from zero percent strain to fifty percent strain. Not all samples are the same length, however adjustments to placement within the tensile strength tester machine grips were made to ensure that the active area for all samples was identical. The active area for all samples as mentioned in the methodology section was 33.5 mm. The results for capacitance value over strain percentage for each subset of sensor can be seen in Figure 4.32 through Figure 4.40. The fluorine rubber ink samples were separated into two charts to add clarity when reading the plots. During the stretch test, two of the five fluorine rubber ink samples exhibited significant separation of the conductive layer on at least one side of the sensor. Examples of the separated layers in the fluorine rubber ink sensor samples can be seen post stretch, Figure 4.23 and Figure 4.24.

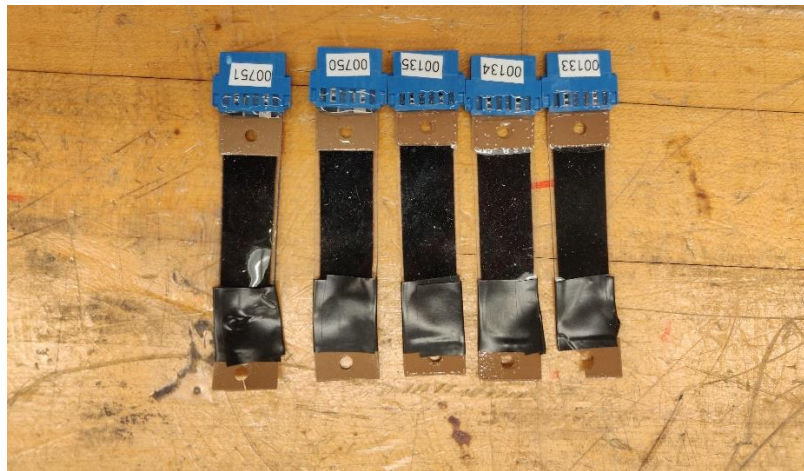


Figure 4.22 - Parker Sensor Samples Post-Stretch Test

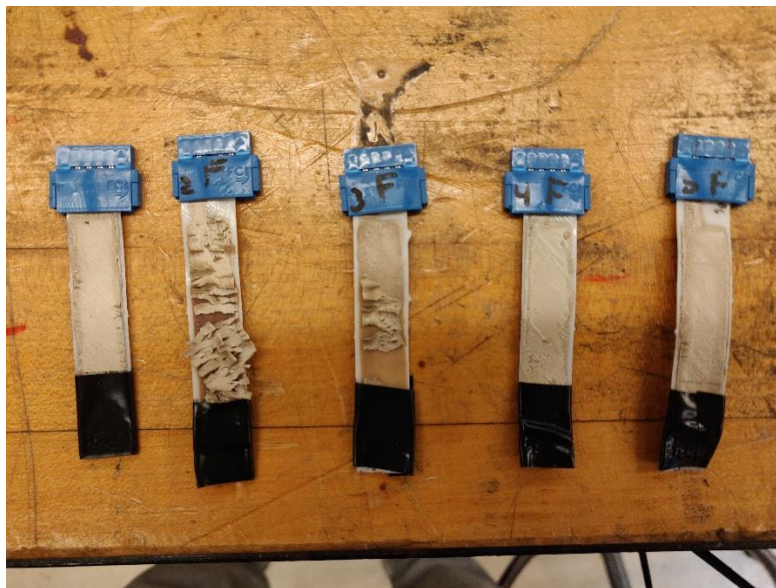


Figure 4.23 - Fluorine Rubber Ink Post-Stretch Test Front Side

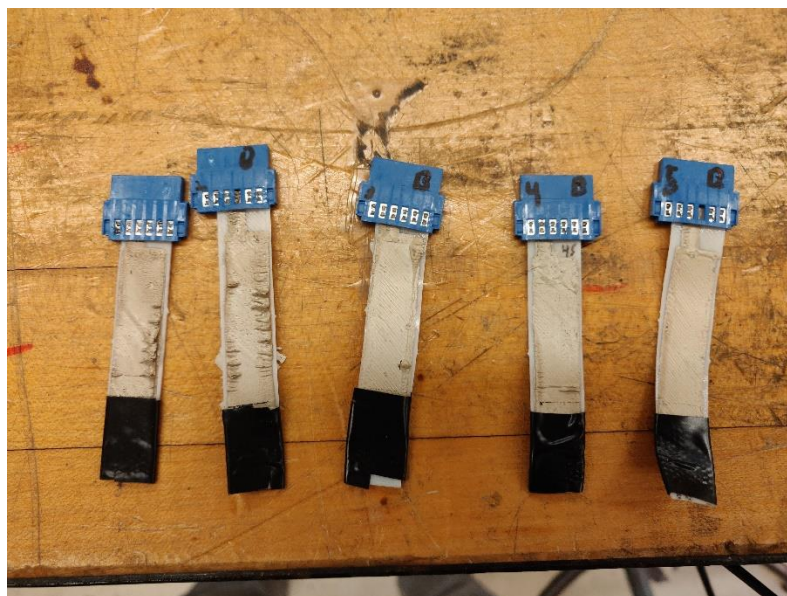


Figure 4.24 - Fluorine Rubber Ink Post-Stretch Test Rear side

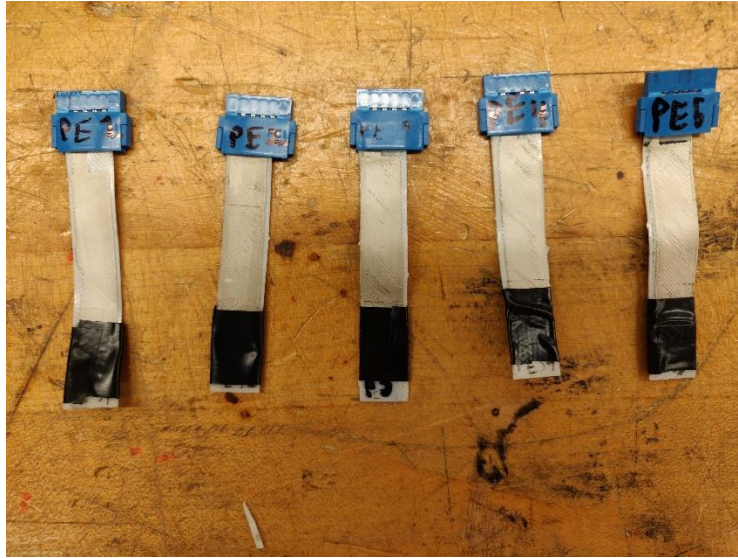


Figure 4.25 – PE873 Post-Stretch Test Front Side

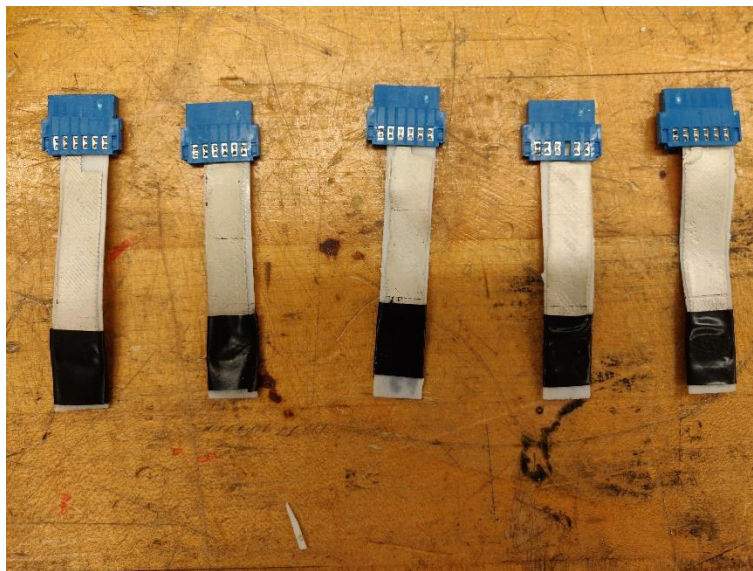


Figure 4.26 – PE873 Post-Stretch Test Rear Side



Figure 4.27 - ETPU initial samples front side post stretch test



Figure 4.28 - ETPU initial samples back side post stretch test

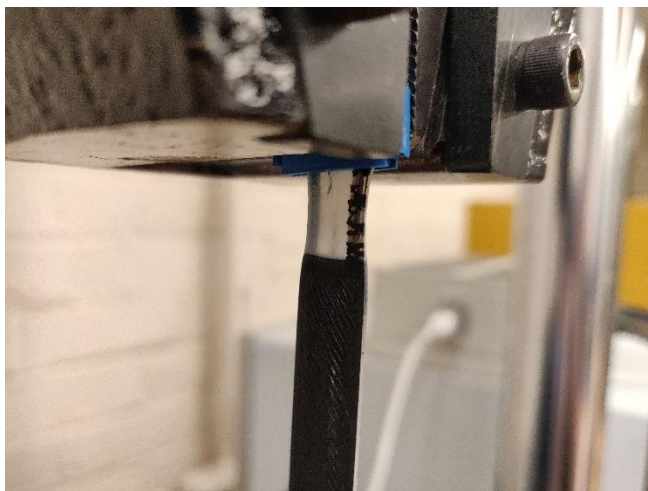


Figure 4.29 - Separation at the reading trace ETPU initial sample

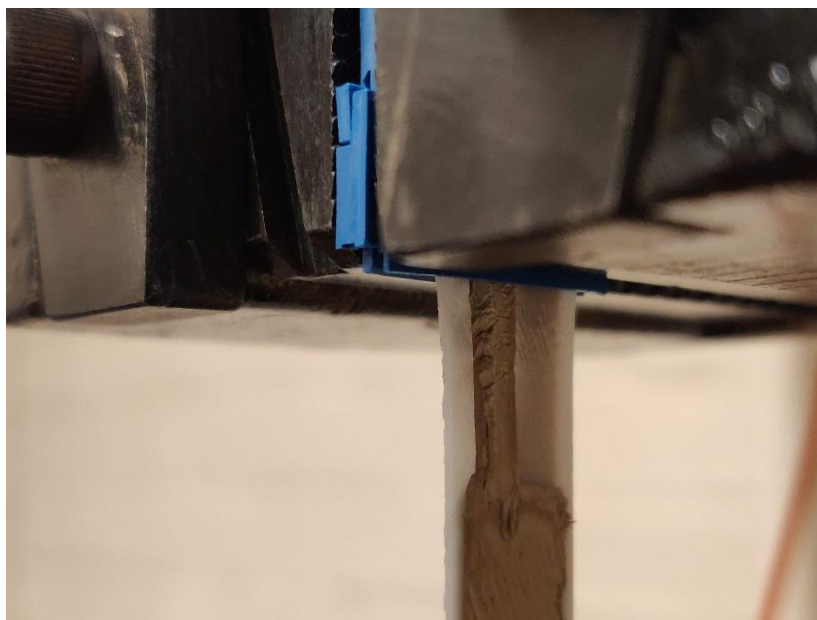


Figure 4.30 - Read trace on Fluorine Rubber Ink Sample



Figure 4.31 - Read trace on PE873 Sample

The capacitance over time graphs have been prefaced with the pictures of the sensor samples post stretch test in order to provide additional context to the plots. Further, the ETPU long samples were not included in the capacitance over time plots as the samples showed no change in capacitance over time. The ETPU initial samples either showed no change in capacitance, or broke due to the slim trace going to the clip separating. The ETPU values were also within the noise floor of the NF ZM2372, as noted in the pre stretch resting values section, making it difficult to accurately assess the legitimacy of the returned values. While separation of the slip trace from the clip was a concern for all samples, the issue only occurred with the ETPU samples.

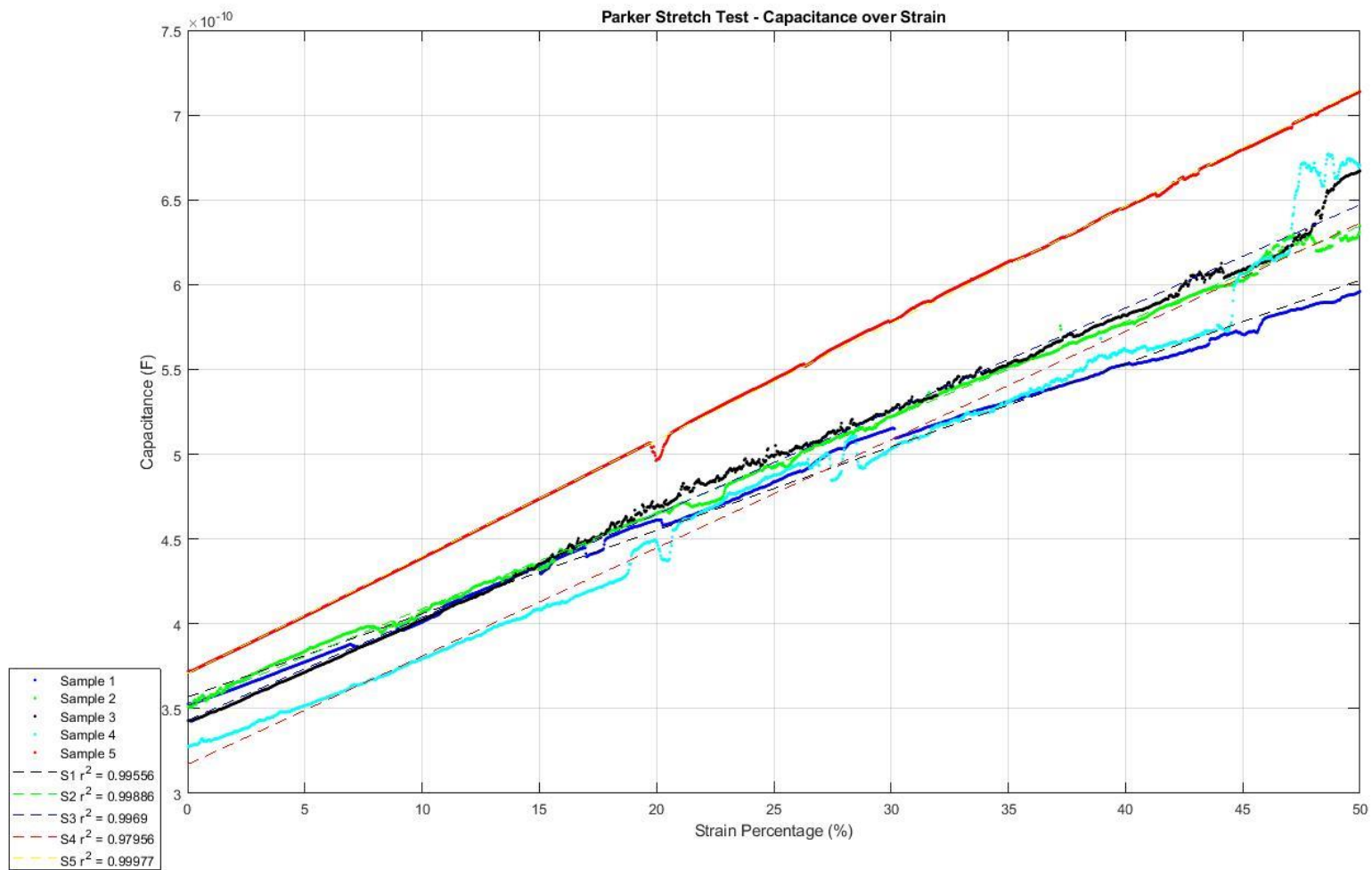


Figure 4.32 - Parker capacitance over strain

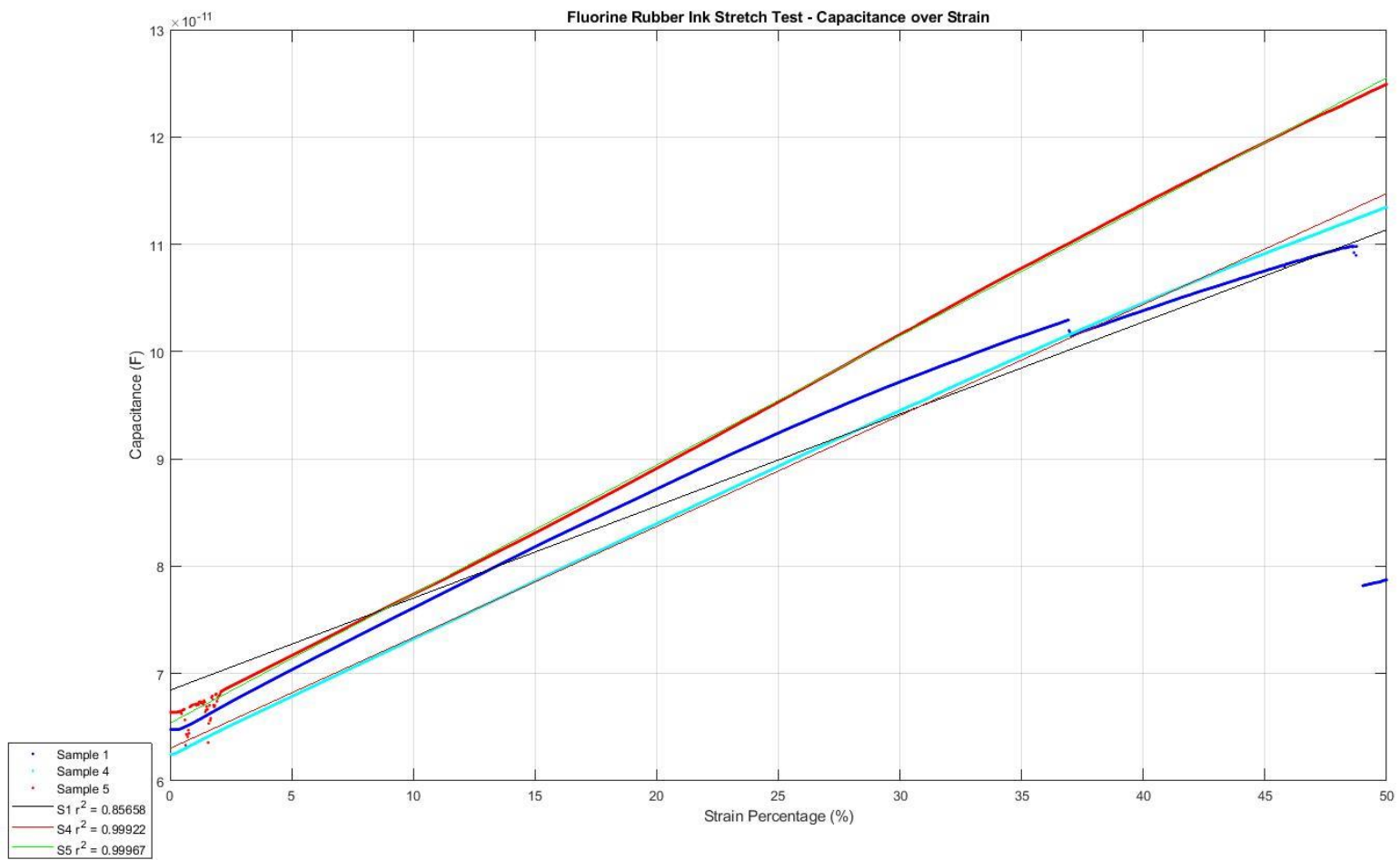


Figure 4.33 - Fluorine Rubber Ink capacitance over strain unbroken samples

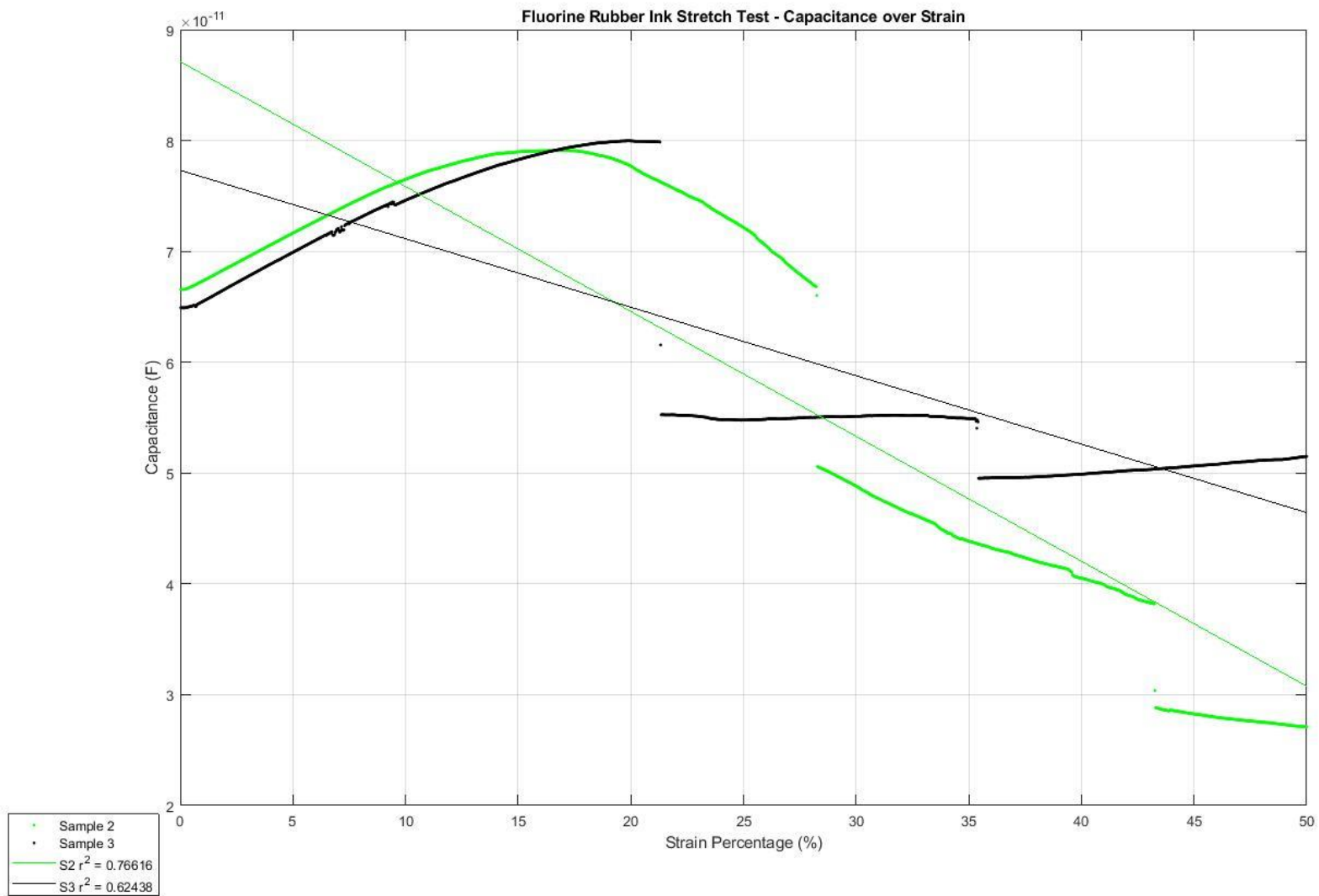


Figure 4.34 – Fluorine Rubber Ink capacitance over strain broken samples

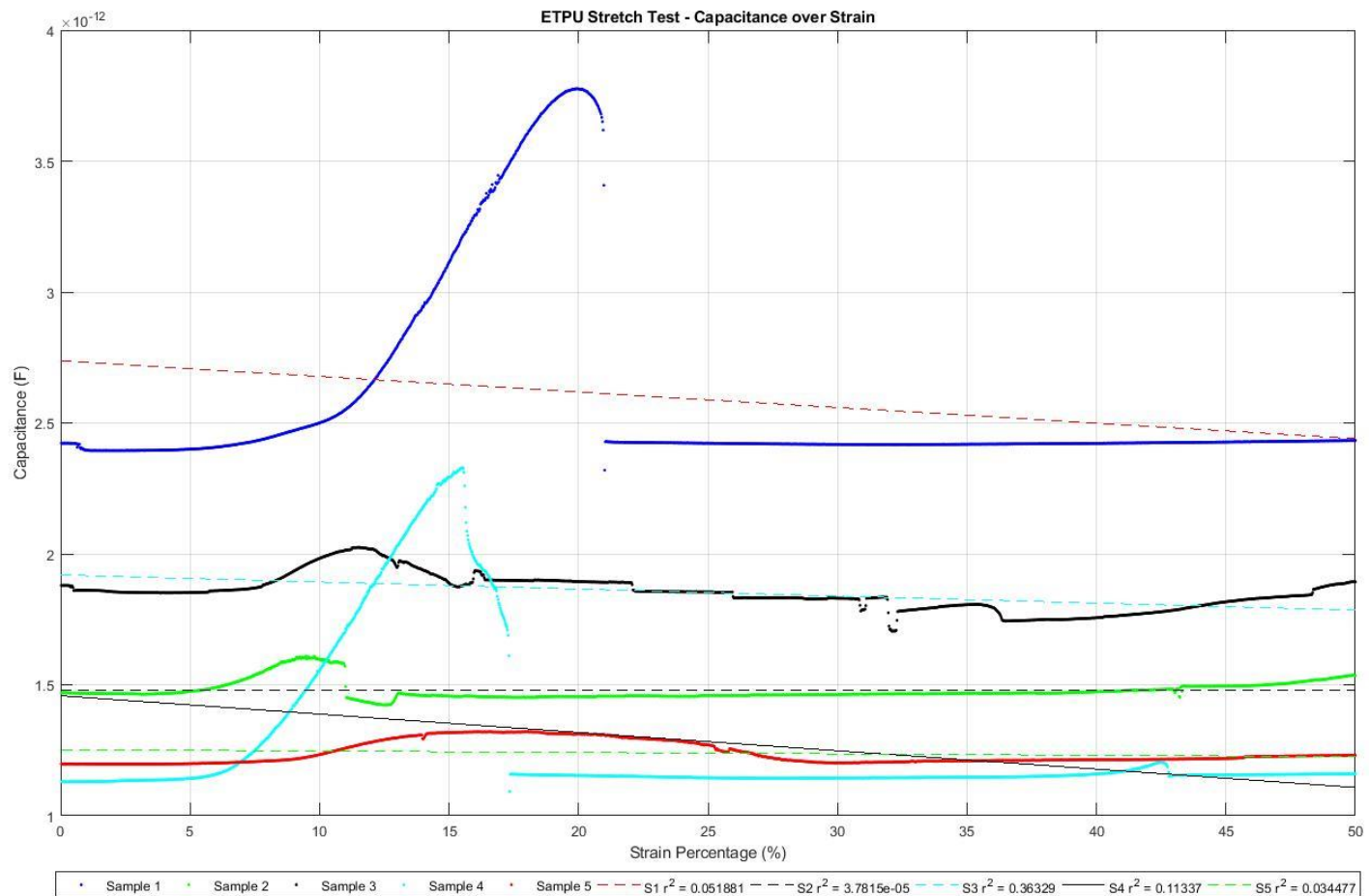


Figure 4.35 - ETPU Samples capacitance over strain

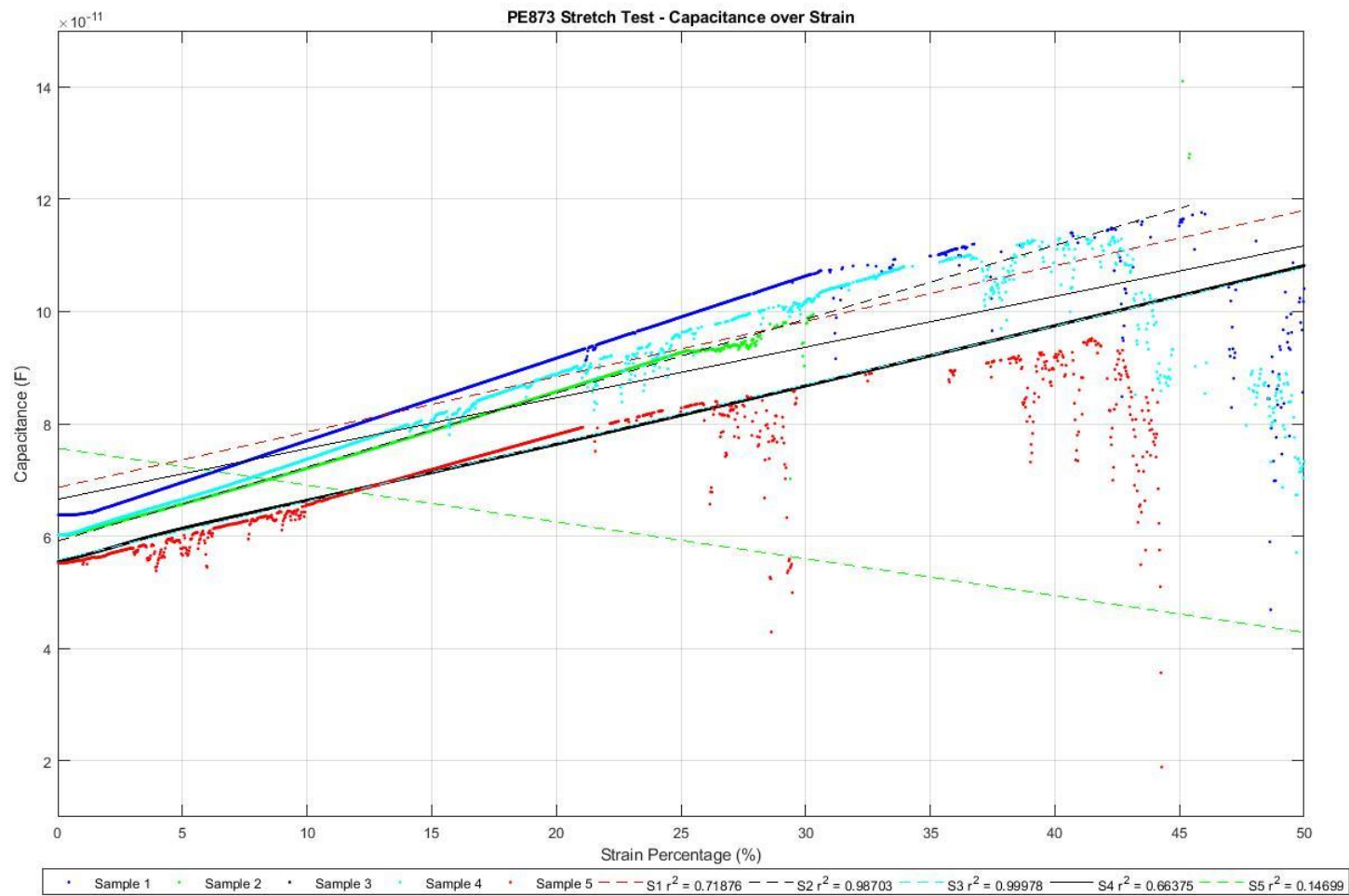


Figure 4.36 - PE873 capacitance over strain

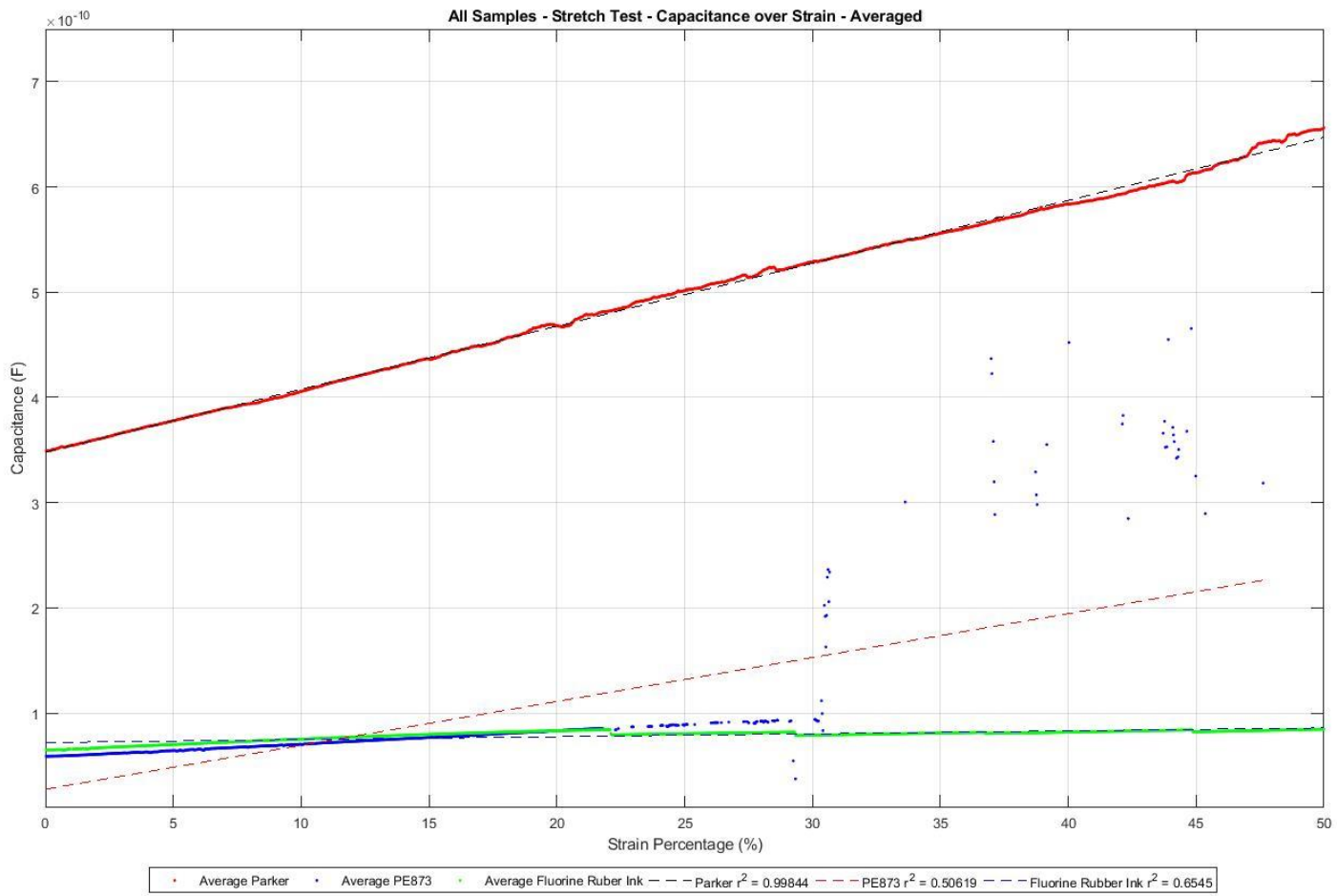


Figure 4.37 - All samples, including Fluorine Rubber Ink broken samples

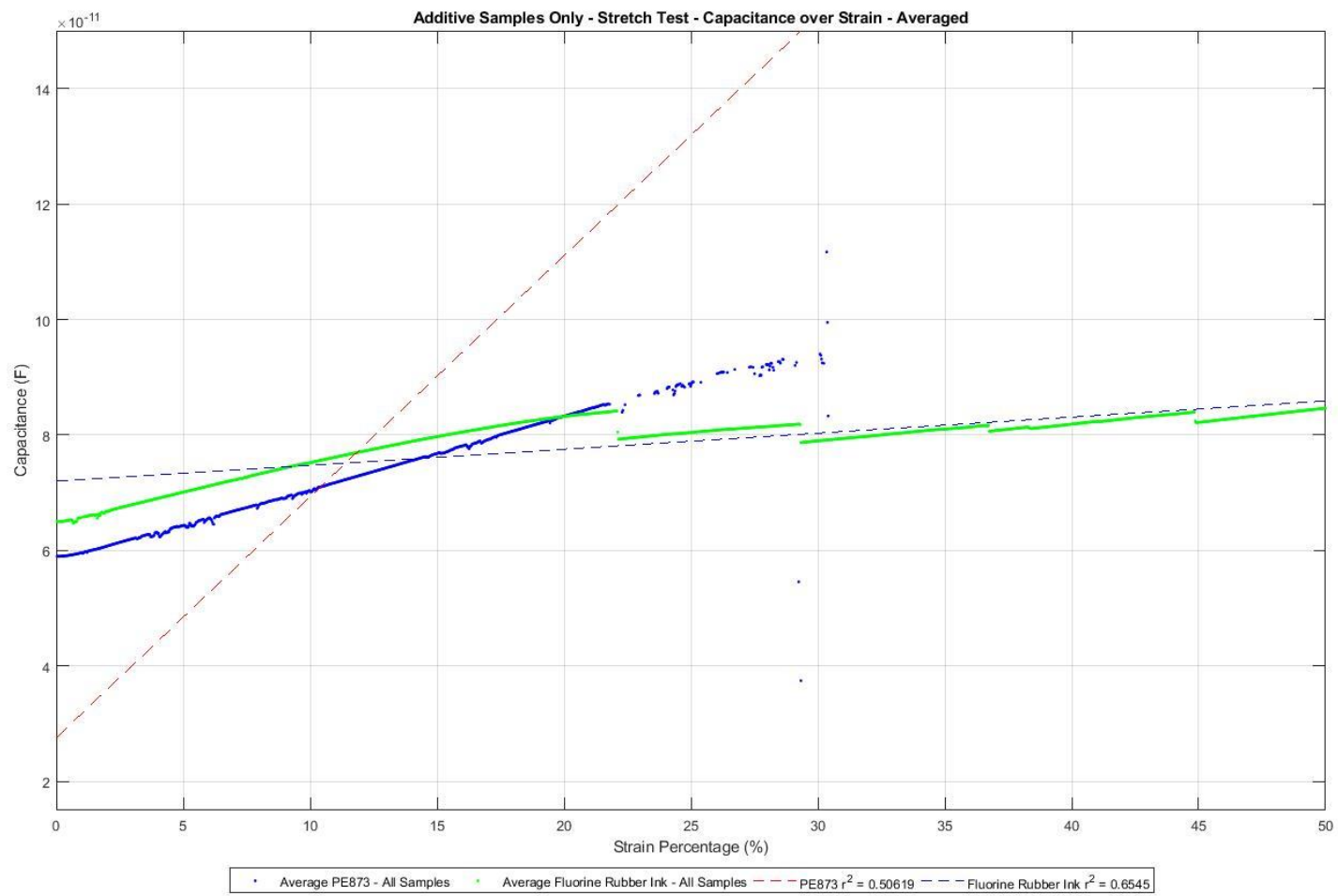


Figure 4.38 - Additive Samples only, including Fluorine Rubber Ink broken samples

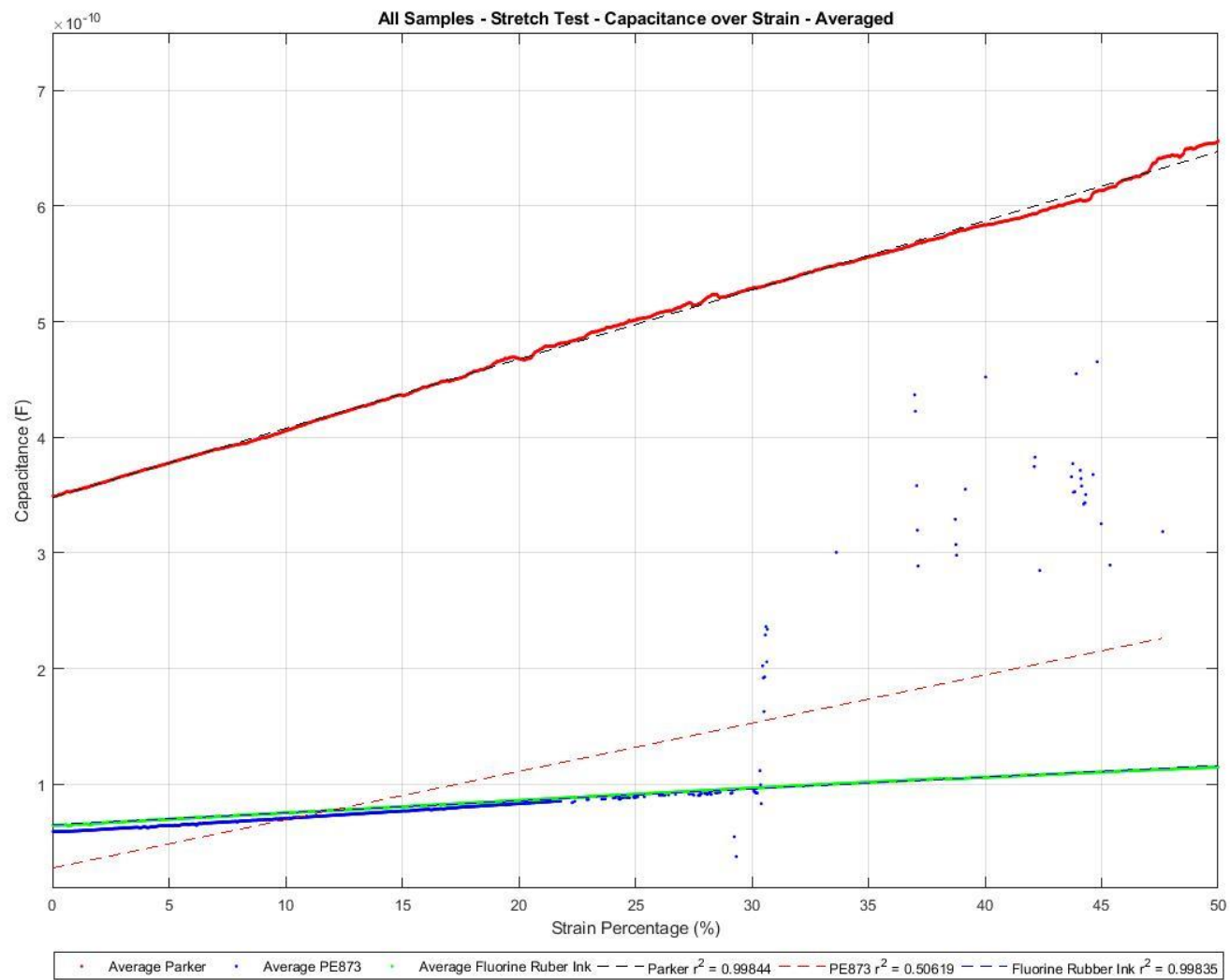


Figure 4.39 - All samples, broken Fluorine Rubber Ink samples removed

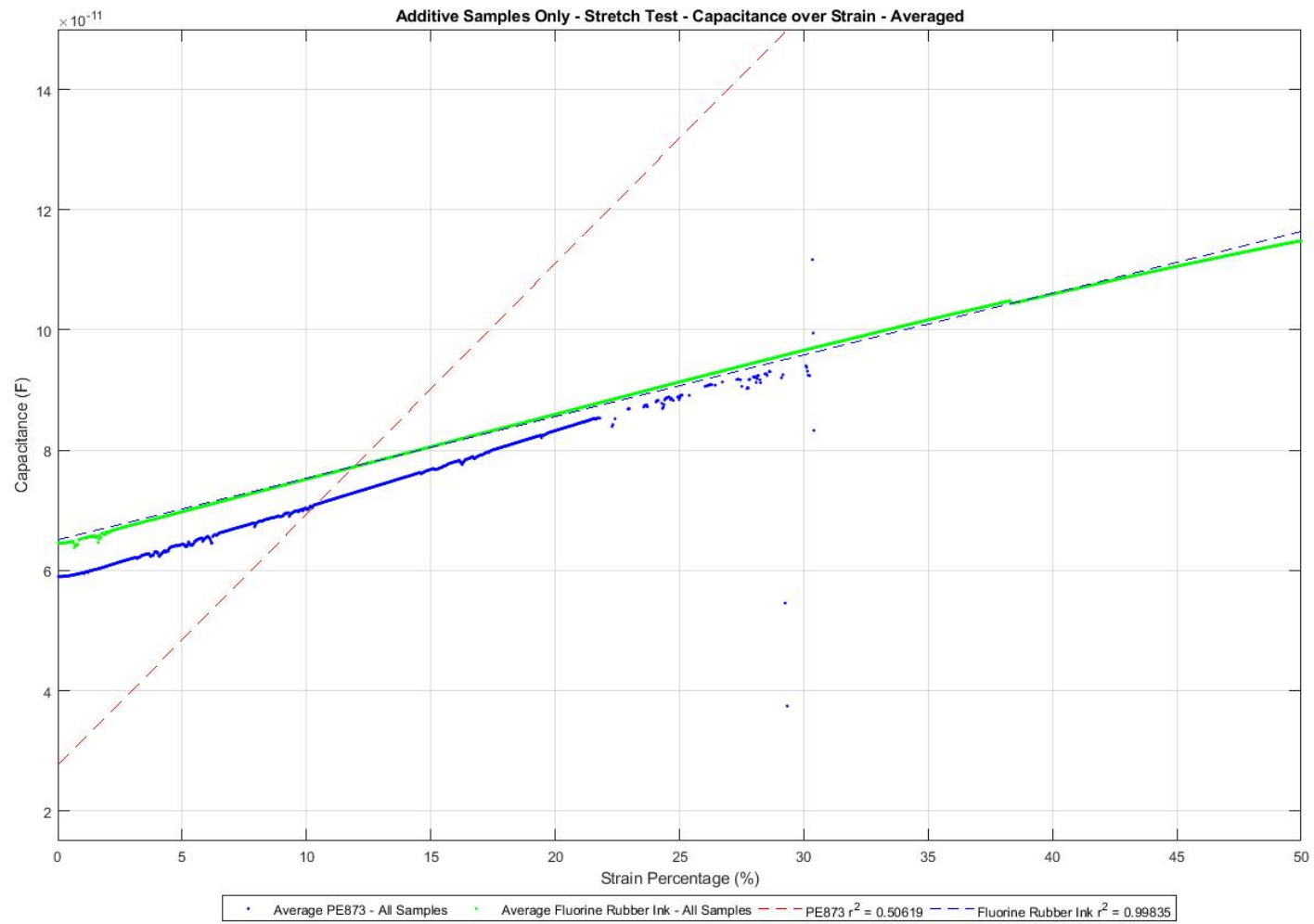


Figure 4.40 - Additive Samples, broken Fluorine Rubber Ink samples removed

Table 4.11 - Number of dropped values during stretch test

Dropped Values			
	Parker	PE873	Fluorine Rubber Ink
Sample 1	0	544	9
Sample 2	0	755	0
Sample 3	0	0	0
Sample 4	0	414	0
Sample 5	0	462	3

Table 4.11 represented the dropped values that occurred during the sensor stretch testing. Dropped values were any values that were below zero or above the 1.5×10^{-9} Farad threshold. The upper threshold was put in place to remove instances where the NF ZM2372 was maxing out, a situation caused by short or false reading that the LCR meter records as a 32×10^{37} Farad value. Both these high bound values and below zero values were seen as errors and thus removed. With the error values in, accurate R^2 values could not be taken, linear best fit could not be accomplished, and plots were skewed to the upper bounds making for ineffective visual representations of the data.

4.4 Resting Values – Post-Stretch

Post-stretch takes on two different meanings when it comes to the sensors and actuators. Post-stretch for the sensors means that the values were taken post stretch testing. Post-stretch testing for the sensors has the sensors returning to the resting state. Post-stretch for the actuators means that the values were acquired once the actuator samples had been strained over the acrylic rings for actuation testing. Post-stretch values for the actuators therefore is under strain, not at resting. Any cell where a value is not recorded is due to the stretch testing having damaged the sample in such a way that the sample is no longer functional enough to acquire a reading from. ETPU samples were not included in the post-stretch capacitance results as the samples were either broken from the sensor testing or still within the noise floor of the LCR meter. Further, ETPU samples are not documented in the post stretch resistance tables for the same reason as the pre-stretch, all readings were wildly fluctuating in the megaohms range. An addition that was not in pre-stretch resting values was the Grease actuator samples. The conductive grease samples are the reference sample for comparison in the actuator subset. The conductive grease sample were

constructed in the same manner as is done in research, as such the conductive grease was applied to the dielectric layer post strain and applied by hand using a foam applicator.

Table 4.12 - PE873 Post-Stretch Resting Capacitance Values

PE 873 Sensor Samples	
	Resting Capacitance (pF)
S1	64.6
S2	62.1
S3	57.1
S4	63.6
S5	57.6
PE 873 Actuator Samples	
	Resting Capacitance (pF)
S1	44.1
S2	113.2
S3	15.4
S4	94.4
S5	N/A

Table 4.13 - PE873 Post-Stretch Resting Capacitance Values Continued

PE873 Sensors				
Average (pF)	Stddev (pF)	Min (pF)	Max (pF)	Broken
61.0	3.1	57.1	64.6	0
PE873 Actuators				
Average (pF)	Stddev (pF)	Min (pF)	Max (pF)	Broken
66.8	38.9	15.4	113.2	1

Table 4.14 – Fluorine Rubber Ink Post-Stretch Resting Capacitance Values

Fluorine Rubber Ink Sensor Samples	
	Resting Capacitance (pF)
S1	56.3
S2	N/A
S3	N/A
S4	61.7
S5	67.5
Fluorine Rubber Ink Actuator Samples Reprint	
	Resting Capacitance (pF)
S1	40
S2	593.3
S3	336.6
S4	384.1
S5	477.5

Table 4.15 - Fluorine Rubber Ink Post-Stretch Resting Capacitance Values Continued

Fluorine Rubber Ink Sensors				
Average (pF)	Stddev (pF)	Min (pF)	Max (pF)	Broken
61.8	4.6	56.3	67.5	2
Fluorine Rubber Ink actuator reprints				
Average (pF)	Stddev (pF)	Min (pF)	Max (pF)	Broken
366.3	185.2	40.0	593.3	0

Table 4.16 – Parker & Grease Post-Stretch Resting Capacitance Values

Parker Sensor Samples	
	Resting Capacitance (pF)
S1	350.2
S2	327.8
S3	321.6
S4	346.6
S5	360.6
Grease Actuator Samples	
	Resting Capacitance
S1	678.2
S2	451.3
S3	486.7
S4	728.3
S5	773.5

Table 4.17 – Parker & Grease Post-Stretch Resting Capacitance Values Continued

Parker Sensors				
Average (pF)	Stddev (pF)	Min (pF)	Max (pF)	Broken
341.3	14.4	321.6	360.6	0
Grease actuator				
Average (pF)	Stddev (pF)	Min (pF)	Max (pF)	Broken
623.6	130.3	451.3	773.5	0

Following the completion of post stretch capacitance measurements, the plots in Figure 4.41 through Figure 4.45 were created to highlight how the sensors were affected by the stretch process and how the active strain on the actuators affects the capacitance value.

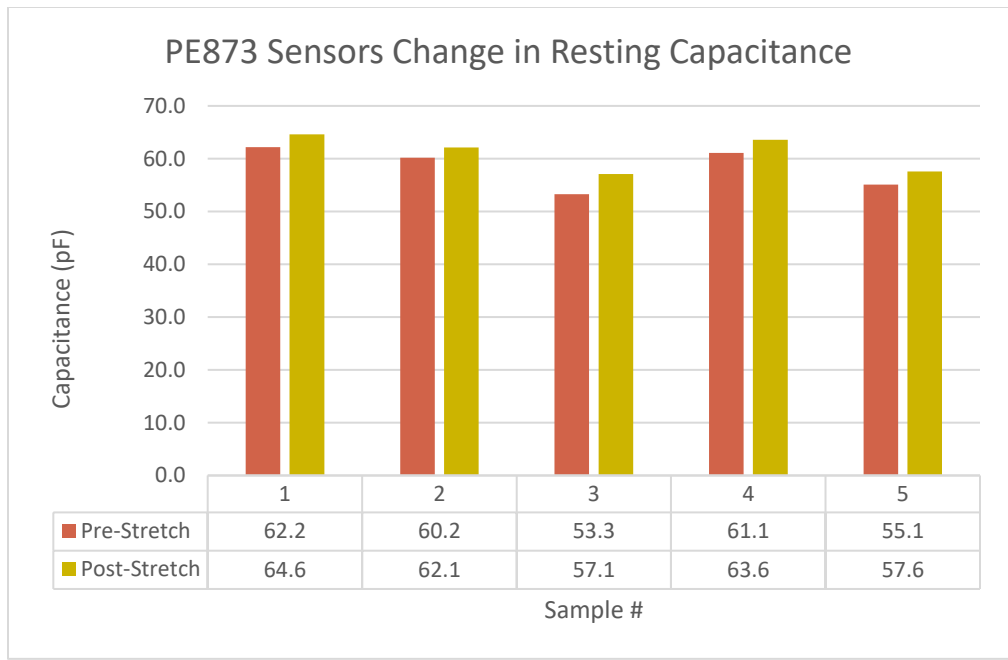


Figure 4.41 - PE873 Sensors Change in Resting Capacitance Plot

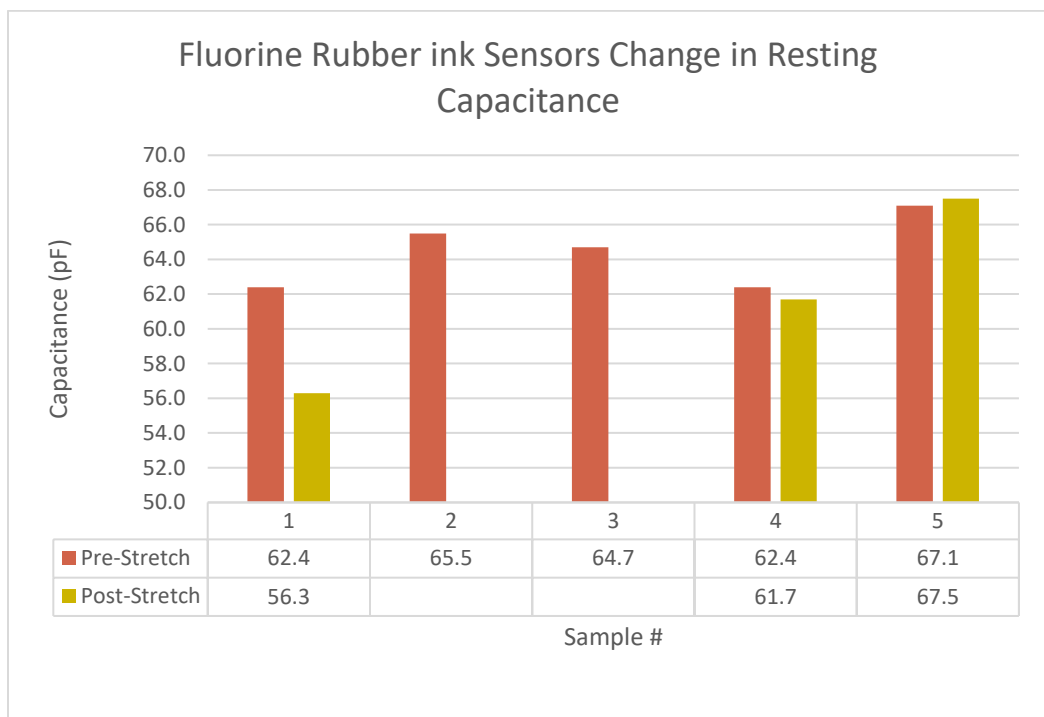


Figure 4.42 - Fluorine Rubber Sensors change in resting capacitance plot

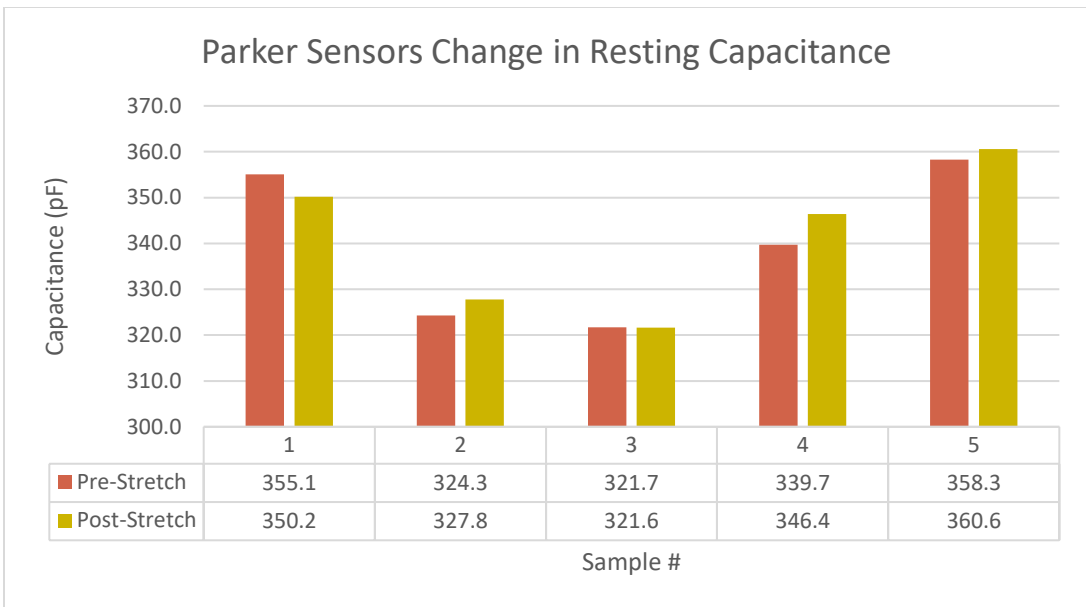


Figure 4.43 - Parker Sensors change in resting capacitance plot

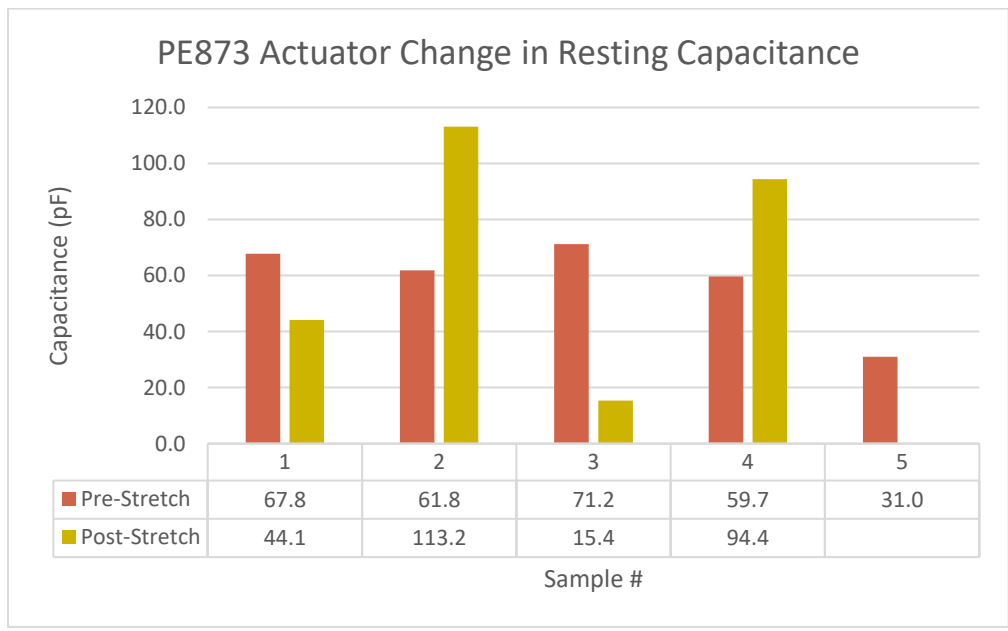


Figure 4.44 - PE873 Actuator sensors change in resting capacitance

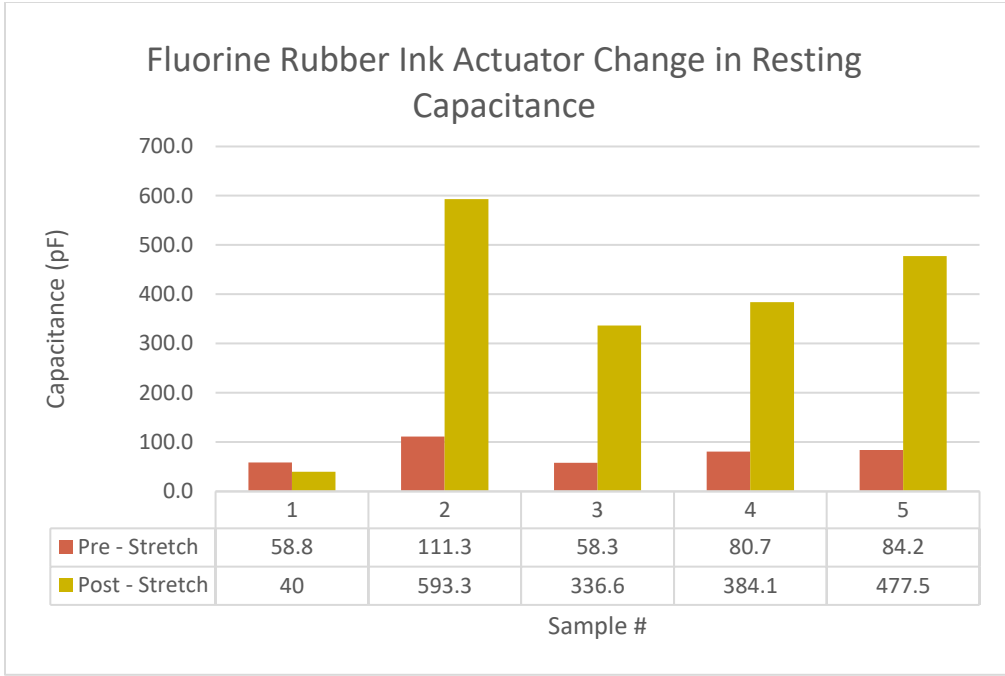


Figure 4.45 - Fluorine Rubber ink actuator changes in resting capacitance

Resting resistance values were again taken post stretch testing. Noteworthy here is the increase in N/A readings due to broken or partially broken samples that occurred for both conductive inks.

Table 4.18 - PE873 Sensors & Actuators Post-Stretch Initial Resting Resistance Values

PE 873 Sensor Samples - Front Side - Ohms						
	Resting Resistance Location 1	Resting Resistance Location 2	Resting Resistance Location 3	Resting Resistance Location 4	Average	
S1	5.001	1.045	2.003	1.561	2.403	
S2	6.450	0.915	1.037	4.263	3.166	
S3	4.809	1.548	1.752	3.293	2.851	
S4	14.441	3.375	11.419	8.859	9.524	
S5	5.969	1.886	2.511	5.156	3.881	
PE 873 Sensor Samples - Back Side - Ohms						
	Resting Resistance Location 1	Resting Resistance Location 2	Resting Resistance Location 3	Resting Resistance Location 4	Average	
S1	3.405	1.725	1.342	1.316	1.947	
S2	8.457	0.980	2.189	7.087	4.678	
S3	31.330	3.274	5.541	22.429	15.644	
S4	7.489	4.770	2.236	4.485	4.745	
S5	12.428	1.386	3.209	10.750	6.943	
PE 873 Actuator Samples - Front Side - Ohms						
	Resting Resistance Location 1	Resting Resistance Location 2	Resting Resistance Location 3	Resting Resistance Location 4	Average	
S1	N/A	N/A	N/A	N/A	0.000	
S2	19.625	38.110	500.290	110.380	167.101	
S3	N/A	N/A	N/A	N/A	0.000	
S4			1200.000	109.000	327.250	
S5	1.064	1.257	1.224	1.384	1.232	
PE 873 Actuator Samples - Back Side - Ohms						
	Resting Resistance Location 1	Resting Resistance Location 2	Resting Resistance Location 3	Resting Resistance Location 4	Average	
S1	N/A	N/A	N/A	N/A	0.000	
S2	26.119	24.773	18.151	10.579	19.906	
S3	N/A	N/A	N/A	N/A	0.000	
S4	N/A	N/A	N/A	N/A	0.000	
S5	5.375	1.633	0.954	1.890	2.463	

Table 4.19 - Fluorine Rubber Ink Sensors & Actuators Post-Stretch Initial Resting Resistance Values

Fluorine Rubber Ink Sensor Samples - Front Side - Ohms					
	Resting Resistance Location 1	Resting Resistance Location 2	Resting Resistance Location 3	Resting Resistance Location 4	Average
S1	8.048	0.197	1.136	6.930	4.078
S2	N/A	0.449	N/A	N/A	0.449
S3	N/A	0.116	N/A	N/A	0.116
S4	1.280	0.305	0.528	0.977	0.773
S5	0.812	0.204	0.213	0.579	0.452
Fluorine Rubber Ink Sensor Samples - Back Side - Ohms					
	Resting Resistance Location 1	Resting Resistance Location 2	Resting Resistance Location 3	Resting Resistance Location 4	Average
S1	3.579	0.397	0.836	2.591	1.851
S2	1.614	0.268	0.285	1.238	0.851
S3	1.741	0.870	0.709	0.762	1.021
S4	2.656	1.511	0.614	0.918	1.425
S5	1.229	0.280	0.506	1.081	0.774
Fluorine Rubber Ink Actuator Samples - Front Side - Ohms					
	Resting Resistance Location 1	Resting Resistance Location 2	Resting Resistance Location 3	Resting Resistance Location 4	Average
S1	20.435	N/A	2.149	1.501	8.028
S2	13.557	13.339	4.961	4.550	9.102
S3	4.789	3.775	1.858	3.320	3.436
S4	1.274	3.163	1.120	0.899	1.614
S5	2.179	2.200	1.702	2.210	2.073
Fluorine Rubber Ink Actuator Samples - Back Side - Ohms					
	Resting Resistance Location 1	Resting Resistance Location 2	Resting Resistance Location 3	Resting Resistance Location 4	Average
S1	N/A	N/A	N/A	N/A	0.000
S2	25.257	43.270	13.585	12.964	23.769
S3	1.816	1.611	1.486	1.585	1.625
S4	1.542	5.515	2.263	1.174	2.624
S5	1.900	2.150	2.016	1.917	1.996

Capacitance frequency sweeps were also taken post stretching to complete the repetition of the resting results pre and post stretch. As with the resting capacitance and resistance measurements, certain samples are reading low or seemingly missing data points because samples broke or were damaged during the stretching process. One noteworthy exception was the grease actuator sample 3, which while successful in producing a resting capacitance value was unable to produce expected and consistent frequency sweep plots despite multiple trials.

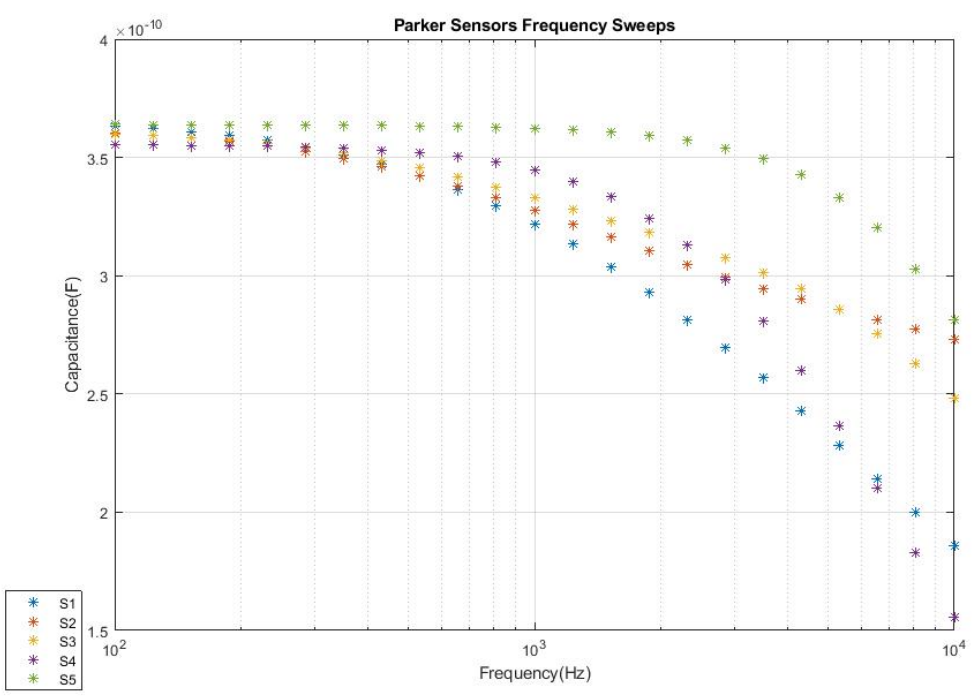


Figure 4.46 - Parker Sensor frequency sweep post stretch test

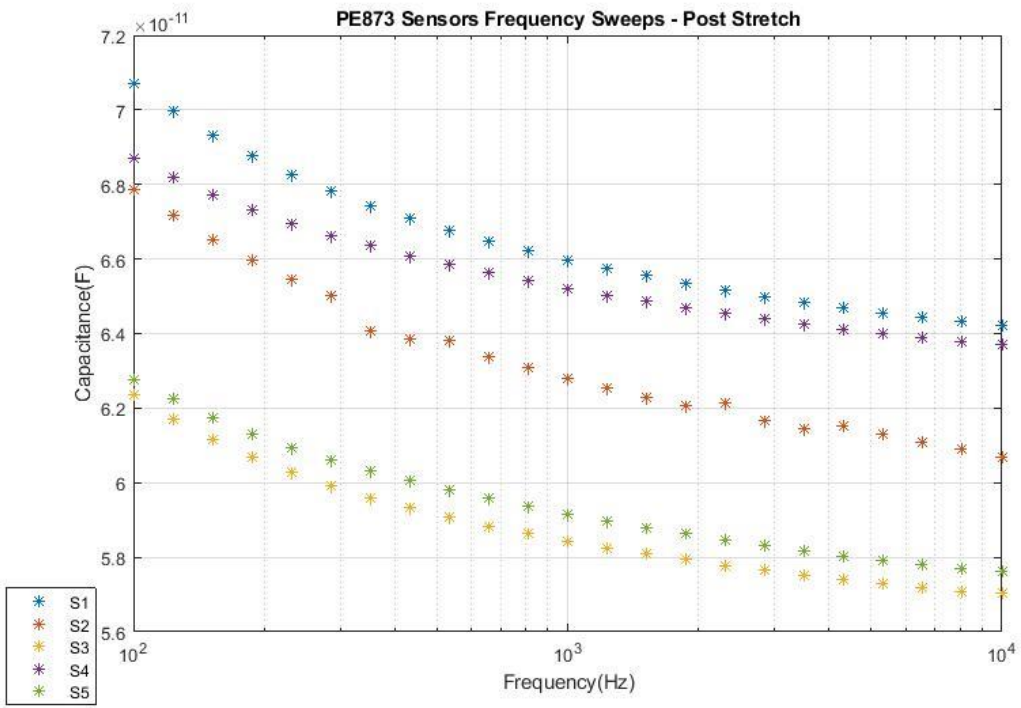


Figure 4.47 - PE873 Sensor frequency sweep post stretch test

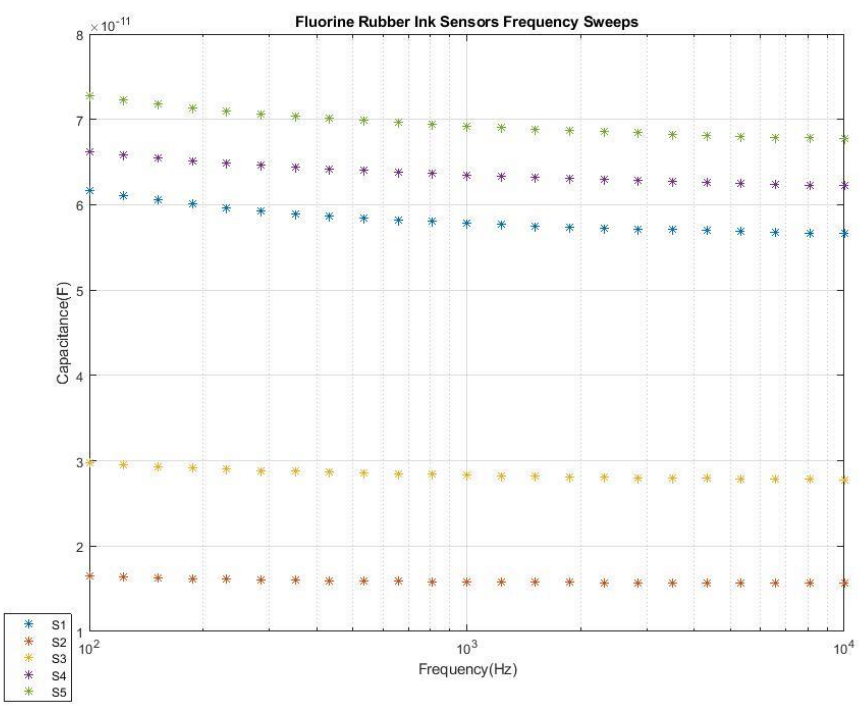


Figure 4.48 - Fluorine Rubber Ink Sensor frequency sweep post stretch test

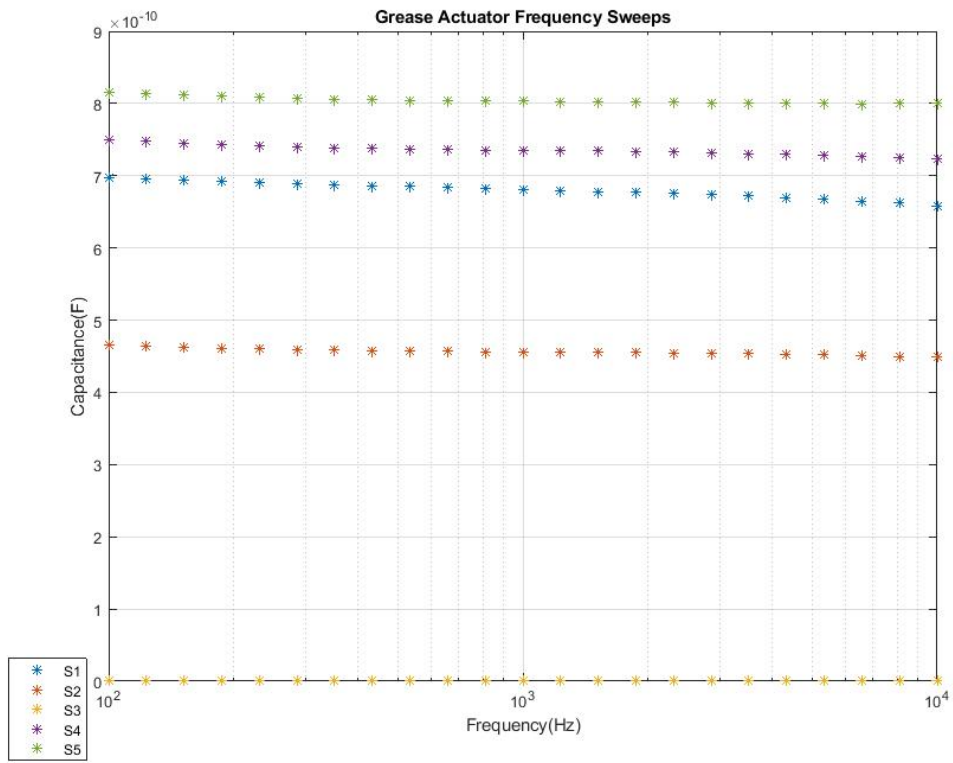


Figure 4.49 – Grease actuator frequency sweep post stretch test

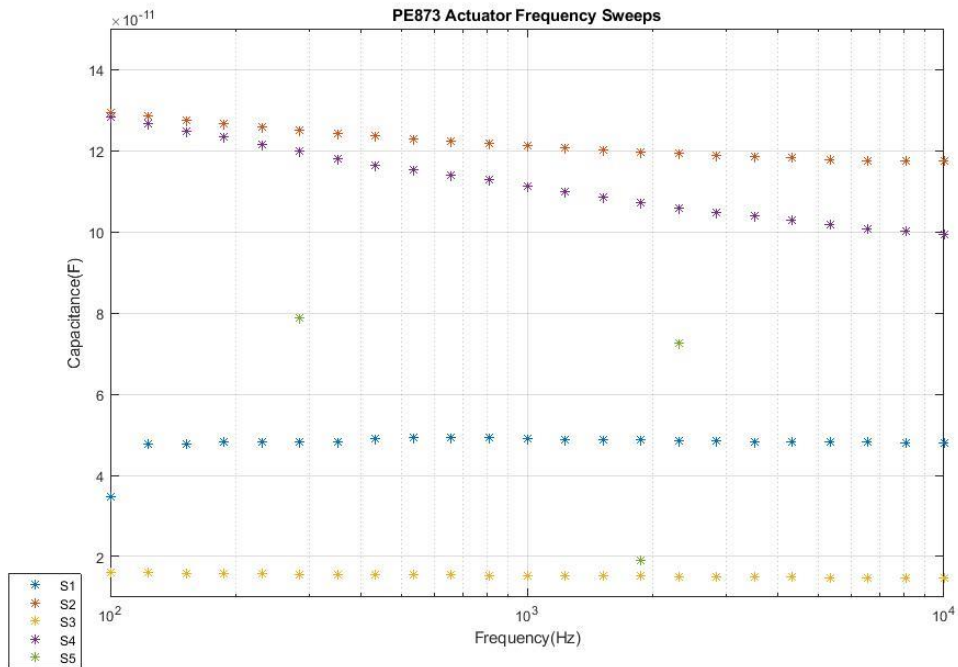


Figure 4.50 - PE873 actuator frequency sweep post stretch test

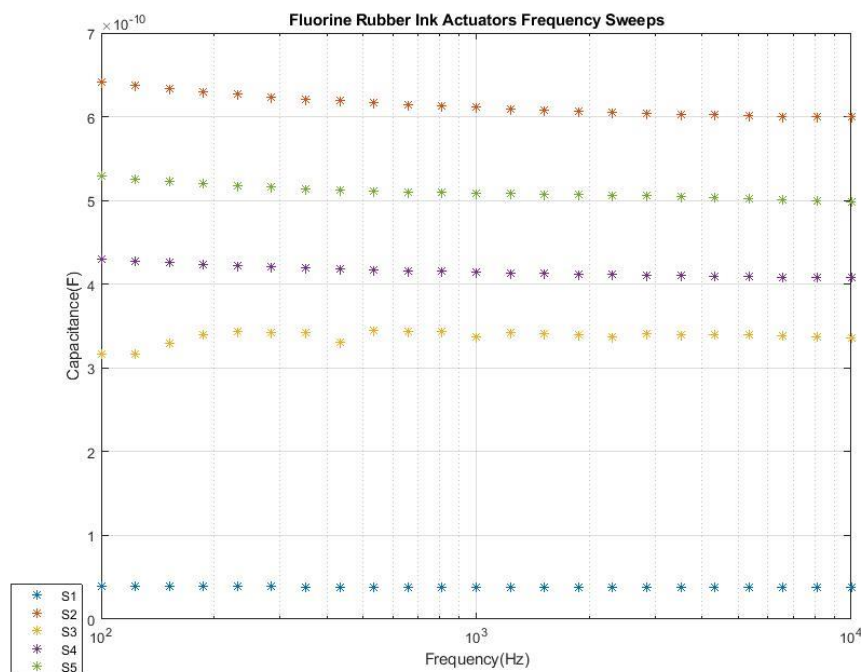


Figure 4.51 - Fluorine Rubber Ink actuator frequency sweep post stretch test

4.5 Application Testing -Actuators

Following the capture of the post-stretch values, the actuator samples were then subjected to actuation testing. The high voltage testing for actuation was utilized to test whether the Coulomb Force produced by exposing the conductive pads to high voltage could overcome the Young's Modulus of the dielectric material. The results for the physical diameter change in the conductive pad for each sample is recorded in Table 4.20. The results for the electrical parameters recorded during actuation testing were recorded in Table 4.22. All samples incurred dielectric breakdown in the form of an electrical arc starting on the electrode layer and tearing through the dielectric material, shorting the samples. The actuation testing for each sample was considered complete at the moment of the short. The grease samples have N/A in the increase from resting to strain cells because the grease samples were constructed as an already strained sample, as previously noted.

Table 4.20 – Actuator high voltage testing physical diameter changes

Grease Actuator Samples									
Sample #	visual actuation	Initial A (mm)	Post A (mm)	Initial B (mm)	Post B (mm)	Increase from resting to strain (mm)	Size before test (mm)	Size at maximum (mm)	Actuation amount (percentage)
S1	1.00	32.13	33.03	31.94	32.96	N/A	32.04	33.00	2.91
S2	1.00	31.37	31.95	32.68	33.35	N/A	32.03	32.65	1.91
S3	1.00	37.54	38.35	32.34	32.91	N/A	34.94	35.63	1.94
S4	1.00	37.00	38.25	37.52	38.51	N/A	37.26	38.38	2.92
S5	1.00	34.68	35.80	37.76	38.56	N/A	36.22	37.18	2.58
PE873 Actuator Samples									
Sample #	visual actuation	Initial A (mm)	Post A (mm)	Initial B (mm)	Post B (mm)	Increase from resting to strain (mm)	Size before test (mm)	Size at maximum (mm)	Actuation amount (percentage)
S1	0.00	21.81	21.81	20.90	20.90	2.85	21.36	21.36	0.00
S2	0.00	21.29	21.29	21.28	21.28	2.78	21.29	21.29	0.00
S3	1.00	23.51	23.97	24.41	24.78	5.46	23.96	24.38	1.70
S4	1.00	28.00	28.26	28.00	28.26	9.50	28.00	28.26	0.92
S5	0.00	22.24	22.24	23.61	23.61	4.42	22.93	22.93	0.00
Fluorine Rubber Ink Actuator Samples									
Sample #	visual actuation	Initial A (mm)	Post A (mm)	Initial B (mm)	Post B (mm)	Increase from resting to strain (mm)	Size before test (mm)	Size at maximum (mm)	Actuation amount (percentage)
S1	1.00	32.02	32.29	29.93	30.64	12.47	30.98	31.47	1.56
S2	1.00	31.62	31.96	29.19	29.47	11.90	30.41	30.72	1.01
S3	0.00	31.43	31.43	30.66	30.66	12.54	31.05	31.05	0.00
S4	1.00	28.06	28.36	28.64	28.75	9.85	28.35	28.56	0.72
S5	0.00	30.53	30.53	34.30	34.30	13.91	32.42	32.42	0.00

Table 4.21 - Average and Standard Deviation for Actuator high voltage testing physical diameter changes

Grease Samples				
	Increase from resting to strain (mm)	Size before test (mm)	size at maximum (mm)	actuation amount (percentage)
average	N/A	34.49	35.36	2.45
stddev	N/A	2.40	2.52	0.50
PE873 Samples				
	Increase from resting to strain (mm)	Size before test (mm)	size at maximum (mm)	actuation amount (percentage)
average	5.00	23.51	23.64	0.52
stddev	2.46	2.75	2.88	0.77
Fluorine Rubber Ink Samples				
	Increase from resting to strain (mm)	Size before test (mm)	size at maximum (mm)	actuation amount (percentage)
average	12.13	30.64	30.84	0.66
stddev	1.32	1.48	16.56	16.93

Table 4.22 - Actuator high voltage testing electrical values

Grease Actuator Samples				
Sample #	Voltage @ breakdown (kVdc)	Amperage Read @ breakdown (mV)	Amperage Actual (uA)	Power (Watts)
S1	4.53	28.50	5.70	0.03
S2	5.97	76.90	15.38	0.09
S3	7.23	29.40	5.88	0.04
S4	6.39	50.10	10.02	0.06
S5	5.82	22.20	4.44	0.03
PE873 Actuator Samples				
Sample #	Voltage @ breakdown (kVdc)	Amperage Read @ breakdown (mV)	Amperage Actual (uA)	Power (Watts)
S1	2.90	1000.00	200.00	0.58
S2	7.42	2986.00	597.20	4.43
S3	4.33	526.00	105.20	0.46
S4	2.88	2667.00	533.40	1.54
S5	0.00	0.00	0.00	0.00
Someya Actuator Samples				
Sample #	Voltage @ breakdown (kVdc)	Amperage Read @ breakdown (mV)	Amperage Actual (uA)	Power (Watts)
S1	7.81	3225.00	645.00	5.04
S2	2.05	3450.00	690.00	1.41
S3	4.17	1187.00	237.40	0.99
S4	6.69	109.80	21.96	0.15
S5	3.11	1094.00	218.80	0.68

Table 4.23 - Average and Standard Deviation for Actuator high voltage testing electrical changes

Grease Samples			
	Voltage @ breakdown (kVdc)	Amperage Read @ breakdown (mV)	Amperage Actual (uA)
average	5.99	41.42	8.28
stddev	0.98	22.44	4.49
PE873 Samples			
	Voltage @ breakdown (kVdc)	Amperage Read @ breakdown (mV)	Amperage Actual (uA)
average	3.51	1435.80	287.16
stddev	2.69	1322.70	264.54
Fluorine Rubber Ink Samples			
	Voltage @ breakdown (kVdc)	Amperage Read @ breakdown (mV)	Amperage Actual (uA)
average	4.77	1813.16	362.63
stddev	3.38	31.87	6.37

CHAPTER 5. SUMMARY, CONCLUSIONS, and RECOMMENDATIONS

5.1 Manufacturing

Reviewing the implemented manufacturing process revealed aspects that are pertinent to the evolving field of EAP manufacturing. Construction of electronic EAPs is commonly done by hand, a complex manufacturing line, or overlooked entirely in documentation focusing on design over manufacturing. Where additive manufacturing is used in EAP construction, it is often the case that additive manufacturing was used to only construct one aspect of the EAP; either the dielectric or the conductive pad but not both (Rossiter et al., 2009). Using exclusively additive manufacturing is a rarity and when it is pursued it is often with traditional EAP materials such as silicone and conductive grease (Cai, 2016). In order to grow the field of exclusively additive manufacturing produced EAPs, more and different materials on a variety of machines will need to be tested. The materials used here are readily available and compatible with readily available machinery. The use of DuPont's PE873, the Fluorine Rubber ink, ETPU, and TPU filament provided evidence for the effectiveness of these materials as additive manufacturing capable EAP components.

In doing so, the manufacturing process also provided insight into the adaptations that will need to be pursued in order to utilize the aforementioned materials effectively in an additive manufacturing context. The most notable observations from the manufacturing process other than the creation of operation samples, were the warping of the samples and the differences in annealing requirements between the materials.

The warping of the samples during the manufacturing process was a side effect of the solvent in the conductive material interacting with the TPU. While the warping did not affect the sensor or actuator samples during the printing process, there exists a possibility that with larger prints the nozzle could collide with the swelled material. Prior to printing across all extrusion style printers, calibration is required to determine the z-axis offset. Calibration of the z-axis offset for prints such as the ones created here is simply adding the height of the substrate (the dielectric material in this case) to the z-axis offset. The swelling of the material throws off the z axis offset, not to mention also potentially moving the sample in the x or y direction further damaging the printing process. The samples printed here were able to avoid issues with swelling

effecting printing because the prints were able to finish before the swelling became severe enough to interfere.

The difference in annealing requirements was another pertinent finding to the EAP manufacturing field. The difference between the annealing requirements between the conductive inks and the ETPU or conductive grease was not unexpected. However, the difference in annealing requirements for the conductive inks demonstrates that even with similar material types, polymers containing silver particles, the annealing process can be different and have drastically different outcomes even when similar annealing strategies are applied. The PE873 was robust when it came to annealing processes. The PE873 retained similar electrical and mechanical properties over different temperatures and times and adapted successfully outside of the exact recommended annealing recommendations. The Fluorine Rubber ink on the other hand required a gentler approach in comparison. The initial annealing strategy based on the provided annealing recommendations produced subpar capacitance values and fluctuating megaohm resistance levels. However, repeating the process again, while successful at improving the aforementioned electrical properties (capacitance of the sensors samples increased on average over 28-fold while the actuator samples increased on average nearly 3-fold), negatively affected the mechanical properties for an EAP use case. The third and fourth step of the annealing process caused a decrease in the ductility of the conductive material while also reducing the cohesion between the electrode and dielectric layers. The reprinted actuator samples were subjected to an altered and carefully observed annealing process. The discovery with the Fluorine Rubber ink is that the conductive ink should be done slowly. What is meant by that is that post initial annealing processes, the Fluorine Rubber Ink samples should then be tested for resting resistance and capacitance values. The samples should then be returned to the annealing process if the tested values are found to be high in resistance and low in capacitance. However, there is a balance to be struck, as annealing at temperatures of above 100C° for extended periods of time produces less surface resistance and higher capacitance, but at the expense of ductility and cohesion with the dielectric material used here.

5.2 Pre & Post Stretch Resting Values

Pre and post stretch values demonstrated two aspects of success for the additive manufacturing exclusive process used here: tangible resistance and capacitance values, and the

ability for the produced samples to have repeatability of use. The use of an additively manufacturing exclusive process brought with it the possibility of all samples being objective failures; not operational in the intended use case and not possessing desirable EAP characteristics. The pre and post stretch resting values demonstrate that when the samples are finished with the manufacturing process, the samples possess desirable electrical properties, retain elasticity, and the ability to return to a nominal value after stretching up to 50%.

The pre-stretch testing results show the consistency capabilities of the manufacturing process to produce samples possessing similar electrical properties. With the focus being producing electronic EAP sensor and actuators, capacitance is the defining trait. Pre-stretch results show a standard deviation of around 3.5 pF for the PE873 sensors and less than 2 pF standard deviation for the Fluorine Rubber samples. Both of the standard deviations for the conductive inks is less than that of the reference Parker sensor samples, which comes in at a standard deviation of 15.12 pF, albeit at a much higher overall capacitance; averaging 339.8 pF compared to 58.4 pF for the PE873 samples and 64.4 pF for the Fluorine Rubber ink samples. The pre-stretch values also demonstrate the consistency of the process to produce samples of the same design using different materials and yet achieve similar outcomes. The PE873 and Fluorine rubber ink samples were within 10% average capacitance values.

Post-stretch testing results depicts the ability of the samples to retain electrical properties post stretch (as was the case with the sensor samples) and also retain electrical properties while strained (as was the case with the actuator samples). The PE873 sensor samples in particular show a robustness in returning to near original resting capacitance levels in all five samples post stretch, the largest difference in pre and post stretch capacitance values being less than 7%. The Fluorine Rubber ink samples were less successful in this regard, as the annealing process left two of the samples destroyed post testing and one sample damaged. When increasing strain on EAP samples it is expected that capacitance goes up, as the surface area of the electrode increases and the distance between the plates decreases as strain increases. With the conductive layer in both cases here being only one layer thick and applied pre strain, there was a potential for capacitance to decrease or drop off entirely as the conductive layer separated during strain. The Fluorine Rubber ink demonstrated its potential for strain capacitance increase, with four of the five actuator samples showing increases in capacitance. Of the four actuators that saw an increase in capacitance, the average increase was 364.3pF. The PE873 ink saw an inconsistent result in

capacitance during strain, seeing only two samples increase in capacitance, two samples decrease, and one sample fall off completely.

5.3 Application Testing - Sensors

In the application testing for the sensors the samples truly started to separate from each other in terms of response. The Parker samples provided the reference set point, with four of the five samples having an R^2 value of higher than 0.99 and one sample having an R^2 value of 0.97. The Fluorine Rubber samples were challenged here, with two of the five samples experiencing damage during the stretching process due to the over annealing. However, the three undamaged samples exhibited similar trends to the Parker samples, albeit at a lower overall capacitance value. When averaged together, the unbroken Fluorine Rubber ink samples possess an R^2 value of 0.99 and exhibit a linear trend.



Figure 5.1 - Fluorine Rubber Ink Sample 2 during stretch testing

The PE873 on the other hand exhibited similar linear trends of capacitance over time but with four of the five samples throwing randomly dispersed values post 15% strain. While the dispersion was not exactly consistent across the four of five samples, the behavior was similar. Additionally, the PE873 sensors produced substantially more dropped values than the Fluorine Rubber ink and Parker sensors samples. One of the PE873 samples dropped nearly 43% of the

recorded values during the capacitance test. DuPont's documentation for other DuPont conductive inks sheds some light on what occurs to the resistance values of the ink as strain is increased, Figure 5.2. While DuPont claims greater than 15% strain with minimal change in resistance (Dupont, 2014), the claim is bundled with the expectation that a strain relief design is used (DuPont recommends a sinusoidal shape). A strain relief design was not used for the sensor design here. The combination of a single layer application leading to layer separation (though layer separation was not visible during the stretch testing), a large increase in resistance post 10% strain, and separation of conductive particles within the polymer may be the culprit behind the behavior exhibited at the higher levels of strain for the PE873 sensor samples.

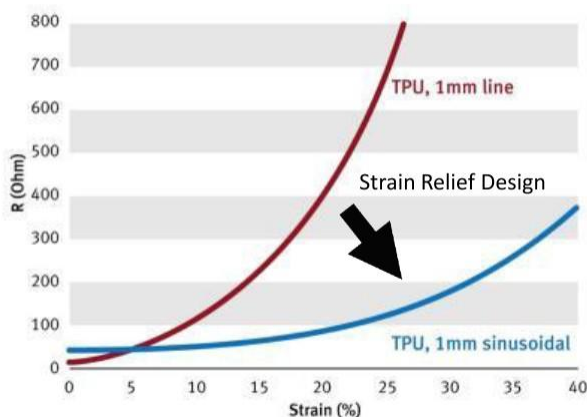


Figure 5.2 - DuPont resistance over strain plot (Dupont, 2014)

5.4 Application Testing - Actuators

The application testing for the actuators produced mixed results with the conductive inks. The grease samples actuated across all five samples and roughly in line with previous research results (Gonzalez et al., 2019). The five grease samples averaged an expansion of 2.45% in diameter prior to dielectric breakdown. Three of the Fluorine Rubber Ink samples actuated, with a 0.66% increase on average in diameter. The PE873 samples were similar to the Fluorine Rubber ink, with two samples exhibiting actuation but only to a 0.52% average increase in diameter. While the actuation results were limited in terms of diameter increase, there were important takeaways. Electronic EAP actuators of the design used here commonly produce limited changes in physical size (Pabst et al., 2011) (Cai, 2016). The crucial take away here is that the samples crossed the minimum threshold into actuation at all. The demonstrations of slight

actuation provide a base for improvement in actuation. Another notable observation was that of the increase in diameter from rest to strain of the PE873 versus the Fluorine Rubber Ink. The Fluorine Rubber ink averaged a roughly 12 mm increase in electrode pad diameter increase whereas the PE873 average only a 5 mm increase in electrode pad diameter. In reviewing the differences of the electrode pad diameter, not only does the Fluorine Rubber ink on average increase the electrode pad more, but it also was more likely to return a sample that increased in capacitance.

5.5 Concluding Statements

In conclusion, the research conducted here was successfully able to produce operational electronic EAP sensors and actuators using an exclusively additively manufactured process. The additively produced sensor samples demonstrated the potential for comparable capacitance over strain trends to the reference counter parts while returning to a resting value of within 11 percent of the original resting value. The actuator samples were able to cross the minimum threshold into successful actuation, actuating as much as 1.7 percent for the conductive inks. Though the actuators actuated less so than the reference counter parts. Additionally, samples such as the ETPU sensor samples demonstrated that it is possible to produce EAP sensors using exclusively additive manufacturing processes on one machine.

5.6 Future Work

The completed research provided a strong basis for EAP production using additive processes. The research can be expanded by fine-tuning annealing settings to balance mechanical and electrical properties of the inks. Since 3D printing EAPs allows for design flexibility, various actuator and sensor designs and geometries should be tested to see how these parameters effect performance. Enhanced accuracy of material deposition is another trend in the additive manufacturing field. Printers such as the Cellink demonstrate precise control over material deposition and can be utilized in the additive manufacture of EAPs. Cellink prints using PE873 ink are depicted in Figure 6.1 through Figure 6.3. Further development can be done using this manufacturing process and materials; but instead focusing on a single aspect as previously mentioned. The placing of both the conductive inks and dielectric TPU onto the same machine

for a one cycle full print (using multiple heads) is another avenue to pursue to bring the goal of an exclusively additive manufacturing process of EAPs closer to reality.

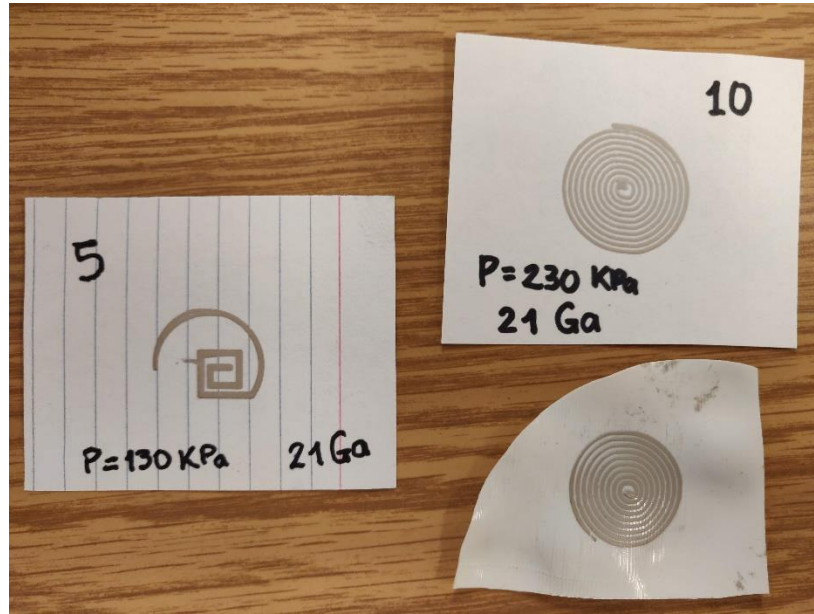


Figure 5.3 - Example of Cellink printer

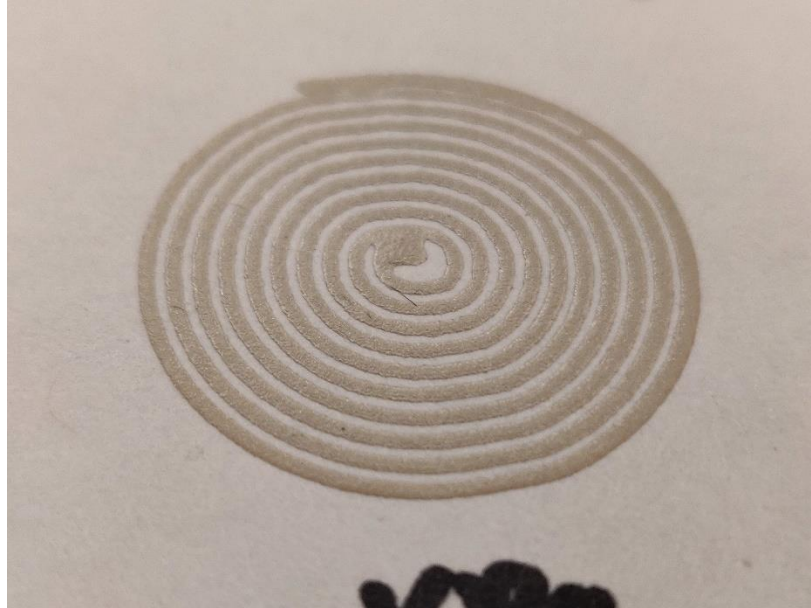


Figure 5.4 - Example of Cellink printer accuracy

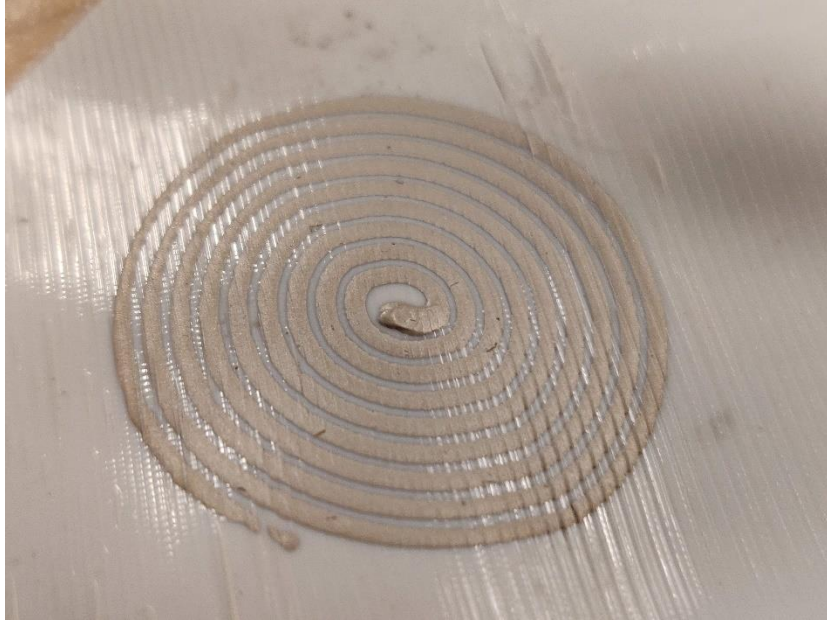


Figure 5.5 - Example of Cellink printer accuracy

LIST of REFERENCES

- 3M. (n.d.). 3M™ VHB™ Tapes No Title. Retrieved from https://www.3m.com/3M/en_US/company-us/all-3m-products/~/All-3M-Products/Adhesives-Tapes/Industrial-Adhesives-and-Tapes/Double-Sided-Bonding-Tapes/3M-VHB-Tapes/?N=5002385+8710676+8710815+8710960+8711017+8713604+3294857497&rt=r3
- Bar-Cohen, Y. (n.d.). EAP material and product manufacturers. Retrieved January 7, 2018, from <https://ndeaa.jpl.nasa.gov/nasa-nde/lommas/eap/EAP-material-n-products.htm>
- Bar-Cohen, Y. (2005). Microsoft Word - EAP-for-medical device.doc, 1–14. Retrieved from <papers2://publication/uuid/FCBAE0D5-FC44-48A3-B888-6F7B6560EC18>
- Bar-Cohen, Y. (2018). EAP and Artificial Muscles. Retrieved April 3, 2019, from <https://ndeaa.jpl.nasa.gov/nasa-nde/lommas/eap/EAP-web.htm>
- Benslimane, M. Y., Kiil, H. E., & Tryson, M. J. (2010). Dielectric electro-active polymer push actuators: Performance and challenges. *Polymer International*, 59(3), 415–421. <https://doi.org/10.1002/pi.2768>
- Burchfiel, B. C., Lipman, P. W., Parsons, T., Soc, G., Bull, A., Tovish, A., ... Joseph, J. (2000). High-Speed Electrically Actuated Elastomers with Strain Greater Than 100 %, 287(February), 836–840. <https://doi.org/10.1126/science.287.5454.836>
- Cai, J. (2016). 4D Printing Dielectric Elastomer Actuator Based Soft Robots, 88. Retrieved from <http://scholarworks.uark.edu/etd/1680/>
- Conductor, S. S. (n.d.). Dupont™ pe873.
- Dupont. (2014). Printed Wearables. Retrieved from <http://www.dupont.com/content/dam/assets/products-and-services/electronic-electrical-materials/assets/datasheets/prodlib/DuPont-Electronic-Inks-for-the-Wearable-World.pdf>
- Dynamics, S., & Forum, G. S. (2001). Paper # 2001-1492 Electroactive Polymers as Artificial Muscles – Reality and Challenges Yoseph Bar-Cohen NDEAA Technologies , JPL / Caltech , Pasadena , CA.
- Gonzalez, D. (2018). SMASIS2018-8011, 1–6.
- Gonzalez, D., García Bravo, J., & Newell, B. (2019). David Journal Paper 032419.
- Hannifin Parker. (n.d.). Electroactive Polymer (EAP) Technology Contact Information :, 2–3.

- HRE Performance Wheels. (2018). Retrieved April 3, 2019, from <https://www.hrewheels.com/wheels/concepts/hre3d>
- Keplinger, C., Kaltenbrunner, M., Arnold, N., & Bauer, S. (2010). Rontgen's electrode-free elastomer actuators without electromechanical pull-in instability. *Proceedings of the National Academy of Sciences of the United States of America*, 107(10), 4505–4510. <https://doi.org/10.1073/pnas.0913461107>
- Kodama, H. (1981). Automatic method for fabricating a three-dimensional plastic model with photo-hardening polymer. *Review of Scientific Instruments*, 52(11), 1770–1773. <https://doi.org/10.1063/1.1136492>
- LulzBot TAZ 6. (n.d.). Retrieved from <https://www.lulzbot.com/store/printers/lulzbot-taz-6>
- Mamer, T., Newell, B., & García Bravo, J. (2018). SMASIS2018-7952 FLEXIBLE 3-D PRINTED CIRCUITS AND SENSORS, 1–5.
- Matsuhisa, N., Kaltenbrunner, M., Yokota, T., Jinno, H., Kuribara, K., Sekitani, T., & Someya, T. (2015). Printable elastic conductors with a high conductivity for electronic textile applications. *Nature Communications*, 6(May), 1–11. <https://doi.org/10.1038/ncomms8461>
- Newell, B., & García-Bravo, J. (n.d.). EAP PPI Grant Newell and Garcia Problem Statement[297].
- Newell, B., & Garcia Bravo, J. (n.d.). *3-D Printed Flexible Electroactive Polymer Sensors, Actuators, and Energy Harvesters*. Purdue University.
- Pabst, O., Perelaer, J., Beckert, E., Schubert, U. S., Eberhardt, R., & Tünnermann, A. (2011). Inkjet printing of electroactive polymer actuators on polymer substrates, (March 2011), 79762H. <https://doi.org/10.1117/12.878873>
- Pelrine, R. E., Kornbluh, R. D., & Joseph, J. P. (1998). Electrostriction of polymer dielectrics with compliant electrodes as a means of actuation. *Sensors and Actuators, A: Physical*, 64(1), 77–85. [https://doi.org/10.1016/S0924-4247\(97\)01657-9](https://doi.org/10.1016/S0924-4247(97)01657-9)
- Pelrine, R., Kornbluh, R. D., Pei, Q., Stanford, S., Oh, S., Eckerle, J., ... Meijer, K. (2003). <title>Dielectric elastomer artificial muscle actuators: toward biomimetic motion</title>. *Smart Structures and Materials 2002: Electroactive Polymer Actuators and Devices (EAPAD)*, 4695(July 2002), 126–137. <https://doi.org/10.1117/12.475157>
- Romo-Estrada, J., Newell, B., & García-Bravo, J. (2018). SMASIS2018-7964, 1–6.
- Rossiter, J., Walters, P., & Stoimenov, B. (2009). Printing 3D dielectric elastomer actuators for soft robotics, 72870H. <https://doi.org/10.1117/12.815746>
- Tracker Video Analysis and Modeling Tool for Physics Education. (n.d.). Retrieved April 16, 2019, from <https://physlets.org/tracker/>

Wang, J., Jiu, J., Nogi, M., Sugahara, T., Nagao, S., Koga, H., ... Suganuma, K. (2015). A highly sensitive and flexible pressure sensor with electrodes and elastomeric interlayer containing silver nanowires. *Nanoscale*, 7(7), 2926–2932.
<https://doi.org/10.1039/C4NR06494A>

Zigon, T. (2017). *LOW-COST PRINTER FOR PROTOTYPING CIRCUITS ON FLEXIBLE SUBSTRATES USING CONDUCTIVE INKS*. Purdue University.